



UNIVERSIDADE FEDERAL DE MINAS GERAIS
FACULTY OF ENGINEERING
DEPARTMENT OF SANITARY AND ENVIRONMENTAL ENGINEERING
POSTGRADUATE PROGRAM IN SANITATION, ENVIRONMENT AND WATER
RESOURCES

RAFAEL PESSOA SANTOS BROCHADO

**Real Time Monitoring of Solids by a Low-Cost Ultrasonic
Sensor: Signal Analysis and Application in Full-Scale
Activated Sludge Systems and UASB Reactors**

MASTERS DISSERTATION

**Belo Horizonte
July of 2022**

RAFAEL PESSOA SANTOS BROCHADO

**Real Time Monitoring of Solids by a Low-Cost Ultrasonic
Sensor: Signal Analysis and Application in Full-Scale
Activated Sludge Systems and UASB Reactors**

Masters dissertation presented to Postgraduate Program in Sanitation, Environment and Water Resources, UFMG, as part of the requirements for obtaining the title of Master in Sanitation, Environment and Water Resources.

Supervisor: Thiago de Alencar Neves
Co-supervisor: Luewton Lemos Felício Agostinho

Belo Horizonte
July of 2022

B863r

Brochado, Rafael Pessoa Santos.

Real time monitoring of solids by a low-cost ultrasonic sensor [recurso eletrônico] : signal analysis and application in full-scale activated sludge systems and UASB reactors / Rafael Pessoa Santos Brochado. – 2022.

1 recurso online (116 f. : il., color.) : pdf.

Orientador: Thiago de Alencar Neves.

Coorientador: Luewton Lemos Felicio Agostinho.

Dissertação (mestrado) Universidade Federal de Minas Gerais, Escola de Engenharia.

Bibliografia: f. 110-116.

1. Engenharia sanitária - Teses. 2. Saneamento - Teses. 3. Esgotos - Tratamento - Teses. 4. Lodo de esgoto - Teses. I. Neves, Thiago de Alencar. II. Agostinho, Luewton Lemos Felicio. III. Universidade Federal de Minas Gerais. Escola de Engenharia. IV. Título.

CDU: 628(043)



UNIVERSIDADE FEDERAL DE MINAS GERAIS
ESCOLA DE ENGENHARIA
COLEGIADO DO CURSO DE PÓS-GRADUAÇÃO EM SANEAMENTO, MEIO AMBIENTE E RECURSOS HÍDRICOS

FOLHA DE APROVAÇÃO

"REAL TIME MONITORING OF SOLIDS BY A LOW-COST ULTRASONIC SENSOR: SIGNAL ANALYSIS AND APPLICATION IN FULL-SCALE ACTIVATED SLUDGE SYSTEMS AND UASB REACTOR"

RAFAEL PESSOA SANTOS BROCHADO

Dissertação de Mestrado defendida e aprovada, no dia **14 de julho de 2022**, pela Banca Examinadora designada pelo Colegiado do Programa de Pós-Graduação **EM SANEAMENTO, MEIO AMBIENTE E RECURSOS HÍDRICOS** da Universidade Federal de Minas Gerais constituída pelos seguintes professores:

Prof. Thiago de Alencar Neves - UFMG

Prof. Luewton Lemos Felício Agostinho - NHL Stenden

Prof. Marcos von Sperling - -UFMG

Prof. Dr. Mateus Pimentel de Matos - UFLA

PhD. Thiago Bressani Ribeiro - UFMG

APROVADA PELO COLEGIADO DO PPG SMARH

Priscilla Macedo Moura - Subcoordenadora do PPG-SMARH

Belo Horizonte, 14 de julho de 2022.



Documento assinado eletronicamente por **Mateus Pimentel de Matos, Usuário Externo**, em 25/07/2022, às 15:04, conforme horário oficial de Brasília, com fundamento no art. 5º do [Decreto nº 10.543, de 13 de novembro de 2020](#).



Documento assinado eletronicamente por **Thiago Bressani Ribeiro, Usuário Externo**, em 26/07/2022, às 10:08, conforme horário oficial de Brasília, com fundamento no art. 5º do [Decreto nº 10.543, de 13 de novembro de 2020](#).



Documento assinado eletronicamente por **Marcos Von Sperling, Professor do Magistério Superior**, em 26/07/2022, às 10:18, conforme horário oficial de Brasília, com fundamento no art. 5º do [Decreto nº 10.543, de 13 de novembro de 2020](#).



Documento assinado eletronicamente por **Thiago de Alencar Neves, Professor do Magistério Superior**, em 27/07/2022, às 11:57, conforme horário oficial de Brasília, com fundamento no art. 5º do [Decreto nº 10.543, de 13 de novembro de 2020](#).



Documento assinado eletronicamente por **Luewton Lemos Felício Agostinho, Usuário Externo**, em 09/08/2022, às 10:51, conforme horário oficial de Brasília, com fundamento no art. 5º do [Decreto nº 10.543, de 13 de novembro de 2020](#).



Documento assinado eletronicamente por **Priscilla Macedo Moura, Coordenador(a)**, em 01/09/2022, às 16:17, conforme horário oficial de Brasília, com fundamento no art. 5º do [Decreto nº 10.543, de 13 de novembro de 2020](#).



A autenticidade deste documento pode ser conferida no site https://sei.ufmg.br/sei/controlador_externo.php?acao=documento_conferir&id_orgao_acesso_externo=0, informando o código verificador **1630234** e o código CRC **751D599F**.

ACKNOWLEDGEMENTS

Mensurar a gratidão que tenho por todos que me ajudaram na minha jornada desse mestrado é algo complicado. Não por falta de equipamentos, técnica ou tecnologia. Mas porque certas coisas são imensuráveis, incalculáveis. Certas coisas simplesmente não cabem no vocabulário da engenharia. A gratidão é uma delas. Mas vamos lá.

Começo pela minha família, mamãe (Adriana) e papai (Francisco Olímpio). Duas pessoas tão diferentes e ao mesmo tempo tão especiais para mim. Não precisam fazer nada para eu me sentir bem (apesar de o fazerem diversas vezes), basta a presença deles, que nem precisa ser física, embora essa ainda seja certamente mais poderosa. E tem meu irmão também, o Pedro, que sempre insisto em me ajudar nos arranjos de composições que faço vez ou outra. Raramente consigo. Mas agradeço a vocês, muito tá?

Agradeço também, obviamente, a quem me ajudou diretamente na pesquisa! O Professor Thiago Neves, meu orientador, que foi tão paciente e me deu tantos direcionamentos. . . às vezes me perdia, mas no final deu tudo certo não é Professor? A essa altura deve estar aliviado de não ter que me responder inúmeras mensagens no whats app sobre problemas advindas do sensor ultrassônico. Muito obrigado por compartilhar um pouco do seu conhecimento comigo, Professor, foi uma honra trabalhar contigo!

Agora temos o meu coorientador, o Prof. Luewton Agostinho! Que honra poder fazer essa pesquisa contigo! Muitos aprendizados e aí até extrapolando os ramos da pesquisa. . . Acolheu a mim e a todos que vieram do Brasil para as terras holandesas, de forma tão orgânica com tanto carinho, certamente foi fundamental para conseguirmos sobreviver ao depressivo inverno holandês. E claro, não posso deixar de agradecer a toda sua família que nos acolheu igualmente, Sílvia, Caio, Tutas, Bruno. . . Saudades de tocar uma viola por aí, Luewton. Muito obrigado por essa oportunidade, foi uma experiência absolutamente transformadora poder passar esse período na Holanda!

Agradeço também à Carolina Carneiro, pelas dicas de gráficos, ajudas na coleta de dados na ETE de Leeuwarden; à Bianca Maiello, que fez diversos experimentos na UFMG, como IC, ao Prof. Cláudio, por todas as contribuições dadas na disciplina do seminário, ao Ronaldo Novaes, que organizava as finanças, reuniões do projeto e virou um grande amigo meu, companheiro dos cinemas holandeses; ao Saulo Nonato, que fez com que fosse possível minha ida a ETE Betim da Copasa, sempre dando todo suporte possível, ao Gabriel Freitas, que sempre deu todo suporte do mundo construindo novos “cases” para o sensor, coletando lodo para Bianca, instalando o sensor na ETE Betim, além de ser uma figuraça do entretenimento; à Priscilla Neves, que começou os estudos com o sensor no seu mestrado e foi comigo até o Cepts para mostrar como ele funciona, além de me contar várias dificuldades que teve e dicas do que fazer. Muito obrigado, vocês ajudaram muito para que isso pudesse acontecer e terminar :)

Agradeço aos membros da banca pelo aceite do convite, Prof. Marcos, Mateus e o Thiago Bressani! Uma honra poder contar com a contribuição de vocês!

Acknowledgments for those who do not understand portuguese

I thank to Mr. Aize, the friendliness in person from the WAC laboratory, always helping

me to built my innumerable setups, and find pretty much everything that I needed; to Mr. Yohan, that borrowed his guitar as soon as I arrived at the lab, and also helped me when things went wrong, for instance, when I needed to seal the sensor to avoid water entrance; to Antônio Munoz, who was a present for me when he arrived at the laboratory, soldering the cables and helping to change the transducer when it broke, furthermore he bought all my furniture when I returned to Brazil, which was a bless; To Doekle (Ynovio B.V), who basically developed the sensor and must also be relieved of not having to receive my messages on whats app with a million questions and problems, but who always gave me precise support; to my colleagues at Wetterskip, Douwe, at RWZI Grou, it was really nice to exchanged so many ideas about the Dutch WWTP and know his vision about them; to Klaas, who made sure that all full-scale application could happen in the WWTP of Grou and Leeuwarden and gave me all the complement data about the optic sensor, temperature, inflow and others parameters in their plants; to Ytzen, who always opened up the little house where the laptop was in so I could collect the data from the sensor in Leewarden, moreover he always send to me suspended solids gravimetric results; to Jonas, that helped me to install the sensor at RWZI Leeuwarden and took a “tour” with me through the plant, it was formidable! To my roommate Razib, from Bangladesh, that taught me a lot of his culture for short time of 3 months in which we lived together and resulted in a good friendship, travels, and music! Hare krishna, brother! To all of you, thank you very much, it was bless and it was essential all this support. I miss you guys already.

Voltando ao português que é uma língua muito mais bonita...

Claro, também não posso deixar de agradecer à equipe que hoje é o CR ETEs, mas que antes compunha o INCT ETEs Sustentáveis, que sempre me deu suporte quando precisei, e que está diretamente envolvida no projeto do sensor ultrassônico. Um agradecimento especial à Lariza Azevedo, que foi quem me deu a ideia da pesquisa e me ajudou tanto no comecinho: como coletar o lodo, como fazer as análises, o passo a passo, além de várias dicas de como viver na Holanda. É uma pessoa incrível e muito querida. Agradeço também ao Thiago Bressani, que também me aguentou diversas vezes no whats app, e sempre com toda paciência do mundo esclarecendo minhas dúvidas. E claro, ao Prof. Carlos Chernicharo, o mentor dessa galera toda, e obviamente um mentor para mim também. Uma pena já ter aposentado quando estava fazendo as disciplinas da pós. Felizmente aproveitei em minha graduação!

Mas nem só quem esteve diretamente envolvido no projeto me ajudou não, tá? Livinha Lobato, rainha, sempre esteve disponível para conversar sobre qualquer assunto. Izabel Chiodi, se não tivesse me chamado para o INCT lá atrás, não sei o que eu estaria fazendo agora, é a pessoa com uma capacidade absurda de lidar com pessoas, saudades das nossas bem humoradas reuniões! Alias essas duas me apoiam desde os tempos da pesquisa do meu TCC sobre papel higiênico!

Tenho que agradecer também à Paulinha, que sempre estava disposta a conversar quando eu precisava, me passando dicas e me confortando nos momentos de escolhas difíceis. Não posso deixar de agradecer ao Prof. Valter, acho que qualquer coisa que eu fizer tenho que agradecê-lo, pois a experiência do internato que ele propiciou a mim e tantos outros alunos é inspiradora,

transformadora e necessária. Nunca esquecerei uma frase que ele repetia para nós “A cabeça pensa a partir de onde os pés pisam“. Agradeço também às companheiras de laboratório, vivemos juntos por um bom tempo e uma ligação muito forte e bacana resultou entre nós: Maria Clara, Bianca, Mônica, Carola, Bruna. Obrigado pela companhia! Espero poder revê-las em breve! Aos meus amigos que estiveram no Brasil durante a minha estadia na Holanda, em especial ao grupo do sopeças, vocês são os reis do entretenimento meus amigos! A todos vocês, muito obrigado! O suporte de vocês foi essencial para que eu seguisse firme na pesquisa!

Thanks to FB oranjewoud to provide the resources for my internship into the Netherlands! It was essential for my staying in the country! Thanks to NHL Stenden and Van Hall Larenstein universities for all the support during my time in The Netherlands.

Thanks to the sanitation company Wetterskip Frislân (The Netherlands) a to allow the installation of the sensor on your plants (RWZI Grou and RWZI Leeuwarden).

Obrigado à Copasa (Companhia de Saneamento de Minas Gerais - Brasil) por permitir e viabilizar a instalação do sensor na ETE Betim.

Obrigado à FAPEMIG, que pagou minha bolsa de mestrado durante grande parte dessa caminhada. Obrigado pela UFMG, uma universidade de excelência que contribuiu tanto em minha formação.

Brasil e Holanda¹

Na Holanda a vida é plana
Bicicleta e aquecedor
Todos têm vida bacana
Do lixeiro ao doutor.

Mas o clima nunca rima
Com o nosso bom humor
Meu Brasil é como um imã
Me atrai com amor.

Ô Brasil, horizonte de montanhas
E um sol de artimanhas
pra aquecer meu coração.

Ô Brasil, chega de apagar o brilho,
Ver a fome como um filho,
e viver na escuridão.

¹ Um poema que fiz que conta um pouco minha percepção sobre a Holanda, meu amor ao Brasil e meu desejo de mudança!

RESUMO

Um dos principais aspectos para o controle operacional das Estações de Tratamento de Esgoto (ETEs) está relacionado ao gerenciamento do lodo. Os sistemas de tratamento de esgoto, aeróbios ou anaeróbios, necessitam de um controle adequado da concentração de sólidos em seus reatores. A falta desse controle pode gerar uma sobrecarga de sólidos que deteriora a qualidade do efluente tratado e, conseqüentemente, o corpo hídrico receptor. O monitoramento em tempo real de sólidos pelo sensor ultrassônico (sensor US) diretamente nos reatores biológicos de tratamento de esgoto é uma alternativa à medição manual e possibilita uma resposta mais rápida ao operador, menor mão-de-obra e um menor custo energético. O sensor US se baseia na técnica pulso-eco para determinação da concentração de sólidos através da atenuação do sinal ultrassônico. Para o uso mais adequado do sensor, a determinação dos fatores intervenientes a sua medição foi realizada. Testes em escala de laboratório mostraram que o tipo de sólido, temperatura e a presença de bolhas podem interferir na leitura do sensor. Para temperatura, o próprio sensor pode medi-la e corrigir sua medição, no entanto, um modelo ainda precisa ser consolidado para a compensação considerando uma coleta contínua de dados. Em testes em escala real foram avaliados primeiramente um reator UASB (*Upflow Anaerobic SLudge blanket*), de grande escala, porém não houve correlação de sólidos totais (ST) com a atenuação do sensor. O sensor esteve localizado na região lateral do reator UASB, possivelmente o posicionamento do sensor seja um fator importante a ser considerado, uma vez que foi testado com sucesso em um reator UASB escala demonstração, sendo posicionado ao centro do reator. O sensor foi também aplicado em duas ETEs na Holanda, em sistemas de lodos ativados. Nesse caso ele foi posicionado em unidades de carrossel e comparado com um sensor de sólidos óptico comercial. Na primeira ETE (ETE Grou), de pequeno porte, o sensor mostrou medições compatíveis com o teste gravimétrico de sólidos suspensos totais (SST) durante o período de uma semana. As medições mantiveram compatíveis durante testes da ETE Leeuwarden, uma ETE de médio porte. Considerando um período de 5 semanas, a estimativa de SST pelo sensor ultrassônico obteve um erro relativo de 1,14% , enquanto o sensor óptico 1,02% em relação ao teste gravimétrico. Após a terceira semana, no entanto, o US sensor apresentou uma superestimativa da concentração de SST, apresentando valores de até 0.08% , enquanto o sensor óptico e o teste gravimétrico mantiveram medições próximas de 0.3%. Esse resultado é um indicativo da necessidade de calibração mensal do sensor. Um dos principais problemas encontrados na aplicação em escala real foi o acúmulo de sólidos no tubo de suporte do sensor, notadamente fios de cabelo, que demandam uma limpeza frequente por parte dos operadores. Testes com um suporte para a superfície refletora do sinal mais limpa e com menos possibilidades de aderência dos sólidos devem ser realizados. O sensor US se mostrou uma tecnologia ainda promissora para competir no mercado com sensores de baixo custo, com a manutenção e comunicação facilitada por se tratar de uma tecnologia nacional.

Palavras-chave: tratamento aeróbio do esgoto, tratamento anaeróbio do esgoto, monitoramento de sólidos em tempo real, técnica pulso-eco, gerenciamento do lodo

ABSTRACT

One of the main aspects for the operational control of Sewage Treatment Plants (STPs) is related to sludge management. STPs with aerobic or anaerobic treatment requires proper control of the solids concentration in their reactors or settlers. The lack of a proper control can generate the solids washout, that deteriorates the quality of the treated effluent, thus polluting the water body. Real-time monitoring of solids by ultrasonic sensor (US sensor) is an alternative to manual measurement, which allows a faster response to the operator, less labor and lower energy consumption. US sensor is based on the pulse-echo technique which determine the concentration of solids through ultrasonic attenuation. Laboratory scale tests showed that the type of solid, temperature and the presence of bubbles can interfere with the sensor reading. For temperature, the sensor itself can measure it and correct its measurement, however, a model still needs to be consolidated for that. Full-scale tests were evaluated in a large-scale UASB reactor in Brazil, which failed to show correlation of total solids (TS) with ultrasonic attenuation. The sensor was located on the lateral region of the reactor. The positioning of the sensor is an important factor to be considered, since it was successfully tested in a demonstration-scale UASB reactor, being positioned at the center of the reactor. The sensor was also applied in two STPs in the Netherlands, in activated sludge systems. The sensor was positioned in a carousel unit and compared with a commercial optical solids sensor. In the first small-sized STP (STP Grou), the sensor showed measurements compatible with the gravimetric test of total suspended solids (TSS) for the period of one week. The measurements remained compatible during tests at STP Leeuwarden, a medium-sized STP for a period of 5 weeks. During that period the US sensor had an relative error of 1.14%, while the optical sensor 1.02% compared to the gravimetric test. After the third week, however, the US sensor showed an underestimation of TSS concentration, presenting values of up to 0.08%, while the optical sensors and the gravimetric test maintained measurements close to 0.3%. This result probably indicates the need for monthly sensor calibration. One of the main problems encountered in full-scale application was the US sensor fouling. Mainly hairs were adhered to the reflection surface support causing the complete attenuation of the signal. For further tests, a cleaner design is recommended to avoid the adherence of solids on the support. Furthermore, the US sensor showed to me a promising technology for the real time monitoring of solids in biological reactors of STPs. Further tests should be done to complete the sensor development and it is expected to be an alternative for low-cost sensors, with the advantage of the know-how allocated in Brazil, which may facilitate maintenance issues and the communication with the developers.

Keywords: Anaerobic sludge. Aerobic sludge. Ultrasonic sensor. Solids real time monitoring. Signal attenuation, sludge management

LIST OF FIGURES

Figure 1 – Typical values of solids distribution in wastewater	21
Figure 2 – US sensor	35
Figure 3 – Different instrumentation of the US sensor for data collection. 1 - Data generated by Arduino and stored by a data logger (no laptop is needed); 2 - Data generated by Arduino and stored by the software Realterm; 3 - Data generated by oscilloscope and treated on MATLAB	36
Figure 4 – Visualization of the module of the signal for still water and peak locations	37
Figure 5 – Signal visualization for still water with the power supply source from a USB connection to a laptop (5 V)	38
Figure 6 – Signal visualization for still water with the power supply source from a 12 V plug connection	38
Figure 7 – Signal visualization for still water with the power supply source from a USB connection to a laptop and a 12 V plug connection	39
Figure 8 – Signal visualization of still water on MATLAB	40
Figure 9 – Transducer case for different distances from the reflection surface	42
Figure 10 – Setup used for different distances from the reflection surface	42
Figure 11 – Visualization of the signal in MATLAB for 15 cm distance (yellow), 23 cm (orange) and 32 cm (blue) from the reflection surface to the transducer.	43
Figure 12 – Echo response time (ERT) for different distances between the reflection surface and the transducer (day 1)	44
Figure 13 – Echo response time (ERT) for different distances between the reflection surface and the transducer (day 2)	45
Figure 14 – Correlation between the maximum potential reflection peak and the distance of the reflection surface to the transducer for day 1 and day 2	45
Figure 15 – Setup for the sludge blanket level measurement	48
Figure 16 – Reflections of the signal for a sludge blanket of 10 cm	49
Figure 17 – Variability of the sound velocity detected by the US sensor - resolution of 2 V - day 1	54
Figure 18 – Variability of the sound velocity detected by the US sensor - resolution of 1 V - day 1	55
Figure 19 – Raw signal obtained from the oscilloscope at a temperature of 21.7 °C and 34.9 °C	55
Figure 20 – Temperature effect on attenuation - data distribution (day 2)	57
Figure 21 – Temperature effect on attenuation - data distribution (day 1)	57
Figure 22 – Maximum potential x temperature (day 1) - linear regression and residuals	58
Figure 23 – Maximum potential x temperature (day 2) - linear regression and residuals	58
Figure 24 – Vertical reactor with air bubble diffusion	62
Figure 25 – Bubbles attached to the ultrasonic transducer surface	63
Figure 26 – Signal area in water for different air flow	64

Figure 27 – Signal area in aerobic sludge with 0.3% of TS for different air flow	64
Figure 28 – Correlation between the area of the signal and the TS concentration at 22 °C and flow rate of 0.58 L.m ⁻² .min ⁻¹	65
Figure 29 – Sludge ash used for the tests	67
Figure 30 – Soil used in the tests	67
Figure 31 – Setup - mechanic mixing	68
Figure 32 – US sensor inside the setup with water	68
Figure 33 – Signal module identification of BRP and maximum potential region	69
Figure 34 – Correlation between TS of soil and the signal potential of the US sensor	70
Figure 35 – Correlation between TS of sludge ash and the signal potential of the US sensor at a range below 0.5%	71
Figure 36 – Correlation between TS of anaerobic sludge and the signal potential of the US sensor at a range below 0.5%	71
Figure 37 – Correlation between TS of anaerobic sludge and the signal potential of the US sensor (until 1.16% TS)	72
Figure 38 – Signal area over time for soil compared to water	73
Figure 39 – Signal area over time for ash sludge compared to water	73
Figure 40 – Signal area over time for anaerobic sludge compared to water	74
Figure 41 – Sludge sampling points along the digester compartment in UASB reactors	77
Figure 42 – ETE Betim Central (STP Betim) - 1: location of the ultrasonic sensor (UASB reactors), 2: aeration tank (activated sludge system), 3: Secondary sedimentation tanks	80
Figure 43 – UASB reactor Betim Central scheme - 1: Ultrasonic sensor position; 2: Support cable; 3: Transmission cable; 4: Gas-Liquid-Solid separator; 5: Deflector; 6: Oscilloscope and control box; 7: Laptop	81
Figure 44 – 1 out of 500 images from the ultrasonic sensor for TS gravimetric measurement of 0.1% at the same height position of the sensor location inside the UASB reactor of ETE Betim Central obtained by an oscilloscope	82
Figure 45 – Solids accumulation on the US sensor after two months inside the UASB reactor from ETE Betim Central	83
Figure 46 – RWZI Grou: 1 - Preliminary treatment; 2 - Carousel units; 3- Secondary sedimentation tanks; 4 - Sludge thickener; 5 - Sludge dewatering units	87
Figure 47 – RWZI Grou carousel unit: 1 - Mixers; 2 - Position of the US sensor and optic sensor for TSS.	87
Figure 48 – US sensor (on the left) and optic sensor (TSS) in the carousel	88
Figure 49 – RWZI Leeuwarden: 1 - Preliminary treatment; 2 - Carousel units; 3- Sludge thickening, dewatering, anaerobic digestors and biogas treatment; 4 - Secondary sedimentation tanks. The circulated area correspond to the carousel unit where the sensors were installed.	89

Figure 50 – RWZI Leeuwarden carousel unit: 1 - Optic sensor location; 2 - Ultrasonic sensor location	89
Figure 51 – US sensor in RWZI Leeuwarden, on the right	90
Figure 52 – Beral uni-seal added to the transducer for water-tight protection	90
Figure 53 – US sensor calibration in RWZI Grou	91
Figure 54 – US sensor calibration in RWZI Leeuwarden	91
Figure 55 – Signal visualization from the oscilloscope in Grou - 17-03-2022	92
Figure 56 – Frequency distribution of US sensor MLSS estimation from 24/03/2022 to 01/04/2022 - RWZI Grou	93
Figure 57 – Frequency distribution for the US sensor estimation of TSS in still water	93
Figure 58 – Time series of the MLSS measurement for the ultrasonic sensor, optic sensor and gravimetric test - RWZI Grou	94
Figure 59 – Solids accumulation on the optic sensor (RWZI Grou)	97
Figure 60 – Solids accumulation on the ultrasonic sensor after one week (RWZI Grou)	97
Figure 61 – Time series - Ultrasonic sensor, optic sensor, gravimetric test for MLSS measurement in RWZI Leeuwarden	98
Figure 62 – Time series of the mixed liquor temperature in RWZI Leeuwarden	100
Figure 63 – Example of signal overrate (DC)	103
Figure 64 – Solids accumulation on the US sensor after two days - RWZI Leeuwarden	104

LIST OF TABLES

Table 1 – Monitoring program for activated sludge systems in terms of suspended solids	23
Table 2 – Cost comparative between different sensors for real time monitoring in STPs	25
Table 3 – Velocity, attenuation coefficient and frequencies of ultrasound waves for different fluids	31
Table 4 – Linear regression coefficients for time response and maximum potential (day 1 and day 2)	46
Table 5 – Hypothesis tests summary for the linear regression ERT x distance and maximum potential x distance	46
Table 6 – Blanket level estimation by the US sensor	49
Table 7 – Temperature estimation by sound velocity (day2)	56
Table 8 – Linear regression - Amplitude of the signal x Temperature	59
Table 9 – Kruskal-Wallis ANOVA table (MATLAB) - Difference of the signal amplitude for different temperatures	59
Table 10 – F-test for attenuation and temperature estimation (linear regression analysis) .	60
Table 11 – Substrates characteristics	67
Table 12 – Signal analysis for the sludge still and mixing compared to water	75
Table 13 – Main factors that can affect the management of sludge from UASB reactors treating sewage	78
Table 14 – Signal amplitude before and during the sludge withdrawal in a UASB reactor	82
Table 15 – Descriptive statistics of the optic sensor, ultrasonic sensor and the inflow rate	94
Table 16 – Correlation parameters in RWZI Grou for a period of one week.	96
Table 17 – Descriptive statistics of the data collected in RWZI Leeuwarden during the period of 18/05/2022 to 20/06/2022	99
Table 18 – Relative error comparative from US sensor and optic sensor in RWZI Leeuwarden	100
Table 19 – Correlation between parameters in RWZI Leeuwarden for a period of one month	102
Table 20 – Comparison of energetic cost for TS and TSS monitoring by US sensor and the gravimetric test	106
Table 21 – Laboratory cost for TS and TSS analysis	107

LIST OF ABBREVIATIONS AND ACRONYMS

ABNT	Associação Brasileira de Normas Técnicas -Brazilian association of technical standards
AC	Alternating current
ANA	Agência Nacional de Água e Saneamento Básico - National water and sanitation agency
ANOVA	Analysis of variance
APHA	American Public Health Association
BRP	Before reflection peak
BW	Bandwidth
COD	Chemical oxygen demand
CONAMA	Conselho Nacional do Meio Ambiente - National environment council
DC	Direct current
DFE	Degrees of freedom
DO	Dissolved oxygen
DOC	Dissolved organic carbon
EC	Electrical conductivity
ERT	Echo response time
H0	Null hypothesis
IEEE	Institute of Electrical and Electronics Engineers
MATLAB	Matrix laboratory
MLSS	Mixed liquor suspended solids
ORP	Oxidation reduction potential
PROSAB	Programa de Pesquisas em Saneamento Básico (Sanitation Research Program)
PVC	Polyvinyl chloride
RMSE	Root mean square error
RWZI	Rioolwaterzuiveringsinstallatie (Sewage treatment plant)

SSE	Sum of squared estimate of errors
STP	Sewage Treatment Plant
TDS	Total Dissolved Solids
TKN	Total kjeldahl nitrogen
TOC	Total organic carbon
TS	Total solids
TSS	Total suspended solids
TVS	Total volatile solids
UASB	Upflow Anaerobic Sludge Blanket
UFMG	Universidade Federal de Minas Gerais (Federal University of Minas Gerais)
US sensor	Ultrasonic sensor
USB	Universal serial bus
UTP	Unshielded twisted pair
VSS	Volatile suspended solids
WAC	Water Application Center
WEF	Water Environment Federation
WS	Worst Scenario
pH	Hydrogen potential
°C	Celsius degree

CONTENTS

1	INTRODUCTION	19
1.1	<i>Research structure</i>	20
1.2	<i>Solids and sludge characteristics in domestic sewage</i>	20
1.3	<i>Solids monitoring in wastewater</i>	22
1.3.1	Real time monitoring in wastewater	23
1.3.2	Data acquisition and transmission	24
1.3.3	Available parameters and cost comparative	24
1.3.4	Real time monitoring of solids in STP	27
1.4	<i>Ultrasonic technology: fundamentals, development and application</i>	28
1.4.1	Physical principles of sound waves	28
1.4.2	Techniques and applications with ultrasound	29
1.4.3	Intrinsic and external variables for the attenuation coefficient	30
2	OBJECTIVES	33
2.1	<i>General objectives</i>	33
2.2	<i>Specific objectives</i>	33
3	INSTRUMENTATION AND DATA TREATMENT FOR THE SIGNAL	34
3.1	<i>Introduction</i>	34
3.2	<i>Methodology</i>	35
3.2.1	Configuration of the system	35
3.2.2	Signal treatment	36
3.2.3	Second reflection peak evaluation	36
3.3	<i>Results and discussion</i>	37
3.3.1	Data treatment	37
3.3.2	Power supply	37
3.3.3	Internal reflection from the setup	39
3.4	Conclusion	40
4	ECHO RESPONSE TIME APPLICATION	41
4.1	<i>Mechanical adjustment for the signal amplification</i>	41
4.1.1	Introduction	41
4.1.2	Methodology	41
4.1.3	Results and discussion	43
4.1.4	Conclusion	46
4.2	<i>Sludge blanket level detection</i>	47
4.2.1	Introduction	47
4.2.2	Methodology	48
4.2.3	Results and discussion	48

4.2.4	Conclusion	50
5	TEMPERATURE EFFECT ON THE ULTRASONIC SIGNAL	51
5.1	<i>Introduction</i>	51
5.2	<i>Methodology</i>	51
5.2.1	Setup	51
5.2.2	Data collection and signal treatment	52
5.2.3	Oscilloscope resolution selection	52
5.2.4	Statistical analysis	52
5.3	<i>Results and discussion</i>	54
5.3.1	Oscilloscope resolution selection	54
5.3.2	Temperature estimation by ERT	55
5.3.3	Temperature effect on attenuation	56
5.3.4	Repeatability	59
5.4	<i>Conclusion</i>	60
6	AIR BUBBLE EFFECT ON THE ULTRASONIC SIGNAL	61
6.1	<i>Introduction</i>	61
6.2	<i>Methodology</i>	61
6.2.1	Setup	61
6.2.2	Signal treatment and sample collection	62
6.3	<i>Results and discussion</i>	63
6.4	<i>Conclusion</i>	65
7	SIGNAL ANALYSIS FOR DIFFERENT TYPE OF SOLIDS	66
7.1	<i>Introduction</i>	66
7.2	<i>Methodology</i>	66
7.2.1	Setup and materials	66
7.2.2	Correlation between attenuation and solids concentration	68
7.2.3	Signal behavior over time	69
7.2.4	Aerobic sludge still and mixing comparative	69
7.3	<i>Results and discussion</i>	70
7.3.1	Correlation between attenuation and TS concentration	70
7.3.2	Signal behavior over time	72
7.3.3	Aerobic sludge still and mixing comparative	74
7.3.4	Conclusion	75
8	US SENSOR FULL-SCALE APPLICATIONS	76
8.1	<i>UASB reactors</i>	76
8.1.1	Introduction	76
8.1.2	Methodology	79
8.1.3	Results and discussion	81

8.1.4	Conclusion	83
8.2	<i>Activated Sludge</i>	84
8.2.1	Introduction	84
8.2.2	Methodology	86
8.2.2.1	<u>STPs overview</u>	86
8.2.2.1.1	Overview of RWZI Grou (small STP)	86
8.2.2.1.2	Overview of RWZI Leeuwarden (medium STP)	88
8.2.3	Calibration	90
8.2.4	Results and discussion	92
8.2.4.1	<u>RWZI Grou</u>	92
8.2.4.2	<u>RWZI Leeuwarden</u>	97
8.2.5	Conclusion	104
9	COST ANALYSIS (US SENSOR X GRAVIMETRIC TEST)	105
9.1	<i>Introduction</i>	105
9.2	<i>Methodology</i>	105
9.3	<i>Results and discussion</i>	106
9.4	<i>Conclusion</i>	107
10	FINAL CONSIDERATIONS	108
10.1	<i>Signal interference</i>	108
10.2	<i>Sludge blanket level</i>	108
10.3	<i>Full-scale application</i>	108
11	RECOMMENDATIONS	110
	REFERENCES	111

1 INTRODUCTION

Sewage Treatment Plants (STPs) have an important role in preventing the pollution of water courses and the spreading of waterborne diseases. Such systems can have a rather complex operational routine, and normally demand continuous monitoring of different variables to guarantee its stable functioning. A very important aspect of such plants is sludge management, which involves solids monitoring, settler drains, dewatering, digestion (in some cases) and transportation/destination. According to Andreoli, von-Sperling and Fernades (2014) such activities can represent 20-60% of the STP OPEX (Operational Expenditure).

The most used technology for sewage treatment in Brazil are the UASB reactors (Upflow Anaerobic Sludge Blanket), representing 37% out of 3668 reported STPs in the country. While activated sludge is the most used technology in the world, in Brazil, it represents 10% of the total reported STP. Nevertheless, in terms of sewage treated volume, activated sludge system are still the most used technology in Brazil (ANA - AGÊNCIA NACIONAL DE ÁGUAS E SANEAMENTO BÁSICO, 2020).

Moreover, several reports include operational problems in UASB reactors, such as the solids washouts due to excess of solids in the settling compartment. The solids washout can deteriorate the quality of the effluent, thus, it compromises the efficiency of the sewage treatment (CHERNICHARO, *et al.*, 2018). In activated sludge the demand of a more complex and sophisticated operational occurs, and the problem of solids washouts occurs as well, specially in developing countries. Abusam and Mydlarczyk (2018) reported aeration problems and organic overload in the aeration tank in Kuwait. In Brazil, Oliveira and von-Sperling (2005) evaluated 166 STPs in the states of Minas Gerais and São Paulo. Despite most of the plants had an organic removal within an expected range, for TSS removal results were below the expected. However, it is relevant to notice that the research was realized in 2005, and a global panorama of the STP performance in Brazil still require more studies.

In order to provide an appropriate control of a STP, it is essential to realize solids monitoring control. The standard method for the examination of water and sewage recommends the gravimetric analytical method for this purpose (APHA/AWWA/WEF, 2017). However, the gravimetric test are usually not realized in an appropriated frequency. Real time solids monitoring is, therefore, currently seen as an important tool to guarantee a good functioning of STPs and allow fast and objective actions of the operators. Moreover, data acquisition for the proper control of the solids in STP's can provide not only an operational improve but also an operational cost reduction (LEONEL, 2016; COLLIVIGNARELLI *et al.*, 2018). Many sensors for solids monitoring are already present in the market. Nevertheless, most of them have a high-cost and are imported products, therefore maintenance is more complicated and may become a barrier for their implementation in the STPs from Brazil. Real time monitoring of solids, despite it may increase sewage treatment efficiency, demands a regular cleaning routine of the sensors to prevent fouling which can result in errors on the measurements.

A partnership between the National Institute of Science and Technology in sustainable STPs (INCT ETEs Sustentáveis), NHL Stenden University of Applied Sciences, YNOVIO

B.V and Lamp-ion BV was established to improve time response for the sludge discharge in STPs with a national technology. A low-cost ultrasonic sensor (US sensor) was developed to estimate the total solid (TS) concentration in UASB reactors and provide a real time monitoring possibility for the operators. Neves *et al.* (2021) tested the sensor in a demo-scale and reported a determination coefficient of 0.97 with the values measured by the sensor compared with the gravimetric test of solids. The present work aims to extend this study to a full-scale UASB reactor and activated sludge systems and to give more technical information regarding the factors that can interfere in the sensor reading. Furthermore, it is expected in the future that the sensor can become a national product for real time monitoring and possibly an automation tool for the STPs in Brazil.

1.1 *Research structure*

This research was structured in chapters for a better understanding of the results that had different setups, therefore different methodology and specific concepts regarding each chapter. A general introduction with contextualization of the theme and its importance was presented on chapter 1. Further items of the introduction will contain the literature review of the main fundamentals used on this research. The second chapter will, then, present the research objective. The next chapters will contain their own introduction, with a short literature review, methodology, results and discussion and conclusion. The two final chapters will contain a general conclusion, with a summary of the main results found on this research, and recommendations for future researches.

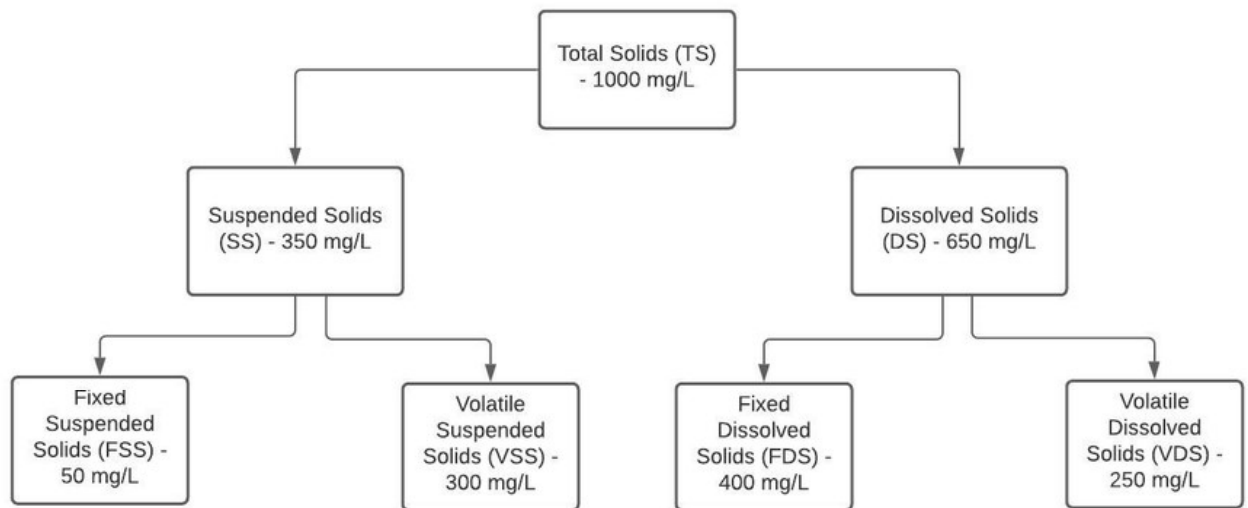
1.2 *Solids and sludge characteristics in domestic sewage*

Raw sewage contents 0.1% of total solids and 99.9% of water. Except dissolved gases, all the water pollutants contribute to compose the 0.1% of solids. Therefore, it is mandatory to treat properly the solids present in sewage in order to preserve the quality of the water bodies or to maintain the viability for water reuse (VON SPERLING, 2014).

The solids classification from the physical aspect's perspective, can be divided by the size of the particles. On this perspective, solids are classified as total suspended solids (TSS), for the retained solids of a 2 μm pore filter (some clays and colloids, may pass through the filter). Particles below 2 μm , that passes through the filter are considered total dissolved solids (TDS) (APHA/AWWA/WEF, 2017). It is relevant to notice that TSS and TD concepts can probably suffer alterations throw the years. With the technology advance, new techniques can be used to measure solids, for instance, suspended nano- particles. Therefore, different classification of solids should occur in the future.

From a chemistry perspective, solids can be volatile when the composition is primarily organic, or fixed solids, when its composition is mainly inorganic matter (VON SPERLING, 2014). The distribution of solids in sewage can be seen at Figure 1:

Figure 1 – Typical values of solids distribution in sewage



VON SPERLING (2014)

The solid phase of the sewage treatment has as main compound the sludge, which can vary according to the technology and process steps. The primary sludge, a sub-product of the primary settler, for instance, will need to pass through all the sludge's treatment steps. The first step is the sludge thickening, which is used aiming at the volume reduction for digestion. Thickening is accomplished in gravity thickeners, dissolved air flotation units, or even in primary sedimentation tanks. It is desirable to have solids concentrations in the raw sludge fed to digestion in the order of 4% to 8%. Higher solids concentrations can be used, as long as the feeding and mixing units are able to handle the solids increase. Solids concentrations lower than 2.5% are not recommended, as excess water has a negative effect on the digestion process. (ANDREOLI; VON-SPERLING; FERNANDES, 2014). The second step is the sludge's stabilization. This procedure is used to eliminate offensive odors and reduce the potential for putrefaction. The third step is the dewatering procedure, which is used to remove the moisture content in the sludge and make its transport feasible (METCALF & EDDY, 2003).

It is known that in non-digested sludge from aerobic systems the relation VS/TS is equal to 0.75-0.80, which means a majority of organic solids, while in digested sludge VS/TS drops to 0.60-0.65 (ANDREOLI; VON SPERLING; FERNANDES; 2014). Unlike most of aerobic treatments such as conventional activated sludge and trickling filters, anaerobic sewage treatment, for instance UASB reactors, provides a thick and stabilized sludge. Therefore, the sludge produced by UASB reactors requires only the dewatering procedure if the final destination is to landfills, which is a common route in Brazil. However, to transform the sludge into a biosolid, and allow that it can be used directly at the soil as a fertilizer or to recovery degraded areas, it has to pass through a disinfection step (CHERNICHARO, 2016; ANDREOLI; VON SPERLING; FERNANDES, 2014). In Brazil, the resolution Conama 498/2020 establishes several criteria for

the disposal of biosolid in the soil (BRASIL, 2020). In Europe, most of the countries have the sludge destination to landfills prohibited, however several countries such as The Netherlands, also cannot apply biosolids directly in their fields, thus the most common practice is the sludge incineration, or even the exportation of this material to other countries (COLLIVIGNARELLI *et al.*, 2019). This restriction in The Netherlands occurs mainly because ground water level is high, thus it is more susceptible to pollutants.

The legislation that determine the standard for effluent discharge in Brazil is CONAMA 430/2011 (BRASIL, 2011). In which concern about solids, the legislation points that solids sedimentation should occur up to 1 mL.L^{-1} . For the discharge into lakes and ponds, settleable materials must be virtually absent. It is also prohibited the presence of floating materials. For the discharge of sewage into submarine emissaries, coarse solids should be absence and the minimum TS removal of 20% should occur before it reaches the sea.

Besides the attendance to the effluent discharge, it is mandatory that the STP respects the standard of the water bodies receptors. In Brazil, it is determined by CONAMA 357/2005 (BRASIL, 2005). The standard depends on the waterbody's class, which can vary from special class to class IV. The classification also depends on their type (saline water, brackish water, fresh water). For solids in fresh water for all water bodies classes, it is established a limit of 500 mg.L^{-1} of total dissolved solids (TDS).

1.3 Solids monitoring in wastewater

For the proper monitoring and control of solids in STP, the standard method recommends gravimetric test (APHA/AWWA/WEF, 2017). For TS determination, the analysis consists on drying the sample at $103\text{-}105 \text{ }^\circ\text{C}$ oven, cooling dish in a desiccator until room temperature is reached and then the sample can be weighted. The procedure should be repeated until the weighting values have a difference below 0.5 mg . It is important to mention that the result obtained from the gravimetric test represents a sample of TS concentration inside the reactor, but there is no perfect mixed system, so the actual value could vary depending on the region that the sample was collected. It will depend on how representative are the collected samples. Nevertheless, the time between two weightings must be at least 1 h. The minimum time consumption for the TS determination, therefore, is 2 h plus the preparation and cooling time. However, in several places, mainly research centers like in the Federal University of Minas Gerais (Brazil) and in Water Application Center (WAC) located in Van Hall Laurenstein University (The Netherlands), the time for TS determination takes usually around 24 h due to the labor of checking the samples in a short time period during the same day.

TS or TVS (total volatile solids) test are usually the parameters used for monitoring the sludge in UASB reactors (CHERNICHARO; BRESSANI-RIBEIRO; LOBATO, 2019), since the high concentration of the sludge make the suspended solids measurement more complicated, considering the high possibility of clogging of the membrane. In UASB reactors, Chernicharo, Bressani-Ribeiro and Lobato (2019) reported sludge concentration of almost 5% ($50\,000 \text{ mg.L}^{-1}$) of TS at the bottom of the reactor, which illustrate the difficult on TSS measurement within the

reactor.

Nevertheless, total suspended solids (TSS) determination can also be a parameter control for the STP. When TSS test can be applied it is usually preferable, since it is necessary only 1 hour to dry the suspended solids (APHA/AWWA/WEF, 2017). In UASB reactors it is used for the efficiency control of the system, by measuring the influent and effluent concentration. In activated sludge system, TSS measurement is performed not only for the efficiency determination, but also for the process control. A daily monitor of TSS in the mixed liquor is recommended (VON-SPERLING, 2016). The concentration range of the mixed liquor for TSS (MLSS) is between 2000 mg.L⁻¹ and 4000 mg.L⁻¹ (METCALF EDDY, 2003). Despite the use of mg.L⁻¹ or g.L⁻¹ to express solids concentration is the most accurate form to express it, on this research % of solids will be adopted, considering 1% of TS or TSS equivalent to 10 000 mg.L⁻¹.

Monitoring frequency will depend on each plant characteristic. However, in general, UASB reactors have to monitor the solids content in the sludge weekly (CHERNICHARO, 2016). However, several UASB reactors in Brazil do not monitor solids at its ideal weekly frequency. Moreover, even STPs that monitor at an ideal frequency, do not use the data for a proper routine of the sludge withdrawal, necessary for a well functioning reactor (CHERNICHARO; BRESSANI-RIBEIRO; LOBATO, 2019). In activated sludge system the frequency of monitoring of solids can be seen in Table 1.

Table 1 – Monitoring program for activated sludge systems in terms of suspended solids

Place	Frequency	Sampling type
Raw sewage	weekly	composite
Primary effluent	weekly	composite
Reactor	daily or continuous	simple/sensor
Return line	daily	composite
Final effluent	weekly	composite

Source: Adapted from Von Sperling, 2016

A more detailed review of UASB reactors and activated sludge systems are present on chapter 8.

1.3.1 Real time monitoring in wastewater

Depending on the purpose of the treatment there are several parameters that have great importance for the operational control of a STP. For the secondary treatment, the objective is the organic matter removal (VON-SPERLING, 2016). However, is also relevant to monitoring the physical characteristic of the sewage and the biological characteristic in terms of pathogens. For a tertiary treatment, nutrients should be monitored and controlled (METCALF EDDY, 2003). More recently micropollutants are also becoming a problem for water quality, thus new forms of monitoring them are emerging. In order to monitor all the parameters to promote a good

control of the effluent quality, sample collection and laboratory analysis are recommended by the standard method (APHA/AWWA/WEF, 2017).

For a well function of a STP, proper operation of the system is essential. Real time monitoring can be a valuable tool therefore. Compared to manual operation it can provide a more rapidly response so the operator can take action. Furthermore, it can provide a more representative data over time for the STP diagnostic compared to simple samples analysis. Moreover, it also opens the possibility of automating several actions, with feedback and feedforward mechanisms which can promote a better control of the plant and reduces costs from laboratories analysis. For the dewatering process, for instance, the use of polymers can reduce up to 50% with the automation of a system (WEF - WATER ENVIRONMENT FEDERATION, 2019). Despite all the benefits of the real time monitoring and automation of the systems, the WEF pointed that:

As is true for all mechanical systems and control elements, the sensors must be installed correctly, maintained, and calibrated to yield accurate, useful data. It is recommended that interested facilities check maintenance requirements and installation details from other installations where these sensors and control systems have been successfully used (WEF - WATER ENVIRONMENT FEDERATION, 2019, p.3) .

1.3.2 Data acquisition and transmission

One relevant aspect for the well functioning of a real time monitoring device is the data acquisition system (DAS). “Data acquisition is the process of sampling signals that measure real world physical conditions and converting the resulting samples into digital numeric values that can be manipulated by a computer”(MURUGAN; SUMATHI, 2017, 1). For an ultrasonic sensor, for instance, one of the mechanisms for DAS is to convert the ultrasonic signal into electrical energy, which can be done by a transducer. The electrical signal can be transmitted by an Unshielded Twisted Pair (UTP) cable until a proper device to transform the analog electrical signal into a digital signal, thus the data can be manipulated by a computer. Besides wired transmission, wireless technology has been reported to be an alternative for the data collection and transmission. It can be done by several kinds of short-range transmission such as Bluetooth (IEEE 802.15.1), Ultra-wideband (IEEE 802.15.3), ZigBee (IEEE 802.15.4) and Wi-fi (IEEE 802.11a/b/g), each one with a different level of security, transmission time and power consumption (LEE; SU; SHEN, 2007). Furthermore, it is ideal for a proper monitoring to have a storage device to save the acquired data, power supplies for the network function and management tools for the proper use of the storage data (CHEN; NI, 2018).

1.3.3 Available parameters and cost comparative

There are several sensors available on the market for the real time monitoring of different parameters in a STP (BOURGEOIS; BURGESS; STUETZ, 2001). Despite developed countries have a majority of STP that are equipped with real time monitoring devices, in developing countries such as Brazil this is still far away to be achieved, mainly due to economic barriers and the lack of national technology for an easier maintenance of the products. The price of the sensors can greatly differ from each other, depending on the parameter, technology that was

used, and the brand. Table 2 show examples of different sensors. It is notable that the most used technology for TSS concentration was optic. Optic sensors function in a similar way compared to US sensors, the difference is that while US sensors measured due to sound attenuation, optic sensors function by the attenuation of light. One crucial difference between light and sound is the sound capacity of avoiding obstacles, which will depend on the sound frequency. However, multiple light beams with different angles can be installed so high concentration of solids can be detected by an optic sensor.

Table 2 – Cost comparative between different sensors for real time monitoring in STPs

Sensor	Brand	*Price (\$)	Description
Multiparameter probe - A	Hanna	\$1,491.64	Mobile device; Paramteres: pH, ORP, DO, EC, temperature, salinity; data transmission: cable (until 100 m without noisy interference).
Multiparameter probe - B	Boqu	\$1,447.67	Parameters: COD, TKN, total Phosphorus.
Multiparameter probe - C	Wtw	\$25,823.54	Parameters: COD,TOC, DOC, TSS.
Dissolved oxygen sensor - A	Boqu	\$1,000.00	DO measurement, Temperature range: 5-50 °C; power supply DC 24 V. Optical sensor.
Dissolved oxygen sensor - B	Boqu	\$999.00	DO range: 0-10 mg.L ⁻¹ , temperature: 0-45 °C; accuracy:± 3%; output RS 485 Modbus. Optic sensor

Sensor	Brand	*Price (\$)	Description
Nitrate sensor (UV)	Boqu	\$5,499.00	Nitrate-Nitrogen concentration range: 0.1-40.0 mg.L ⁻¹ ; Accuracy ±5%; repeatability: ±2%; output RS485 Modbus; life time: 2-3 years
Nitrate sensor (ion)	Boqu	\$929.00	Nitrate measurement range: 0.02-1000 mg.L ⁻¹ ; accuracy: 5%; cable length 5 meters; life time: 6 months.
Phosphorus real time analyzer	Boqu	\$6,399.00	Measurement range: 0-500 mg.L ⁻¹ ; measurement period: minimum of 30 minutes; sewage must be pumped into the analyzer, or a sample must be taken.
Optic Sensor TSS - A	Hach	\$4,587.67	TSS concentration; Range: 0-50 000 mg.L ⁻¹ .
Optic Sensor TSS - B	Boqu	\$1,999.00	TSS Range: 0-50 000 mg.L ⁻¹ ; suitable temperature : 5-60 °C. Output signal: 4-20 mA.
Optic Sensor TSS - C	Winmore	\$1,048.00	TSS Range: 0.01 - 250 000 mg.L ⁻¹ . Communication RS485 Modbus. Life time of 10 years. Suitable temperature: -5 °C to 40 °C. Self-cleaning. Bubble compensation algorithm.
Sludge blanket level	Hach	\$6,404.02	Ultrasonic sensor for measuring the sludge blanket level.

*quotes from different companies from 2021 and 2022

Most of the sensors presented a high-cost, however, TSS optic sensor from Winmore presented a lower cost compared to others TSS sensors. Despite the lower cost, the brand is not consolidated in the market as Hach or Hanna, for example, but the sensor could be a promising low-cost alternative to compete with the US sensor. The advantage for the US sensor is that the technology would be national, and Winmore is from China, thus, maintenance and communication from the US sensor would be facilitated in case of the use in Brazil.

It is relevant to notice that there was a wide variation of models for TSS determination, but most of the asked quotations did not receive a response. However, temperature compensation and bubbles compensation were two aspects that were on the sensors descriptions and will be evaluated on this work. Moreover, even the sensors with self-cleaning descriptive had the recommendation of weekly cleaning. The TSS optic sensor (A) was used for the comparison with the gravimetric test and the US sensor performances in two activated sludge systems that

will be detailed on chapter 8.

1.3.4 Real time monitoring of solids in STP

Several techniques can be used for real time solid concentration monitoring in a STP. Microwaves, ultrasonic sensors, electromagnetic probes, optic probes, image pattern, are some examples of non-destructive methods, that are important to maintain the biological system intact (PARRA *et al.*, 2018; ROCHER *et al.*, 2018; WEF - WATER ENVIRONMENT FEDERATION, 2019; NEVES *et al.*, 2021; BOURGEOIS; BURGESS; STUETZ, 2001).

Optic sensors are widely used for solids concentration evaluation. Parra *et al.* (2018) developed a low-cost turbidity sensor, that can differentiate sediment matter, and two species of algae: brown and green. However, scattering at high levels of solids concentration may greatly reduce the light signal received by optic sensors, increasing the error in the sensor measurement. Winata *et al.* (2019) conclude that in photo bioreactors the biomass algal control can be done in real time by image pattern technique. Furthermore, Rocher *et al.* (2018) developed an electromagnetic transducer composed by two coils and a microprocessor module, a low-cost system for solids monitoring in real time. Nevertheless, the presence of metals, even in low concentration could interfere on the sensor measurement for solid concentration.

For dewatering and thickening solids evaluation, WEF - WATER ENVIRONMENT FEDERATION (2019) reported the use of microwave “time-of-flight” flow-through devices to measure TS in the solid processing unit feed line, thickened solids outlet from thickeners, or dewatered cake; optical devices to measure TSS in filtrate/centrate/pressate; and microwave resonance devices to collect, convey, and measure cake solids moisture content (dry solids, or DS) in dewatered cake.

Ultrasonic sensors for real time monitoring of solids in STP are largely reported in the literature. In activated sludge system, Abda *et al.* (2009) developed a method using an ultrasonic transducer to predict the profile of the settling velocity in real time. Locatelli *et al.* (2015) reported settling velocities in secondary sedimentation tanks of activated sludge system, moreover the solids concentration of the top layer of the sludge blanket ($7800 - 8600 \text{ mg.L}^{-1}$) and the bottom layer ($30\ 030 - 33\ 100 \text{ mg.L}^{-1}$). More recently, Neves *et al.* (2021) reported a good linear correlation between the results from the gravimetric test and the attenuation measurement of the ultrasonic transducer in bench scale, in a range of 0-1% of TS. Moreover, in the same research, in a demo scale UASB reactor the linear correlation observed in the range of 0-1% of TS had an R^2 coefficient of 0.97 and accuracy of 0.1%. However, most of the data were obtained in the upper part of the reactor, 2.1 m from the ground, corresponding to a range of 0-0.2% of TS. Furthermore, Neves *et al.* (2021) points out that despite the control of solids in STP by means of an ultrasonic sensor is promising, the hydrodynamics of biological reactors may bring challenges to their implementation, requiring adjustment in the processing of the ultrasonic signal for a full-scale application.

Real time monitoring in STP is already a reality in many developed countries, but are usually quite expensive. Currently, many promising technologies for real time monitoring at a

low-cost are emerging. In developing countries the main concern in STPs is still the removal of organic matter, since universalization of sewage collection and treatment did not occur yet. However, most of the STPs still need to achieve a proper operational routine. Regarding that, the ultrasonic transducer that was used by Neves *et al.* (2021) showed that it can be a useful tool for the Brazilian reality with a national technical staff following its development.

1.4 Ultrasonic technology: fundamentals, development and application

The next sub-session will explore the fundamentals of this technology and how it was developed.

1.4.1 Physical principles of sound waves

The physical properties of sound are relevant to understand the variables that can interfere in the signal emitted by the ultrasonic transducer that is going to be used in this work.

Sound is the energy produced by the vibration of material bodies. For sound waves to propagate it is necessary a medium (solid, liquid or gaseous) which means that in a vacuum there is no sound. When sound waves propagate in a medium, they cause successive compression and rarefaction. The wavelength is given by the distance between two successive compression, while the frequency is given by the inverse of the wavelength. The human ear is capable perceiving sound in a frequency range between 20 and 20 000 Hz, although those values can vary from one individual to another. Frequency bands below 20 Hz are defined as infrasound, while bands above 20 000 Hz are defined as ultrasound waves. The intensity by which the wave is propagated is related to the energy transport capacity it has. The amplitude of the wave is one of the factors that can make it more intense, as well as the frequency. High frequencies and amplitudes are capable of transmitting a greater amount of energy, therefore require more power per unit area to be produced. On the other hand, a bigger distance from the source carry out in a smaller intensity of the sound for the observer (BORGES; RODRIGUES, 2017).

The velocity of sound depends on the characteristics of the medium in which it propagates, such as density, structural organization and rigidity (CHEEKE, 2002). Depending on these characteristics, the sound waves can propagate in different ways, which can be observed by surface wave velocity, longitudinal wave velocity, transverse wave velocity and flexion wave velocity (BOLLER; CHANG; FUJINO, 2009).

According to Morais *et al.* (2017), more than one type of wave propagation can occur simultaneously in the same material, resulting in different velocities for each one. Ultrasonic techniques can provide these different forms of propagation, in order to draw conclusions about the structure of the target material. However, in liquids and gases, the transverse waves, the flexion waves and the surface waves are very weak due to the low stiffness and shear of the medium in these physical states (CHEEKE, 2002)

A sound wave, when impacted an object, can cause three different phenomena: reflection, diffraction and refraction. Reflected sound waves, when target an object returns totally or

partially to the original means of propagation. When the reflected wave returns to the source in a period less than 0.1 seconds, there is the specific phenomenon of reverberation, which acts as a reinforcement of the sound. The refraction occurs due to the change of medium propagation, hence, is possible that the direction, velocity and wavelength changes as well. The frequency, however, remains the same. Usually, part of the wave is reflected and another part is absorbed, depending on the type of material on which the wave is impacting. Smooth substances tend to reflect better (eg. glass), while porous substances tend to absorb / refract better.

Another important characteristic of the sound wave is its diffraction capacity, that is the ability to circumvent obstacles and extremities. The degree of diffraction is greater the greater is the wavelength of the sound wave emitted and lesser, the smaller the width of the object to be circumvented by the wave (BORGES; RODRIGUES, 2017).

1.4.2 Techniques and applications with ultrasound

Ultrasonic sensors have different uses. According to Wade (2000) some uses for ultrasound are: speed of a submarine determination, measuring the flow rate of a liquid, motion detection, catalyst in chemical reaction, investigation of the viscosity of materials, investigation into living cells, locating schools of fish, and for counting and sorting items in an assembly line.

The sinking of Titanic in 1912 due to an unseen iceberg which promote the death of 1517 people, was a big motivator for the developing of ultrasound systems to ensure a more secure navigation (WADE, 2000). More recently, in the medicine field, ultrasonic techniques are used to promote non-invasive methods for abdominal, cardiac, maternity, gynecological, urological and cerebrovascular examination, breast examination, and small pieces of tissue as well as in pediatric and surgical operational review (CAROVAC; SMAJLOVIC; JUNUZOVIC, 2011). For the sanitation sector, the most relevant applications are the possibility of determining the particle size of solids, water and sludge blanket level, concentration of solids, sedimentation velocity, detection of fractures in water and sewage pipes, flow rate of a liquid, cell lysis and more recently acoustic fields for the selection of particles in water (POWLES *et al.*, 2018; PÉTRIER, 2015; KANDEMIR *et al.*, 2020; ABDA *et al.*, 2009; BAMBERGER; GREENWOOD, 2004). Martin (2012), also reports that ultrasonic waves, through the surface waves known as creeping, can be used to identify internal or external corrosion of a structure. This can be quite useful in sewage treatment technologies that uses anaerobic digestion and are susceptible to this kind of adversity.

Ultrasound measurements have been applied to characterize solids, liquids and gases for over 60 years. Ultrasonic sensors can provide information in real time and work through compact, robust and low-cost systems (BAMBERGER; GREENWOOD, 2004).

Several ultrasound techniques have been developed over the years. The A-scan visualization is a technique derived from the echo pulse technique. It is capable of receiving and interpreting the arrival of longitudinal and transverse waves, in order to allow the inference of defects in the analyzed structure, such as cracks, geometry of target objects, size and location. Over the years, it was possible to improve the technique, making it possible to obtain two-dimensional (B-scan and D-scan) and three-dimensional (C-scan and S-scan) ultrasonic images (MARTIN,

2012; CHEEKE, 2002).

The B-scan and C-scan resulted from an improvement in the pulse-echo technique, which resulted in the technique known as ToFD (Time of Flight Diffraction). In this technique the interpretation of the travel time occurs not only by the reflected waves, as in the pulse-echo, but also by waves originating from diffraction (MORAIS *et al.*, 2017).

The development of computing since the 1970s and the drop in the cost of piezoelectric electronic components, enabled the emergence of a third ultrasonic technique, called Phased Array. This technique consists on the additional use of a guided wave, that is, a parallel wave with low potential to suffer attenuation. Phased Array function can be described as the automation of multiple ultrasonic heads, so that the angles of attack and flight of the ultrasonic waves can be determined by means of an algorithm. This technique allows high-resolution B-scans and C-scans, from larger areas and in a short time. However, despite this technique has been commercially available since the beginning of the 21st century, acquisition and operational costs are still very high, compared to the echo-pulse technique and ToFD (OLYMPUS, 2007 apud MORAIS, 2017).

From the 1990s with the consolidation of the guided wave technique a new type of ultrasonic transducer was created, no longer piezoelectric, but capable of causing excitation of sound waves by means of electromagnetic force. These were called electromagnetic acoustic transducers. They are capable of generating longitudinal, transverse and surface waves, but the great advantage over piezoelectric transducers is the absence of contact between the surface of the transducer and the inspected surface, which allows the inspection of surfaces with high temperatures (MORAIS *et al.*, 2017; OLYMPUS, 2007; HIRAO; OGI, 2003).

1.4.3 Intrinsic and external variables for the attenuation coefficient

In ultrasonic tests, the attenuation occurs due to the loss of sound energy. The main factor for that loss is through absorption (i.e. conversion of sound energy into thermal energy) by the suspended solids and through scattering that they provoke. The attenuation coefficient α_T indicates the level of attenuation, and depends mainly on the frequency of the signal and the characteristics of the media through which that the signal is getting through (STAKUTIS *et al.*, 1955; ZHANG *et al.*, 2021). In theory, it can be calculated according to the equation 1.1 presented by Stakutis *et al.* (1955):

$$I = I_o \cdot e^{-2 \cdot \pi \cdot x \cdot \alpha} \quad (1.1)$$

Where I is the final intensity and I_o the initial intensity of the beam in parallel planes x m apart. α_T can also be determined by the sum: $\alpha_T = \alpha_P + \alpha_F$, where α_P is the attenuation coefficient of the solids particles' and α_F is the attenuation coefficient of the fluid medium. Attenuation can also be determined by the sum of absorption coefficient and scattering coefficient (BOUDA; LEBAILI; BENCHALA, 2002). Zhang *et al.* (2021) reported that the greater the frequency of ultrasonic signal the greater the attenuation coefficient. Despite high attenuation coefficient

provide a lower superior limit for suspended particles' detection, small variations in solids particles's concentration can be easier detected.

There are several aspects that can interfere on the ultrasonic signal. Some of them are intrinsic to the sound source, such as frequency and amplitude. However, there are external aspects that may interfere on such measurements. This work will approach four aspects: temperature, bubbles, solids concentration and different types of solids. These topics will be discussed in further chapters.

Table 3 shows different velocity and attenuation coefficient for different media. As the media density decreases, the media increases its capacity to attenuate the ultrasonic signal, considering the same source frequency. In STPs the presence of fat and bubbles could be quite big, which can cause a greater attenuation than predicted by an ultrasonic sensor, for example. Nevertheless, Treeby *et al.* (2009) reported that the influence of temperature on ultrasonic attenuation depends on the frequency range, which may also be applied for other variables such as bubbles, density and different type of solids. Moreover, the elevated coefficient attenuation of air, shown in Table 3 indicates that the presence of air bubbles can greatly contribute for the attenuation of the signal.

Table 3 – Velocity, attenuation coefficient and frequencies of ultrasound waves for different fluids

Sample	Velocity (m.s ⁻¹)	Density (g.L ⁻¹)	Attenuation coefficient (dB.m ⁻¹)	Frequency (MHz)	Reference
Distilled water	1483	997	0.87-7,82	2.1	(MCCLEMENTS; FAIRLEY, 1991)
Water	1483	1000	0.20 *	1.0	(ITIS FOUNDATION, 2021) (ALPEN, 1998)
Fat	1440	900	63.00	1.0	(ALPEN, 1998) (ITIS FOUNDATION, 2021)
Olive Oil	1464	917	46.90	2.1	(MCCLEMENTS; FAIRLEY, 1991)
Air	343	1.3	1200	1.0	(ITIS FOUNDATION, 2021) (ALPEN, 1998)

*water indicates a quadratic frequency depending on attenuation

Errors greater than 20% were observed due to diffraction in ultrasonic attenuation methods. However, Error Diffraction Correction (EDC) can be applied in pulse-echo techniques, hence the method could have a greater accuracy (JONATHAN *et al.*, 1995). Diffraction correction

should be done especially in small transducers that use low frequencies, since diffraction will occur greatly as wavelength is bigger than the obstacle that sound wave is going through.

2 OBJECTIVES

2.1 *General objectives*

Evaluate the application of the US sensor as a real time monitoring tool for solids control in full-scale aerobic and anaerobic STPs.

2.2 *Specific objectives*

- Evaluate intrinsic and external variables that can interfere on the US sensor signal.
- Determine the sludge blanket level with the US sensor.
- Evaluate the US sensor performance in full-scale activated sludge system reactor compared to the gravimetric test and a commercial optic sensor.
- Evaluate the application of the US sensor position in the lateral part of a full-scale UASB reactor.

3 INSTRUMENTATION AND DATA TREATMENT FOR THE SIGNAL

3.1 Introduction

Echo-pulse technique needs, in summary, three items: a transducer, a device to amplify and filter the analog signal and a device to convert the analog signal into digital so it can be treated. Transducer is a device which converts one form of energy to another form. Electrical, mechanical, chemical, kinetic and thermal energy are some example of energy forms. A piezo-electric transducer, specifically converts electric energy into mechanic energy (such as ultrasonic waves) and vice versa in a specific resonance frequency. A proper piezoelectric material for transmitting and/or receiving the ultrasonic wave includes stability, piezoelectric properties, and the strength of the material (SHUNG; ZIPPURO, 1996).

Amplifier has an essential function for echo-pulse analysis, because it can provide high amplifications gain, thus a better visualization of the signal. However, it is also necessary to filter the signal, since noise must be avoided (SANCHEZ *et al.*, 2012).

Two devices for data collection by the US sensor are a microcontroller and an oscilloscope. Microcontrollers can be defined as a system that can control features and actions of a device (RAFIQUZZAMAN, 2011). They have both hardware and software components (GRIDLING; WEISS, 2006). Microcontrollers can be found in process control systems, medical devices, automobile engine control systems, remote control systems, industrial instrumentation devices, voltmeter, office equipment, electronic appliances and power tools (GÜVEN *et al.*, 2017). Most of these devices and products are automatically controlled, have dedicated input devices and tiny LED/LCD display outputs. They are used mostly because of the low-energetic consumption and because they are programmable and reusable. The most known microcontroller is Arduino, which is a open source hardware and software enterprise. Unlike most microcontrollers Arduino is an inexpensive platform and is used for innumerable application (KONDAVEETI *et al.*, 2021).

An oscilloscope is a basic tool for measuring electrical quantities, as well as studying all types of waveforms. Generally, measurement of a quantity is regarding peak voltage, frequency, phase difference, pulse width and delay time (PANDIN, 2021).

On this work, data collection occur with both Arduino and oscilloscope. The difference between both is related to data collection duration and data treatment. Oscilloscope can provide a more malleable data, since it gives the raw signal that can be treated in different ways. Nevertheless, data is not continuously generated. Arduino, on the other hand, can provide a continuously data, however it must follow a pre-determinate routine for data treatment, thus is not possible to add new routines for its treatment.

3.2 Methodology

3.2.1 Configuration of the system

Since most of the data produced was used with the same instrumentation, this chapter characterizes the main compounds of the setup used for the signal analysis and explains how the sensor works and how it was tested.

For the solids measurement in real time it was used an ultrasonic sensor that can measure the attenuation and the velocity of the signal. The sensor can be described as a single piezoelectric ultrasonic transducer, that can be used either as an emitter and a receiver of the signal. The transducer (\varnothing 50 mm) was attached to a hollow PVC tube (\varnothing 55 mm). The tube contained a parallel reflection surface made of glass at a distance face-to-face of 25 cm from the transducer. A picture of the sensor can be seen in Figure 2.

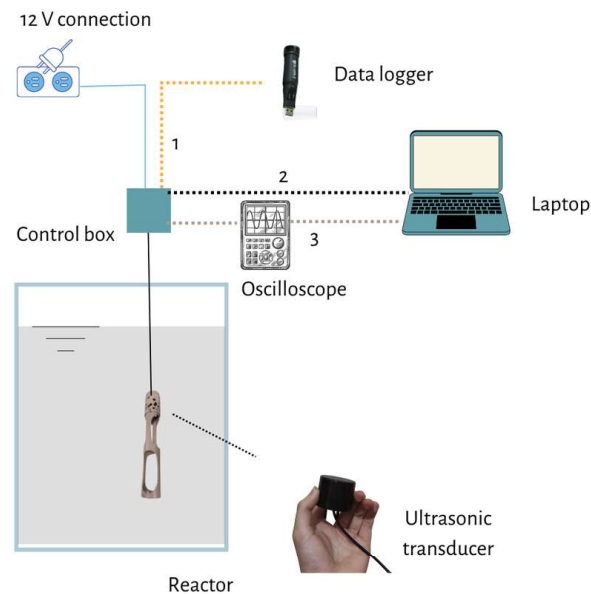
Figure 2 – US sensor



For the data collection of the signal two different configurations were used, one from an oscilloscope and the other from an Arduino Nano. The transducer was connected to a homemade control box (design to receive 12 V), which has the objective of filter and amplify the incoming signals in the frequency of 200 kHz. The control box also contained an Arduino Nano that was responsible to provide the data in real time. One output of the control box was connected to the laptop via USB to store the data from the Arduino by using the software Realterm. For the oscilloscope reading it was used two probes connected from the oscilloscope on the pin gates of the control box's board. The oscilloscope was connected to the laptop via USB. For the oscilloscope reading it was used the software picoscope. The power was supplied only by the laptop via USB connection or either the laptop and a 12 V plug connection to continuous current circuit system. Both forms were adopted because the amplification level of the signal was over ranged in the oscilloscope, thus it was used only the laptop power until the amplification level was adjusted by a potentiometer reduction. A scheme of the configuration's system for data

collection can be seen on Figure 3.

Figure 3 – Different instrumentation of the US sensor for data collection. 1 - Data generated by Arduino and stored by a data logger (no laptop is needed); 2 - Data generated by Arduino and stored by the software Realterm; 3 - Data generated by oscilloscope and treated on MATLAB



Instrumentation of the US sensor data collection

This setup will be used for the determination of the variables that can interfere on the US sensor signal and on full-scale tests that will be further detailed. On this chapter, the sensor was submerged on still water for a better understanding of its basics functioning.

3.2.2 Signal treatment

The transducer functions as either an emitter and receiver of the signal. The emitted signal reflects into a reflection surface back to the transducer, which correspond to the first reflection peak. A second reflection was observed in bench scale tests. Depending on the media characteristic, signal attenuation may occur. The oscilloscope operates in alternating current mode (AC) and generates 1 out of 500 images for further treatment.

3.2.3 Second reflection peak evaluation

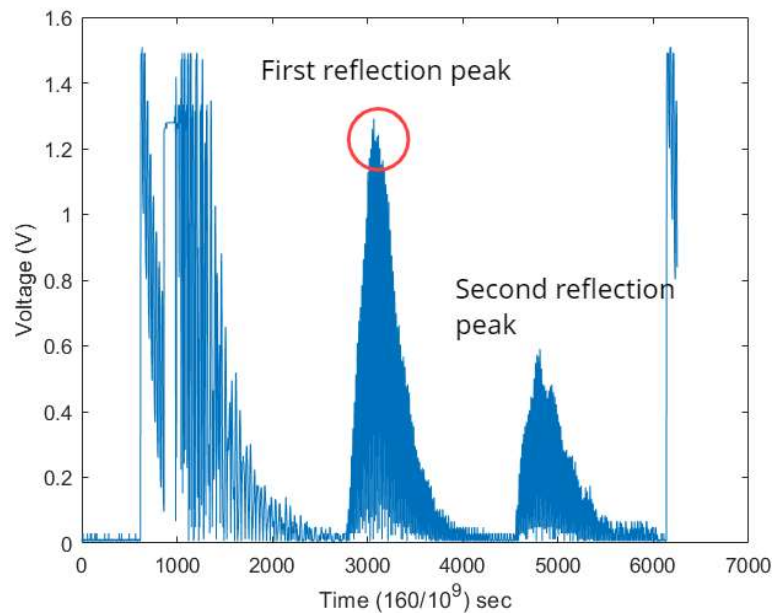
In order to evaluate the second reflection peak generated by the US sensor, the signal between the reflection surface and the setup walls was blocked with the author's hands .

3.3 Results and discussion

3.3.1 Data treatment

Since the potential signal follows a senoid distribution, with positive and negative values, the module of the signal was used for a better treatment in MATLAB (Figure 4). For the oscilloscope data, attenuation was measured according to the maximum potential of the first reflection peak. The routine elaborated in MATLAB consists in an average of 500 images of the maximum potential observed on the first reflection peak. For the Arduino data it was calculated the correspondent area of the first reflection peak, since the Arduino routine could not change during the experiments, otherwise the obtained data would not be comparable.

Figure 4 – Visualization of the module of the signal for still water and peak locations



3.3.2 Power supply

There were three forms to provide power to the US system. Power source only from the laptop, only from a 12 V connection to a plug and from both. While the power from the laptop (5 V) may be more unstable and provide a lower power signal, the power provided from the laptop and the plug together (5 V+12 V) assures better stability for the signal. It is important to notice that depending on the power supply configuration the signal will have a different peak value, as seen in Figure 5, Figure 6 and Figure 7. In the figures the signal from all configurations were taken at 19.2 °C with the sensor in still water.

Figure 5 – Signal visualization for still water with the power supply source from a USB connection to a laptop (5 V)

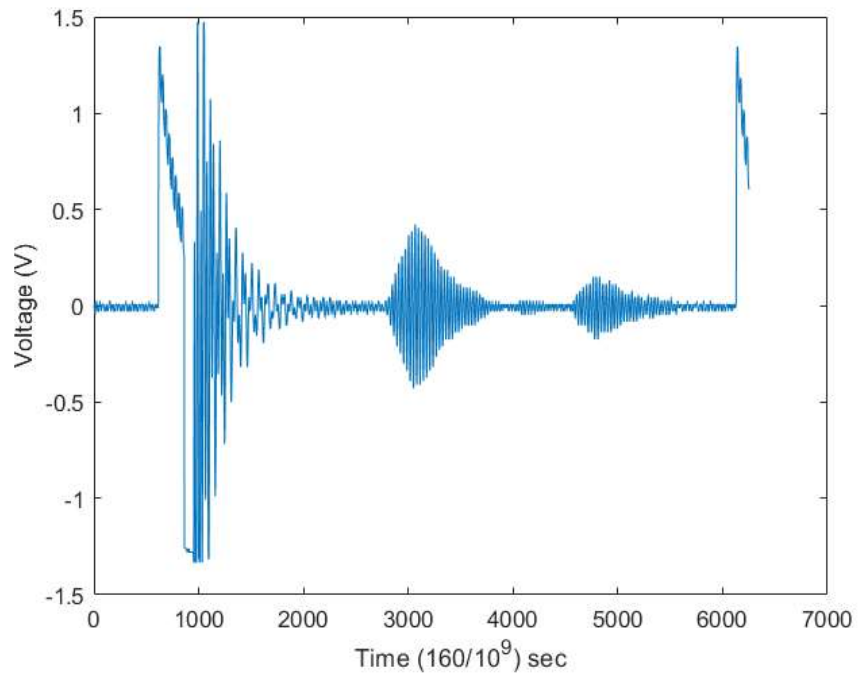


Figure 6 – Signal visualization for still water with the power supply source from a 12 V plug connection

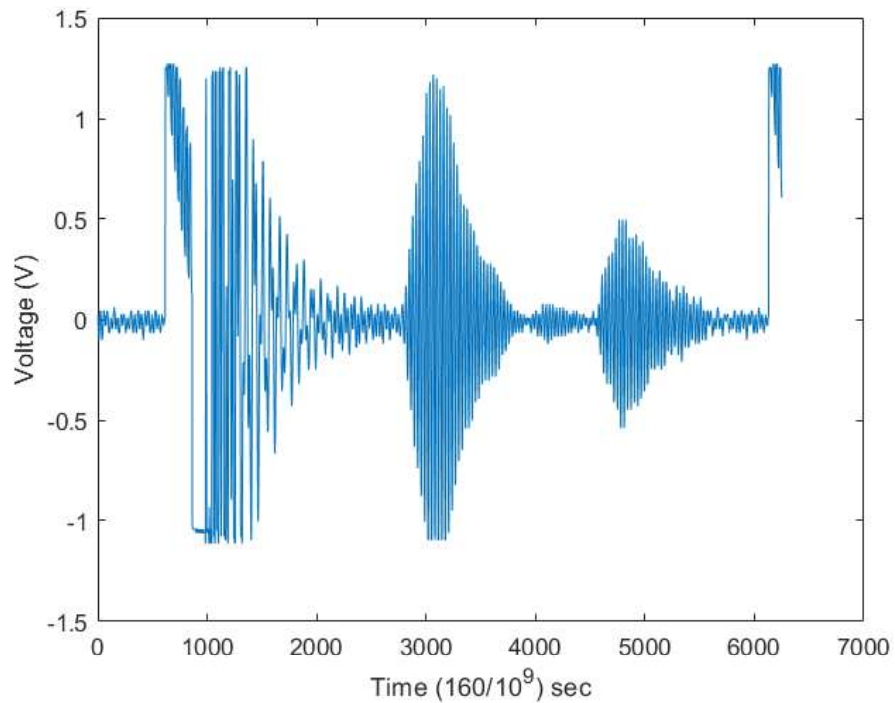
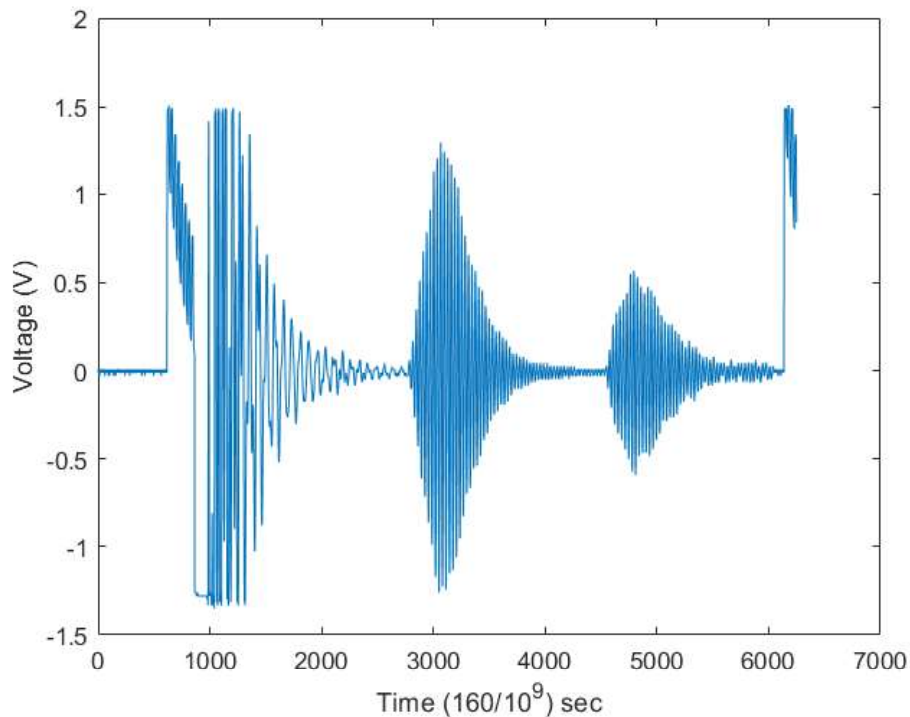


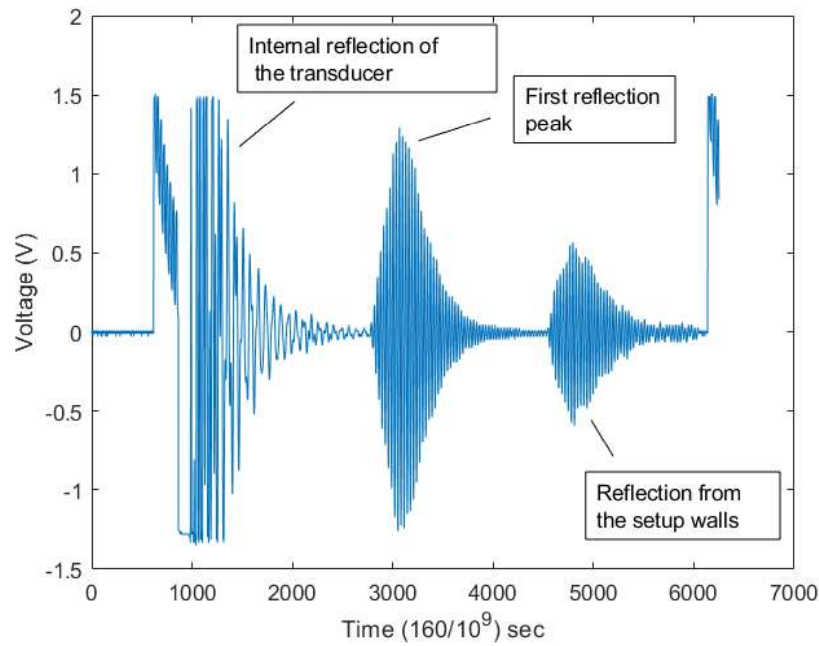
Figure 7 – Signal visualization for still water with the power supply source from a USB connection to a laptop and a 12 V plug connection



3.3.3 Internal reflection from the setup

When the author's hand was placed in between the reflection surface and the setup walls, the second peak immediately responded with complete attenuation. However, the first peak remained intact. This short experiment clarifies that the second peak is originated from setup walls reflections. Furthermore, the interference that the setup walls may play into the first peak is not completely understood, since sound waves propagates in every direction. It is known, however, that either a constructive or destructive interference on the first peak may occur depending on the reflections conditions and distances from the wall. To guarantee no interference at all on the first peak, there must be no reflection surface in a 25 cm ratio, since that is the distance from the transducer to the reflection surface. Its is relevant to notice that in bench scale such conditions are very difficult to be avoided due to the small setups available.

The interpretation of the signal peaks obtained by the oscilloscope considering the sensor submerge in still water in bench scale, can be seen in Figure 8

Figure 8 – Signal visualization of still water on MATLAB

Signal visualization for water on MATLAB

3.4 Conclusion

MATLAB treatment routine of the oscilloscope data was developed considering the module of signal. For both Arduino and oscilloscope data collection, power supply greatly influence the data. For application in STP, 12 V plug connection without a USB connection is recommended. The first peak may suffer interference from internal reflections of the setup walls in small setups. Considering that in bench is very difficult to avoid those situations, every result should be critic analyzed considering these possibilities.

4 ECHO RESPONSE TIME APPLICATION

4.1 *Mechanical adjustment for the signal amplification*

4.1.1 Introduction

Amplification level of the signal can variate according to electrical or mechanical adjustments. For electrical adjustment, a potentiometer can be used to increase or decrease the resistance in the circuit, thus change the amplification level (greater or lower values for the voltage detected by the sensor). This item will evaluate the possible mechanical adjustment.

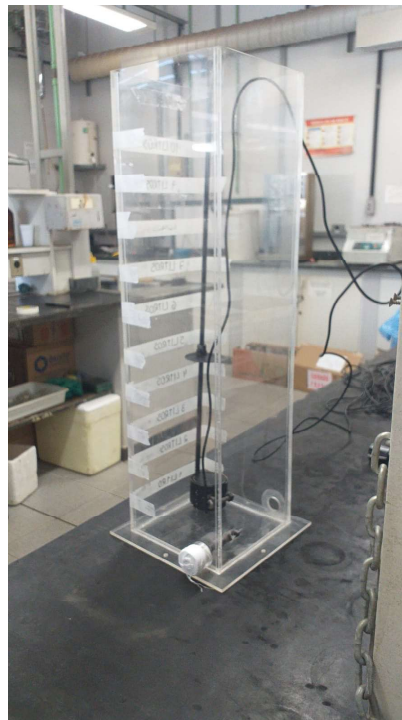
Attenuation increases or decreases depending on the course made by the emitted signal (STAKUTIS *et al.*, 1955). Greater distances means the energy loss during the signal course will be greater as well. For that reason attenuation coefficient it is written as $\text{dB}\cdot\text{m}^{-1}$. Using this principle, it is possible to increase or decrease the amplification of the signal by changing the distance between the reflection surface and the transducer.

4.1.2 Methodology

In order to evaluate the attenuation for different distances between the transducer and the reflections surface, it was build a specific support for the US sensor (Figure 9). The support contained a metal reflection surface that can be fixed in different heights compared to the position of the transducer. The tests were performed in the physico-chemical laboratory of UFMG, in the city of Belo Horizonte (Brazil). The control box used in that test did not have an Arduino, thus the oscilloscope was the only way to retrieve the data from the sensor. The power supply of the system was a laptop, connected to it with a USB connection. This setup was arranged because in Brazil the control box did not posses an output for 12 V plug connection.

The US sensor was placed inside an acrylic reactor with dimensions of 14.4 cm x 14.4 cm x 44.5 cm (Figure 10). 10 liters of distilled water was added to the system. The minimum distance of the reflection surface from the transducer was evaluated considering that the reflection peak does not cause overlays with the internal reflection peak.

The distance was adjusted outside the reactor and for each new adjusted distance the sensor was placed inside the reactor again. After 10 minutes the sample from an oscilloscope was taken and 300 images were saved and analyzed in the software MATLAB, as described in chapter 3. A home made routine in MATLAB calculated the maximum potential of the reflection peak and the ERT (Echo response time).

Figure 9 – Transducer case for different distances from the reflection surface**Figure 10 – Setup used for different distances from the reflection surface**

It was tested the hypothesis whether the coefficients from day 1 and day 2 were significantly different from each other or not, so repeatability of the data can be evaluated. Gao *et al.* (2008) pointed that parametric and non-parametric variance analysis (F-Test and Mann Whitney) can produce reliable results with a “n” superior to 15. Therefore, F-test was performed in order to compare repeatability of the measurements evaluating the slope coefficient.

H0sMP: The slope coefficient from day 1 and day 2 for the linear regression of maximum potential x distance are not significantly different for a confidence level of 99%.

HAsMP: The slope coefficient from day 1 and day 2 for the linear regression of maximum potential x distance are significantly different for a confidence level of 99%.

H0sRT: The slope coefficient from day 1 and day 2 for the linear regression of ERT x distance are not significantly different for a confidence level of 99%.

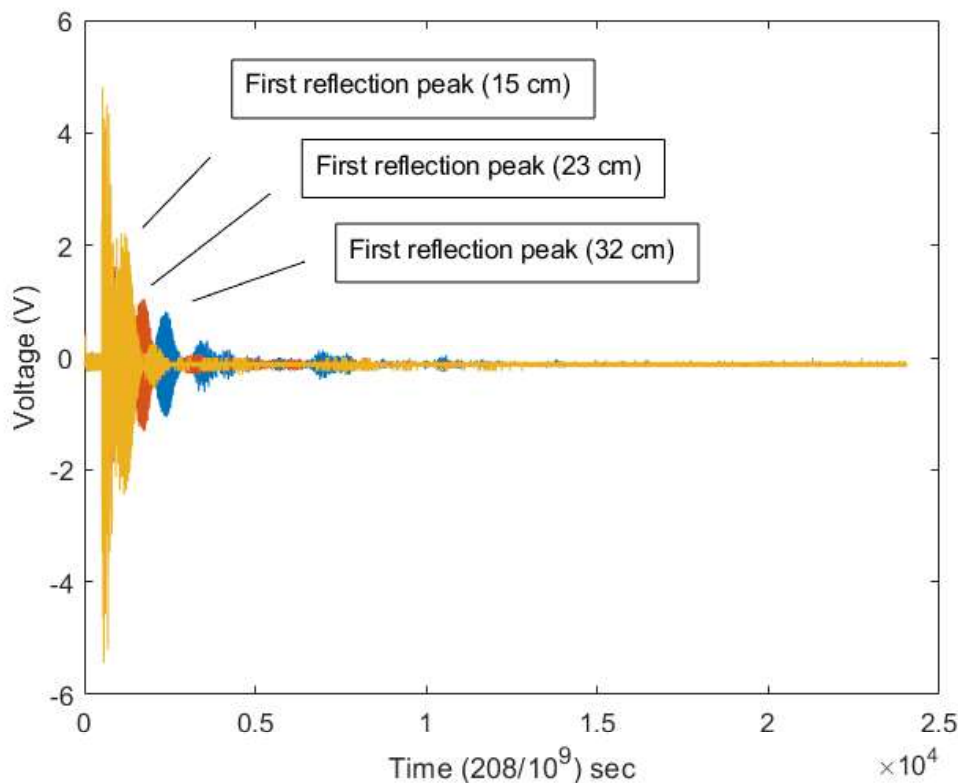
HAsRT: The slope coefficient from day 1 and day 2 for the linear regression of ERT x distance are significantly different for a confidence level of 99%.

For the statistical analysis it was used the software STATGRAPHICS 19 for the comparison of the coefficients from the linear regression.

4.1.3 Results and discussion

The visualization of the signal for different distances between the reflection surface and the transducer can be seen on Figure 11. If the distance between the transducer and the reflection surface is too small, it will happen an overlay of signals. Internal reflection from the transducer will interfere in the first reflection peak as shown in the yellow signal of the figure. It was found that a safe distance to avoid the overlay is 23 cm.

Figure 11 – Visualization of the signal in MATLAB for 15 cm distance (yellow), 23 cm (orange) and 32 cm (blue) from the reflection surface to the transducer.



The results obtained from the linear regression for either the maximum potential and the ERT (Figure 12, Figure 13 and Figure 14) provide important information regarding a wider application of the US sensor. The graphics correspondent to ERT were not in the same figure because the points overlay each other. Moreover, the starting values from x and y-axis were adjusted to improve the visualization of the linear regression and the data tendency. One important aspect is that distance variation between the transducer and the reflection surface carry out in a

linear variation of the maximum potential and ERT in a range between 22 cm and 34 cm. Despite greater distances decreases the amplification level, it can provide to the operational system a more representative data, covering a higher area of influence. Therefore, mechanical adjustment can be used to regulate the distance between the transducer and the reflection surface in order to adjust not only amplification level but the representative of the measurements.

Figure 12 – Echo response time (ERT) for different distances between the reflection surface and the transducer (day 1)

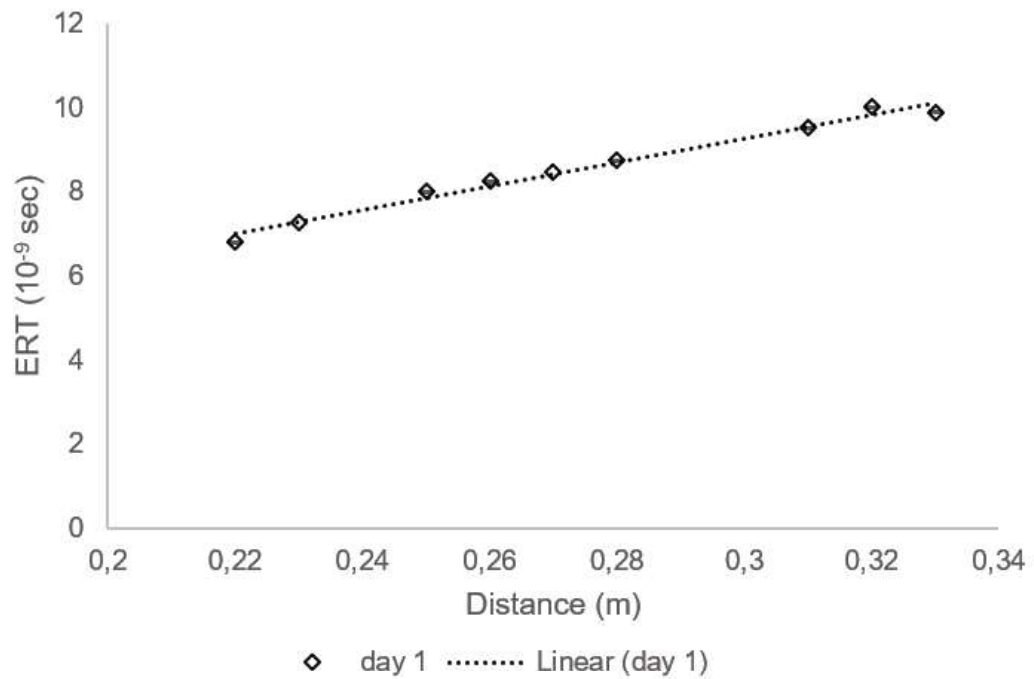


Figure 13 – Echo response time (ERT) for different distances between the reflection surface and the transducer (day 2)

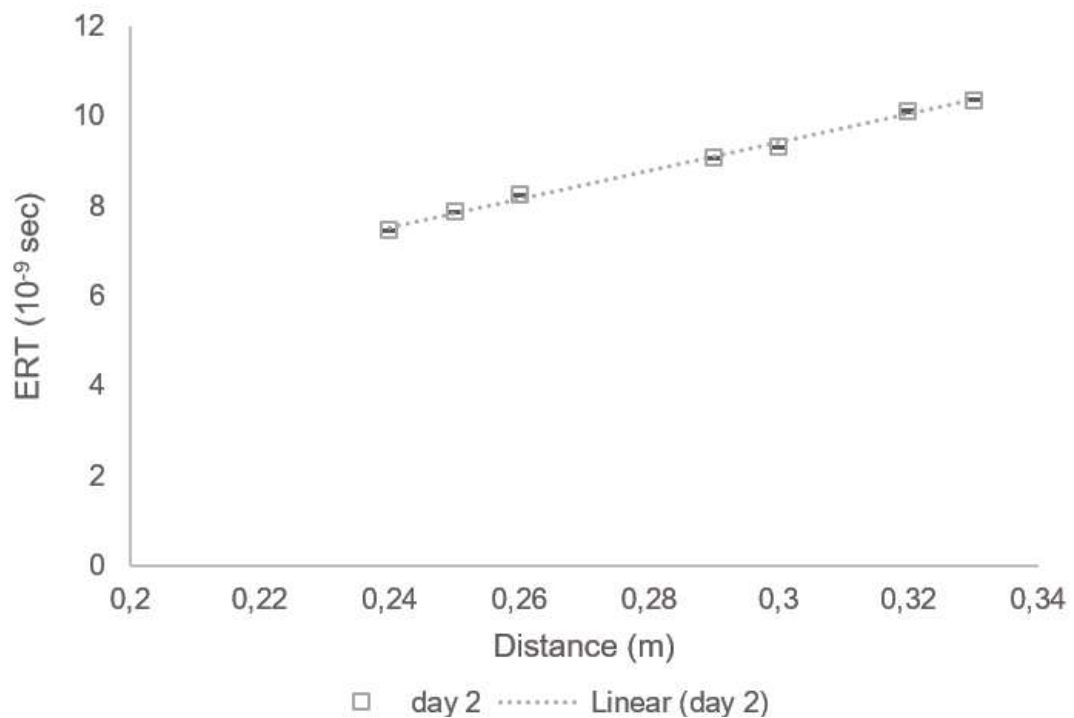
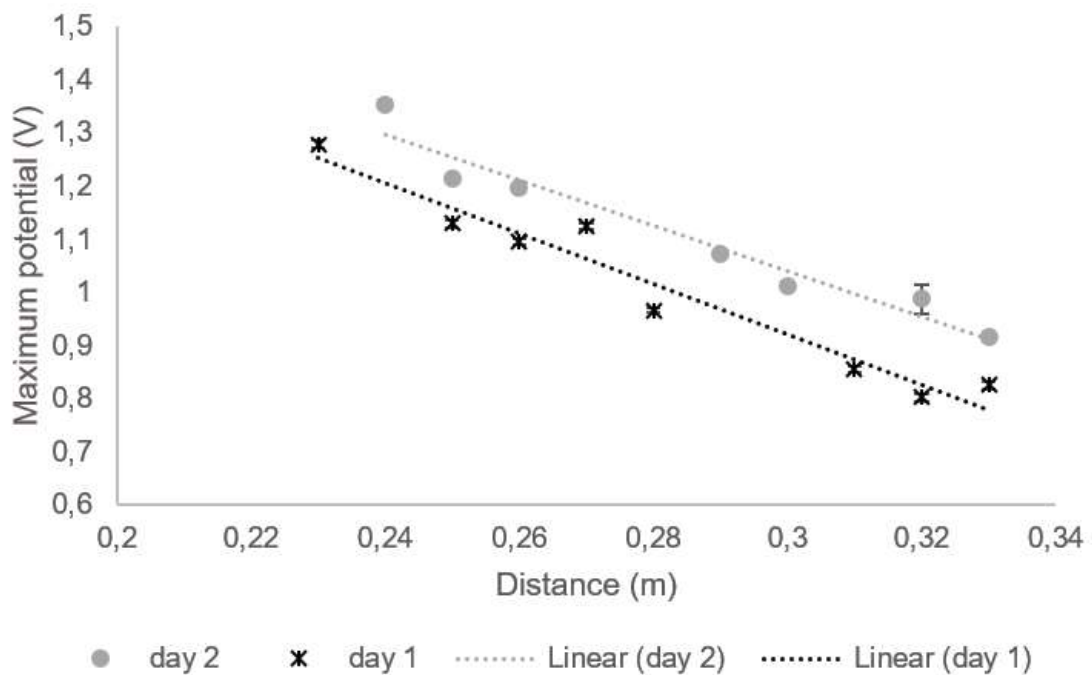


Figure 14 – Correlation between the maximum potential reflection peak and the distance of the reflection surface to the transducer for day 1 and day 2



A second aspect, is that different ERT for each distance may indicate that the US sensor is also capable to estimate the distance between a reflection surface from the transducer. This can be calculated knowing the *in loco* velocity of sound in the fluid, which will depend on

the temperature, and the time of the signal trajectory until the first reflected signal back to the transducer. The bases of the routine used for this is experiment will be used for the sludge blanket level measurements in section 4.2.

Results obtained from Table 4 showed a high R^2 (coefficient of determination) value for either maximum potential x distance and ERT x distance. All the linear regression also presented a low RMSE, which indicate a good accuracy of the data. A summary of the hypothesis test regarding the repeatability of the experiment can be seen on Table 5. The hypothesis had the null hypothesis regarding the slope coefficients were not rejected by a confidence level of 99%, with p-value superior to 0.12. The results indicate that distance estimation and maximum potential prediction from distance between the reflection surface and the transducer are repeatable and precise to be performed by the US sensor.

Table 4 – Linear regression coefficients for time response and maximum potential (day 1 and day 2)

Regression	Slope	Intercepts	N	R^2	RMSE
ERT (day 1)	28.4518	0.7453	300	0.9965	14.80
ERT (day 2)	31.4845	-0.0150	300	0.9836	31.89
Maximum potential (day 1)	-4.264	2.32	300	0.9486	0.04
Maximum potential (day2)	-4.733	2.34	300	0.9474	0.04

Table 5 – Hypothesis tests summary for the linear regression ERT x distance and maximum potential x distance

Hypothesis	Mean square	F-ratio	P-value	Decision	Conclusion
H0sMP/ HAsMP	0.3302	216.17	0.4528	Do not reject H0sMP	The slope coefficient from day 1 and day 2 for the linear regression of maximum potential x distance are not significantly different for a confidence level of 99%
H0sRT/ HAsRT	0.0316	2.00	0.1830	Do not reject H0sRT	The slope coefficient from day 1 and day 2 for the linear regression of ERT x distance are not significantly different for a confidence level of 99%

4.1.4 Conclusion

ERT can be used to predict distances from the transducer and the reflection surface in a range of 22 cm to 34 cm. For the same range, maximum potential also showed linear dependence to the distance variations. A minimum distance of 23 cm between the transducer and the reflection surface is recommended to be use in order to optimize the maximum potential and avoid overlays into the first reflection peak.

4.2 Sludge blanket level detection

4.2.1 Introduction

Sludge blanket depth are an important parameter to evaluate the performance of the clarifier (primary or secondary). The variations on the sludge blanket in a STP (clarifier) with a consistent operation are usually low (0.3 - 0.6 m). An abrupt change in the blanket level may be caused by an increased amount in the influent flow rate or a malfunction in the sludge withdrawal system (WEF, 2005).

In primary clarifiers, sludge blanket depth is one of the main parameters that triggers initiation of sludge withdrawal. In secondary clarifiers, this parameter can be influenced by a number of activated sludge system performance changes, and its fluctuations over time provide critical information for the overall health of the activated sludge system. Therefore, sludge blanket depth is one of the most frequently monitored parameters in wastewater treatment plants (WEF, 2005, p.601) .

The measurement of the blanket level can be done manually or automatic. In UASB reactors, to maintain anaerobic conditions, the reactor must operate closed. In that way, manual measurements of the blanket level it is not recommended, but are not critical, since by monitoring the solids content in the digestion compartment it is already an appropriate operation routine. Manual measurement is the most common measurement in full-scale activated sludge systems. To check the blanket level the operator usually use a clear plastic tube (core sampler) until the bottom of the settler tank. After removing it, solids will be adhered at the tube until a certain level which will give the operator the blanket level measurement. Manual measurement of the blanket is cheap, easy to operate and is recommended especially for small STP (WEF, 2005).

On the other hand, the automated sludge blanket level measurement are recommended for medium and large STP. Dakers (1985) found that sludge volume could be reduced by approximately 50% if automated sludge blanket control is used instead of manual clarifier desludging. Automatic control could provide a more efficient system to remove the excess sludge, hence generate the sludge production reduction. Many other authors reported about the benefits of using automatic sludge measurement (WEF, 2005).

Optic and ultrasonic sensors are the most used systems for automatic blanket level detection, but they still have a high cost. Both ultrasonic and optic sensors have a similar accuracy ($\pm 1\%$) and range (between 1 m and 11 m) (WEF, 2005). More recently, Schewerda, Förster and Heinrichmeier (2014) reported good approximation from the manual measurements in a full-scale plant (secondary clarifier) by using a low-cost technique based on the different pressure on the sludge zone and the clean water zone. The same authors also pointed that ultrasonic sensor failed several times and the pressure technique fitted better with the manual measurement.

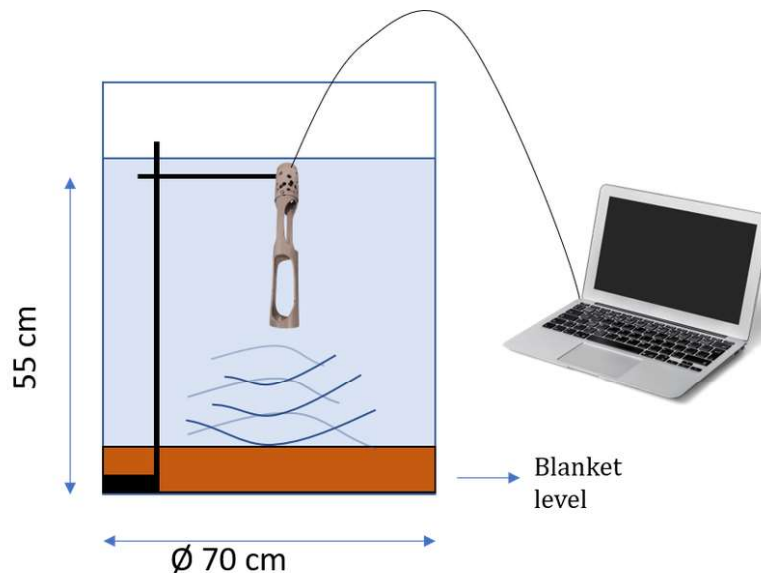
WEF (2005) pointed that the ultrasonic sensor use for the blanket level measurement works better when the sludge present good settleability. A sludge with bulking or floating issue compromise the reading of the sensor, since this type of sludge does not have a well-defined echo. In that case, optic sensor, despite the higher cost, are recommended.

4.2.2 Methodology

In order to evaluate a wider use of the low-cost ultrasonic sensor from this research, it was evaluated the measurement of the blanket level in the laboratory located in the WAC in Leeuwarden. The frequency used by the already commercial ultrasonic sensors are unknown, however the high prices indicate that it is probably used a higher frequency compared to the US sensor (200 kHz).

For the test it was used a plastic bucket, and the sensor was fixed in a position at 55 cm from the bottom (Figure 15). The bucket was filled with water, and the peak position was saved to serve as a parameter for the different sludge blanket measurements. To have such measurements it was added sludge from the recirculation line of the activated sludge system of Leeuwarden, which has an average concentration of 1.0 % of TSS. Temperature was measured inside the bucket as well, since it may affect the peak's position.

Figure 15 – Setup for the sludge blanket level measurement



One hour after the sludge was added to the system, when it was already settled at the bottom, the signal from the sensor was saved and treated on MATLAB. The blanket level was estimated according to the equation obtained in section 4.1 (Figure 13).

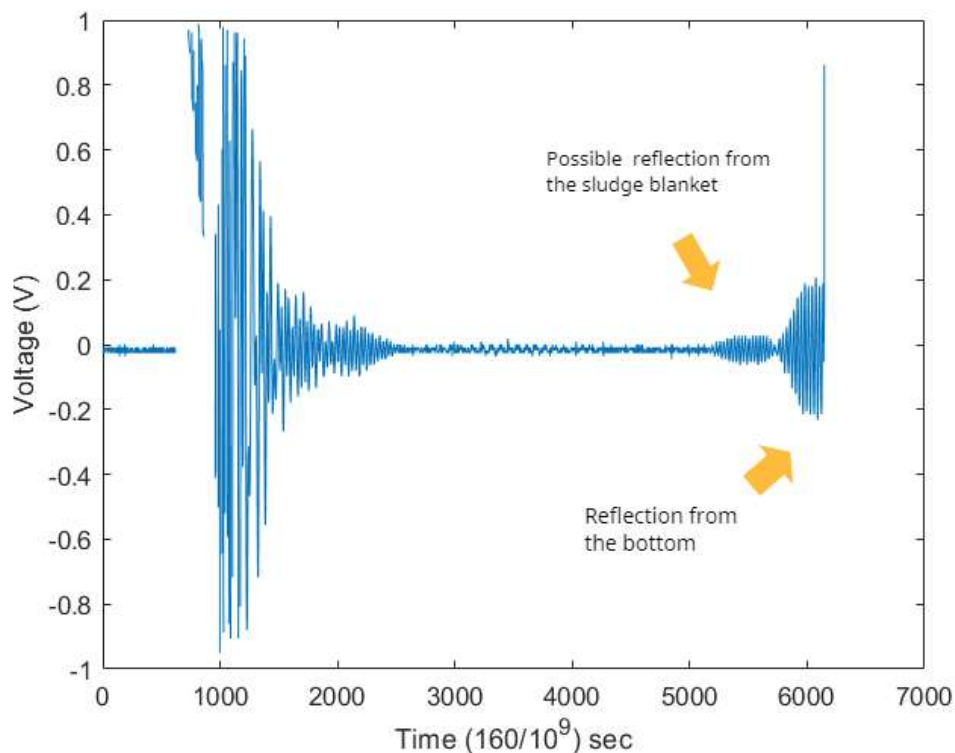
4.2.3 Results and discussion

The estimation by the US sensor for the blanket level detection did not occur as expected (Table 6). The results did not correspond to the resolution of 0.03 m present in WEF (2005). Temperature measured were in the same range, except for water (blanket level equal to 0.00 m), thus it is probably not a reason to explain the difference on the manual and estimated measurements.

Table 6 – Blanket level estimation by the US sensor

Temperature (°C)	Manual blanket measurement (m)	Blanket level estimation by the US sensor (m)
14.6	0.00	0.00
18.2	0.05	0.03
18.0	0.06	0.05
18.3	0.07	0.03
18.6	0.08	0.07
19.2	0.10	0.05

It is important to notice that the reflection peak in between the initial peak and the reflection from the bottom of the bucket only appeared after the position of the sensor was adjusted inside the bucket. Depending on the sensor position (but maintaining the height level) only its reflection from the bottom appears. Probably the regions that has bubbles adhered into the sludge blanket carry out in the earlier reflection compared to the bottom (Figure 16).

Figure 16 – Reflections of the signal for a sludge blanket of 10 cm

It is relevant to notice that the range tested for the sludge blanket level were between 0.05 and 0.10 m of height. A wider range is recommended for further tests, considering that typical variations on the blanket level are between 0.3-0.6 m (WEF, 2005). For a better precision of the sensor, probably a higher frequency must be used for the transducer, which means a higher cost

for the sensor. Moreover, the real necessity of investigating a low-cost US sensor for the sludge blanket detection should be better evaluated, considering the efforts necessary, the limitations (frequently cleaning routine) and the presence of others low-cost alternatives such as pressure technique reported by Schewerda, Förster and Heinrichmeier (2014).

4.2.4 Conclusion

Sludge blanket level determination in real time is an effective way of controlling the sludge from clarifiers of primary and secondary sedimentation tanks. However, the US sensor did not shown a positive correlation with the manual test, although it was only tested for the range between 0.05 and 0.10 m. The results are still inconclusive, but if a higher precision is necessary, probably the sensor will need to use a higher frequency which will carry out in a higher cost for the sensor. In that case, testing the US sensor with a wider range and expecting a lower accuracy may be a better option for further tests.

5 TEMPERATURE EFFECT ON THE ULTRASONIC SIGNAL

5.1 Introduction

Temperature is a parameter that is usually relevant for most applications regarding sensors. For the analysis of the signal from the ultrasonic sensor, two aspects are relevant to evaluate, velocity of sound and the attenuation of the signal.

Sound propagation velocity depends on the characteristics of the medium in which it is being propagated, such as density, structural organization and rigidity (CHEEKE, 2002). Depending on these characteristics, the sound waves can propagate with different velocities. In water, main component of sewage, one of the factors that can interfere on the velocity of sound is temperature due to the shift of the viscosity (BOLLER; CHANG; FUJINO, 2009).

Several studies reported the dependence of temperature and ultrasonic attenuation, mainly for medical application in bones or tissues (TECHAVIPOO *et al.*, 2004; CUCCARO *et al.*, 2015). In sanitation application, temperature dependence on attenuation may be very relevant. In Brazil the amplitude of sewage temperature can be above 10 °C. For example, in the city of Curitiba (Paraná-Brazil) during one year of monitoring, it registered a minimum temperature in the effluent of 14.8 °C, while the maximum was 23.8 °C, (PAULA, 2019). In Teresina (Piau -Brazil) the temperature registered on the influent of the current STP was a minimum of 30.0 °C and a maximum of 34.5 °C (MARÇAL; SILVA, 2017). In the Netherlands, the temperature in the mixed liquor variates more according to the seasons. During this research within the STP of Grou and Leeuwarden, temperature of the mixed liquor had variate gradually from 9 °C to 22 °C during the months of March, April, and May of 2022. Due to the household heating system of the water, the minimum temperature rarely reach values below 8°C, even in the winter, according to one of the operators from Rioolwaterzuiveringsinstallatie (RWZI - ‘‘STP’’) Grou (The Netherlands) .

This chapter has as objective to evaluate the temperature influence on the signal treatment generated by an ultrasonic transducer. In order to achieve this objective is necessary that the sensor can also measure temperature, which is possible by calculating the velocity of sound. Depending on the range of temperature Lubbers and Graaf (1998) recommend different coefficient to be used for the estimation of temperature. For the range of 15-35 °C in water they recommend the equation 5.1:

$$c = 1404.3 + 4.7T - 0.04T^2 \quad (5.1)$$

where, c is the velocity of sound and T the temperature of water.

5.2 Methodology

5.2.1 Setup

Temperature analysis was evaluated inside of the WAC laboratory, located in the city of Leeuwarden (Netherlands). The US sensor was used according to the set showed on Figure 2.

Only the oscilloscope data was evaluated. The US sensor was fixed inside a warm bath with recirculation of water. The recirculation increases the homogeneity distribution of temperature inside the warm bath, to simulate a dynamic system and, therefore, a more representative system.

An external temperature sensor was placed inside a warm bath (accuracy of 1 °C) and it was double-checked with the warm bath its self temperature measurements. The range of temperature evaluated was 21.7-35.0 °C. Lower temperature was not evaluated because 21.7 °C was the minimum temperature of the water in the laboratory. The test was repeated in two different days (day 1 and day 2) to evaluate its repeatability.

5.2.2 Data collection and signal treatment

For each selected temperature a sample was taken containing 500 images of the signal by the software picoscope, the resolution of the images were set in 1 V AC (alternate current). Samples were collected after the temperature was stabilized. Further details of the instrumentation can be found on chapter 3.

The generated files were treated with a homemade routine in MATLAB, that evaluate two aspects of the signal. Firstly, it was determined the ERT, which indicate an estimation of the velocity of sound (equation 5.2).

$$velocity = \frac{distance}{time} \quad (5.2)$$

Since the ultrasonic signal goes to the reflection surface and get back to transducer, the distance considered was 25 cm x 2. Time was measured considering the location of the reflection peak for the maximum value of the signal measured by the oscilloscope. Secondly the maximum potential response from the US sensor was evaluated for temperatures from 21.7 °C to 35.0 °C.

5.2.3 Oscilloscope resolution selection

It was evaluated the sound velocity measurements by the oscilloscope with a resolution of 1 V (higher detail level) and 2 V. (lower detail level). The tests considered the measurements obtained in day 1. The objective aimed to evaluate if a lower resolution could be used for the velocity determination. While the resolution of 2 V allow the visualization of all signal, resolution of 1 V allows only the visualization of the first reflection peak, considering the adopted signal amplification level.

5.2.4 Statistical analysis

A linear regression was made correlating temperature and the signal maximum potential median. For each temperature a sample of the signal (500 images) was saved and the mean value of each sample was the output for this variable. In that way, temperature was the independent variable and the maximum potential the dependent variable.

For the temperature estimation by the sound velocity, a comparison was made between the estimated temperature by a linear regression and the estimated temperature considering equation 5.1.

- **Normality of the data**

To evaluate the normality of data a routine in MATLAB execute a code for Shapiro-Wilk or Shapiro-Francia test, depending on the sample being Leptokurtic ($kurtosis > 0$) or Platykurtic ($kurtosis < 0$). The Shapiro-Wilk and Shapiro-Francia null hypothesis is: “the sample is normal with unspecified mean and variance.” While the alternative hypothesis indicate that the sample do not have a normal distribution (BENSAÏDA, 2009). The test was applied with a significance level of 5%. The result of this test will be presented in this section, since the normality of the data is a necessary information in order to choose a proper statistical test (parametric or non-parametric) for further analysis.

The null hypothesis of normal distribution for the data of attenuation and temperature estimation were both rejected for a significance level of 5%. Hence, a non-parametric hypothesis test was used.

- **Confidence level of the data**

To evaluate if there is significant difference between the attenuation for different temperatures, the medians of the maximum potential from each sample (500 images) were compared, considering the corresponding temperature. The hypothesis for this test are:

- 1) H_0 : Maximum potential signal median is not significantly different for different temperatures for confident level of 99%.
- 2) H_A : Maximum potential signal median is significantly different for different temperatures for confident level of 99%.

Since the data is not normally distributed and the samples are independent, Kruskal-Wallis hypothesis test was applied on MATLAB. For day 1, it was compared the amplitude of the signal for 7 different temperatures. For day 2, the comparison was for 7 different temperatures.

- **Repeatability**

To evaluate the repeatability of the experiment a statistical hypothesis test was performed (F-test). First evaluating the slope of both linear regression for day 1 and day 2, and secondly for the interception coefficient.

Attenuation analysis

- 1) H_{SA0} : Linear regression slope of day 1 and day 2 for the signal maximum potential x temperature are not significantly different for confident level of 95%

- 2) H_{SA} : Linear regression slope of day 1 and day 2 for the signal maximum potential x temperature are significantly different for confident level of 95%
- 3) H_{IA_0} : Linear regression interception coefficient from day 1 and day 2 for the signal maximum potential are not significantly different for confident level of 95%.
- 4) H_{IA} : Linear regression interception coefficient from day 1 and day 2 for the signal maximum potential are significantly different for confident level of 95%.

The statistical hypothesis were performed by the software STATGRAPHICS 19.

5.3 Results and discussion

5.3.1 Oscilloscope resolution selection

The medians readings from the oscilloscope showed a considerable difference for the sound velocity calculation at the temperature of 26.4 °C and 35.3 °C when using alternating current (AC) with a resolution of 1 V or 2 V for day 1 (Figure 17 and Figure 18). Besides the median values, the variability of the data is noticeable greater for the set resolution of 2 V, which can be observed by the greater amplitude of the interquartis box-plot. Hence, the set resolution of 1 V, because it shows a linear correlation with the median velocity of sound x temperature without outliers, was the configuration adopted for temperature analysis.

Figure 17 – Variability of the sound velocity detected by the US sensor - resolution of 2 V - day 1

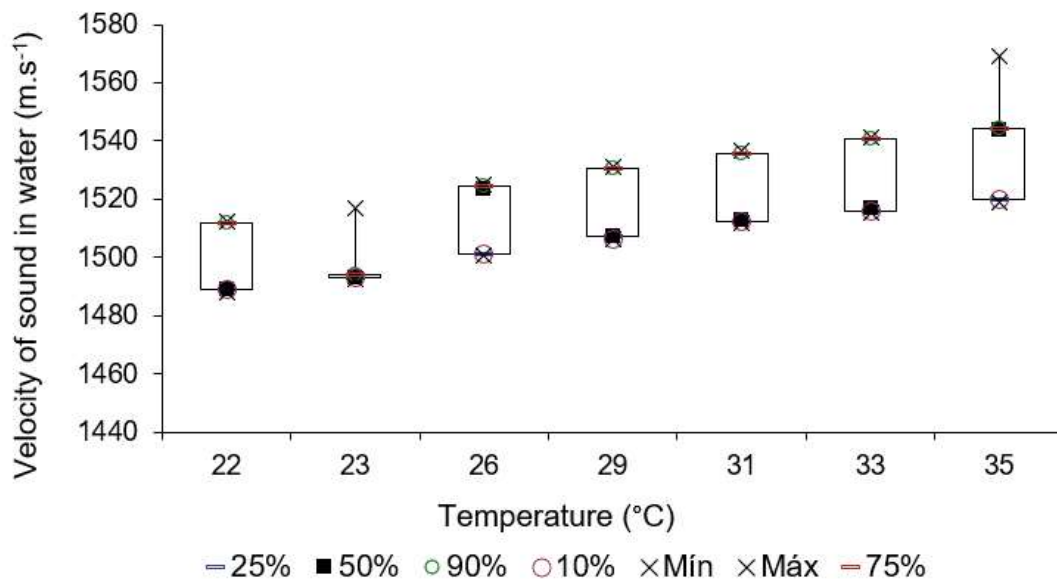
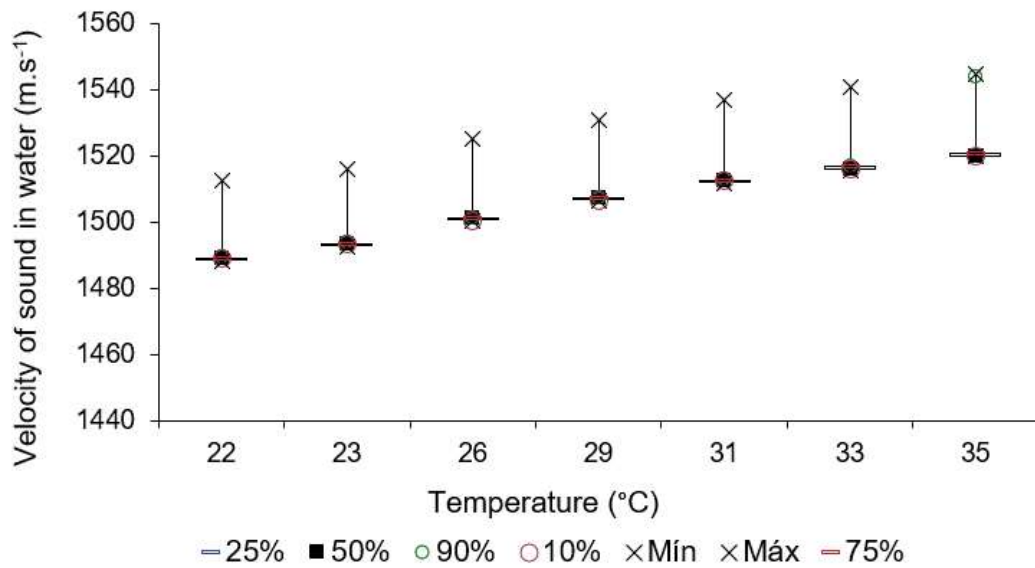


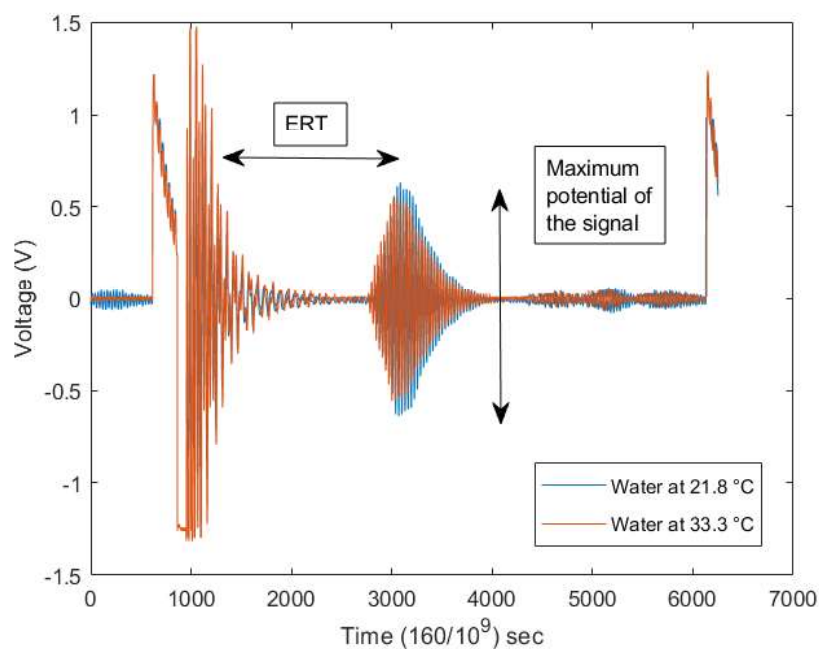
Figure 18 – Variability of the sound velocity detected by the US sensor - resolution of 1 V - day 1



5.3.2 Temperature estimation by ERT

Temperature effect on attenuation and sound velocity can be visually seen by the oscilloscope image in Figure 19. The difference between the signal at 21.8 °C and 33.3 °C can be seen either for signal (maximum potential) amplitude and the ERT because of the sound velocity shift.

Figure 19 – Raw signal obtained from the oscilloscope at a temperature of 21.7 °C and 34.9 °C



ERT values were used for sound velocity calculation. The equation obtained from the linear regression generated from the sound velocity x temperature (day 2) measured in day 2 carry out in an equation to estimate temperature. The results obtained from Table 7 show that the model predicted by Lubbers and Graaf (1998) had a more reliable output, comparing to the linear regression output, although both had a good match comparing with the measured temperature in the range of 23.7-35.0 °C. Considering the oscilloscope data collection, variation of temperature could be auto corrected during the application of the sensor. However, two aspects still need a better investigation: effect of temperature when the US sensor is placed in sewage (not water) and the development of an Arduino routine for the continuously correction of temperature influences.

Table 7 – Temperature estimation by sound velocity (day2)

Measured temp. (°C)	Temp. estimation in °C (linear regression)	Temp. estimation in °C (LUBBERS; GRAAF, 1998)	Standard Error (linear regression)	Standard Error (LUBBERS; GRAAF, 1998)	ERT (160.10 ⁹ seconds)	Sound velocity in water (m.s ⁻¹)
21.7	21.2	21.9	2.4	1.0	3087	1488.1
23.4	23.0	23.4	1.6	0.1	3081	1492.5
25.1	25.5	25.6	1.7	0.58	3073	1498.3
26.3	26.5	26.4	0.6	0.4	3070	1500.5
28.4	28.7	28.5	0.9	0.2	3063	1505.7
31.1	31.5	31.4	1.3	0.8	3054	1512.4
33.2	33.1	33.1	0.3	0.2	3049	1516.1
34.9	34.7	35.0	0.5	0.4	3044	1519.9
			$\Sigma = 9.3$	$\Sigma = 4.9$		

5.3.3 Temperature effect on attenuation

Figure 20 shown the variability of the signal for different temperature in day 2, the variability occurred similarly in day 1 (Figure 21). From the box-plot it seems that temperature variations considering 500 images for each temperature, was similar in both days.

Figure 20 – Temperature effect on attenuation - data distribution (day 2)

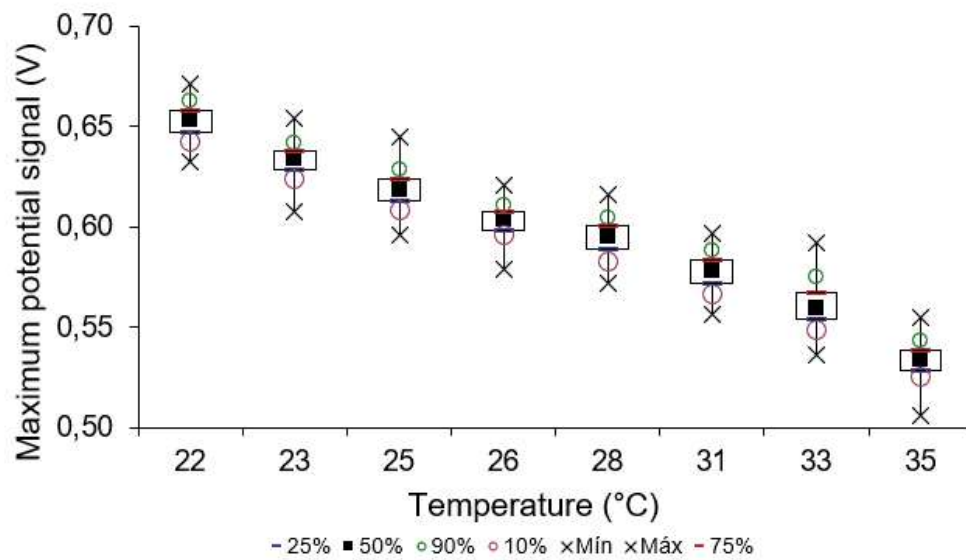
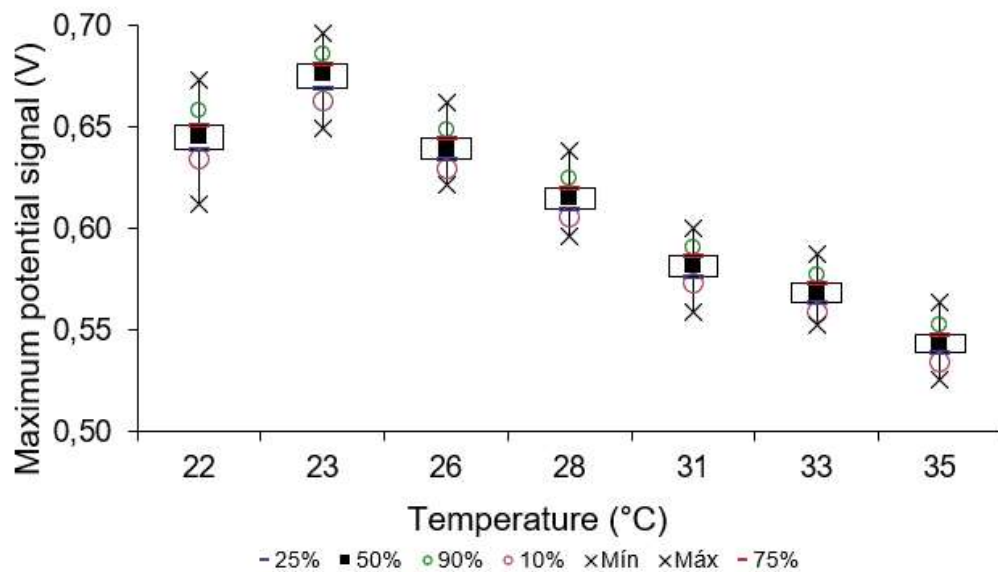


Figure 21 – Temperature effect on attenuation - data distribution (day 1)



The results obtained from the linear regression analysis for the maximum potential x temperature (Figure 22 and Figure 23) show that all observed measurement were within a confidence level of 95% for the estimated value of y. The residual distribution can be seen in both Figures, and indicates that the linearity principle of the residuals was attended.

Figure 22 – Maximum potential x temperature (day 1) - linear regression and residuals

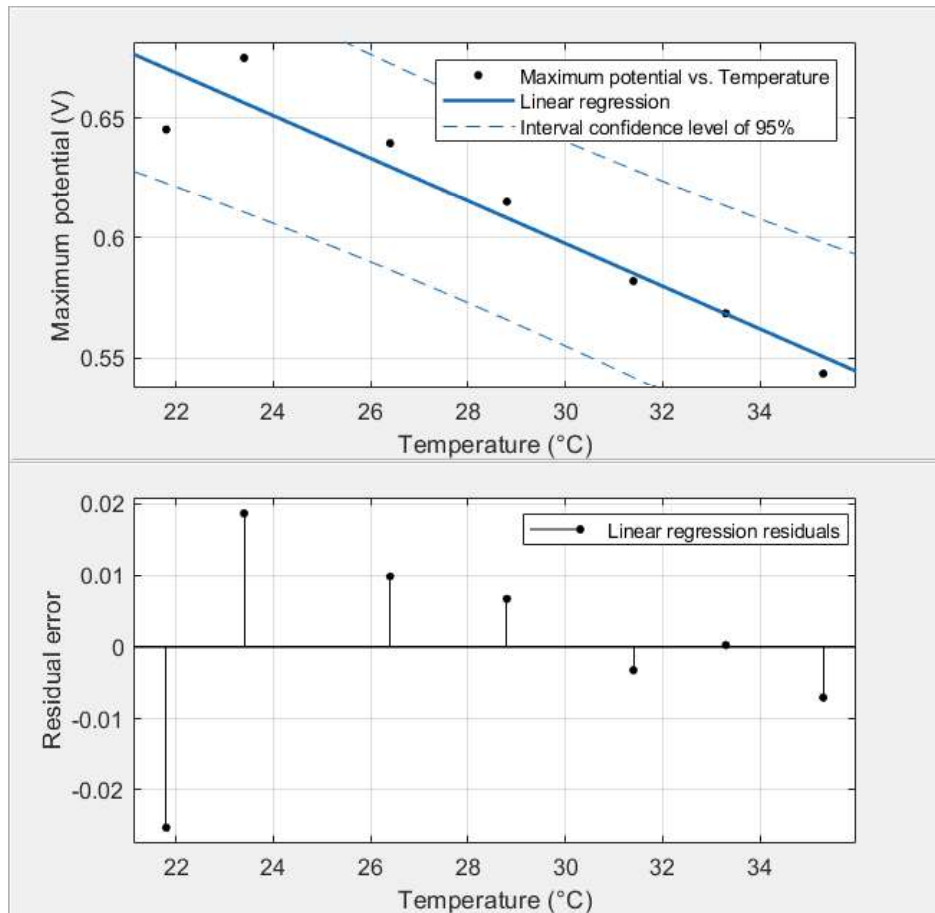
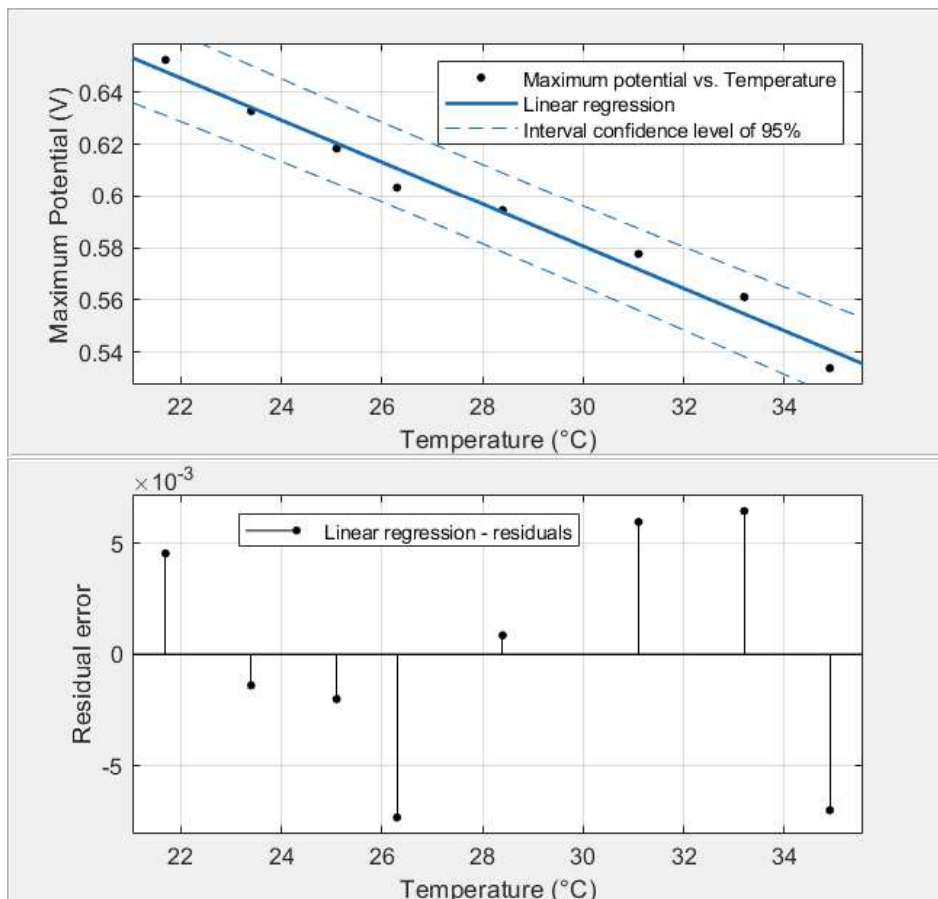


Figure 23 – Maximum potential x temperature (day 2) - linear regression and residuals



The R^2 from day 1 and day 2 show that most of the data can be explained by the linear regression model, and the low value of the RMSE, confirms a good fit of the model (Table 8).

Table 8 – Linear regression - Amplitude of the signal x Temperature

Day	SSE	R-Square	DFE	Adjust R-square	RMSE
1	0.0012	0.9103	5	0.8923	0.0154
2	0.0002	0.9802	6	0.9769	0.0059

The results from kruskal-Wallis and Dun test (Table 9) indicate that there is a significant difference between the potential detected by the sensor in different temperature for a confidence level of 99% in day 2 and day 1. This result reinforces that temperature have a significant effect on attenuation.

Table 9 – Kruskal-Wallis ANOVA table (MATLAB) - Difference of the signal amplitude for different temperatures

Day	Number of groups compared	chi-square	p-value	Decision	Conclusion
1	7	3125	<0.001	Reject H_0	Maximum potential signal median is significantly different for different temperaturesfor confident level of 99%
2	8	3820	<0.001	Reject H_0	Maximum potential signal median is significantly different for different temperaturesfor confident level of 99%

Despite attenuation x temperature was proven to be correlated,a multi linear correlation it is recommended to be tested. For example, considering TSS, bubbles and temperature as variables of the regression. For that, the variables must not be auto correlated (VON-SPERLING; VERBYLA; OLIVEIRA, 2020). Therefore, further test should evaluate temperature in real application, considering other variables.

5.3.4 Repeatability

The results presented on Table 10 show that HSA_0 cannot be rejected, with a p-value of 0.5917. Hence, there is no significantly difference from the linear regression of day 1 and day 2, considering the attenuation variation due to temperature swift. These results show that the attenuation is proportional in two different independent tests, therefore an indication of

measurements repeatability. However, more tests are necessary for a more conclusive result about repeatability.

Table 10 – F-test for attenuation and temperature estimation (linear regression analysis)

Hypothesis	Mean square	F-Ratio	p-value	Decision	Conclusion
$H_{S A_0} / H_{S A_A}$	0.00004	0.31	0.5917	Do not reject $H_{S A_0}$	Linear regression slope of day 1 and day 2 for the signal maximum potential x temperature are not significantly different for confident level of 95%
$H_{I A_0} / H_{I A_A}$	0.00126	9.80	0.0096	Reject $H_{I A_0}$	Linear regression interception coefficient from day 1 and day 2 for the signal maximum potential are not significantly different for confident level of 95%.

5.4 Conclusion

The results indicate that it is possible to predict the attenuation due to temperature and to estimate the temperature as well, following Lubbers and Graaf (1998) equation. Furthermore, these predictions can support a more precise estimation of solids concentration by attenuation, since the swift of temperature can greatly affect attenuation, which was the parameter used to estimate solids concentration on this work. Although MATLAB routine for ERT was successful for sound velocity calculation, the routine have to be adapted and tested with an Arduino system, so it can be applied in full-scale reactors. Visual analysis indicate a repeatability of the tests, however, more samples should be analyzed statistically in order to confirm its repeatability. Further tests should evaluate temperature in real application, considering other variables and its possible auto correlation.

6 AIR BUBBLE EFFECT ON THE ULTRASONIC SIGNAL

6.1 Introduction

The influence of air bubbles in attenuation was already reported by several researches (BHASKARAN, 2014; RAVEAU, 2016; HAN *et al.*, 2020). Han *et al.* (2020) found out the attenuation of bubbles were smaller at ultrasonic frequency between 50 kHz and 100 kHz, and greater in the frequency below 40 kHz and above 100 kHz. The same research also reported the influence of the size on attenuation, and found out that larger bubbles contribute to greater attenuation. Besides bubbles size, it influences with different air flow was rarely discussed at the frequency of 200 kHz. The presence of air bubbles influence the attenuation signal measured by the transducer, because air has a high attenuation coefficient (ALPEN, 1998).

This chapter has the objective of evaluating the response of the ultrasonic signal for different air flows in water and sludge.

6.2 Methodology

6.2.1 Setup

To evaluate how the air bubbles may influence the signal attenuation for water and sludge measurements a setup was built in Water Application Center, located in the city of Leeuwarden (Netherlands). The setup was a reactor made of glass, of 120 cm of height, and internal diameter of 9.92 cm. The reactor contained a drainage tube with a control valve to drain the sludge outside the reactor after the test was completed. For the bubbles supply a tube of pressurized air was used, and connected to a manual air flow meter, which was attached to a spherical diffuser made of stone, inside the reactor. The pressure of the air could be controlled by a regulation valve and the flow meter had a range of 0.19-1.62 L.m⁻².min⁻¹. The reactor also contained an external layer for temperature control. The image of the setup can be seen in Figure 24.

Figure 24 – Vertical reactor with air bubble diffusion

Bubbles effect were evaluated in three scenarios. In the first scenario 4 liter of water was placed inside the reactor and the air flow varying from $0.19 \text{ L.m}^{-2}.\text{min}^{-1}$ to $1.62 \text{ L.m}^{-2}.\text{min}^{-1}$ at $22 \text{ }^\circ\text{C}$. Second scenario contained 4 liters of sludge with a concentration of 0.3% of TS varying to $0.19\text{-}0.71 \text{ L.m}^{-2}.\text{min}^{-1}$ at $22 \text{ }^\circ\text{C}$. The third scenario kept the air flow constant at $0.58 \text{ L.m}^{-2}.\text{min}^{-1}$ as the sludge concentration varied from 0.11% to 0.57% of TS. The sludge used was obtained from the anaerobic digester of the STP of Leeuwarden, and the different concentration was obtained through a dilution serial.

6.2.2 Signal treatment and sample collection

Before each signal reading there was a time interval of 10 minutes so that the signal could be stabilized. The data of the sensor was obtained in two ways. Firstly, through an Arduino that calculated the area of a specific region on the reflection peak (Y). The average of the area calculated in the interval of 10 minutes was the final output indicator of the sensor for this sample. The second way was through a MATLAB routine that calculated the average of 500 images of the reflection peak of interest in a specific region. The images were collected two times, first one on the beginning of Arduino collection time, and the second one after the 10 minutes.

In order to calibrate the sensor reading with the solids concentration present inside the reactor, the gravimetric test was performed in duplicate, before and after 10 minutes of data collection by the Arduino. The samples were obtained through a beaker at the same height where the upper part of the sensor was located.

6.3 Results and discussion

When the bubbles were attached to the transducer (Figure 25), which was located against the ascendant bubble flux, the signal was completely attenuated. That probably explain why NEVES (2020) reported that the signal was completely gone in some occasions in the demo scale UASB reactor, that contained a certain quantity of biogas bubbles. In that case, after swinging the sensor the signal appeared again. In that sense, if the sensor is perpendicular to the flux, it is unlikely that the bubbles will be attached to the sensor surface.

Figure 25 – Bubbles attached to the ultrasonic transducer surface



The results obtained on Figure 26 and Figure 27 showed that the attenuation increased together with the air flow. The main reason for that is because air has a high attenuation coefficient (ALPEN, 1998), therefore, more air will cause greater attenuation of the sensor signal. Between $0.32 \text{ L.m}^{-2}.\text{min}^{-1}$ and $1.62 \text{ L.m}^{-2}.\text{min}^{-1}$ the attenuation seems to reach its maximum level, probably because the amount of bubbles that fits in the reflection surface of glass was saturated. It is relevant to notice that the minimum area detected by the sensor, in air, is below 200 a.u, considering the area calculated by Arduino. Therefore, this stabilization did not occur because of the lower detection limit of the sensor, considering the test with water. Furthermore, the standard deviation of the signal area represented on the graphics decreases as the air flow increases, which make sense considering that the saturation of bubbles will stabilize the signal at that point.

Figure 26 – Signal area in water for different air flow

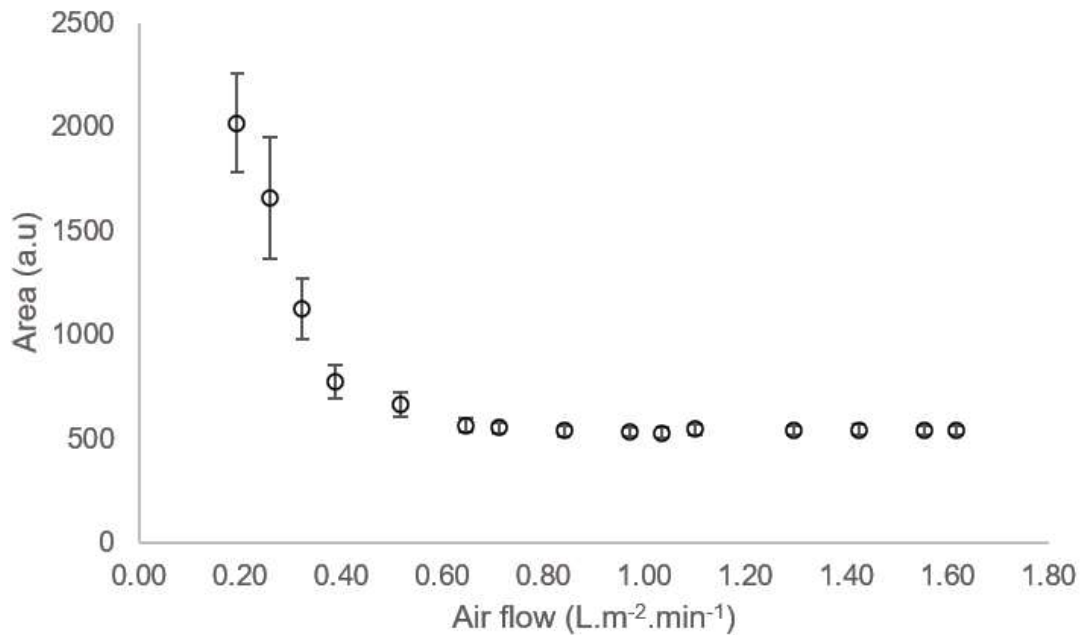
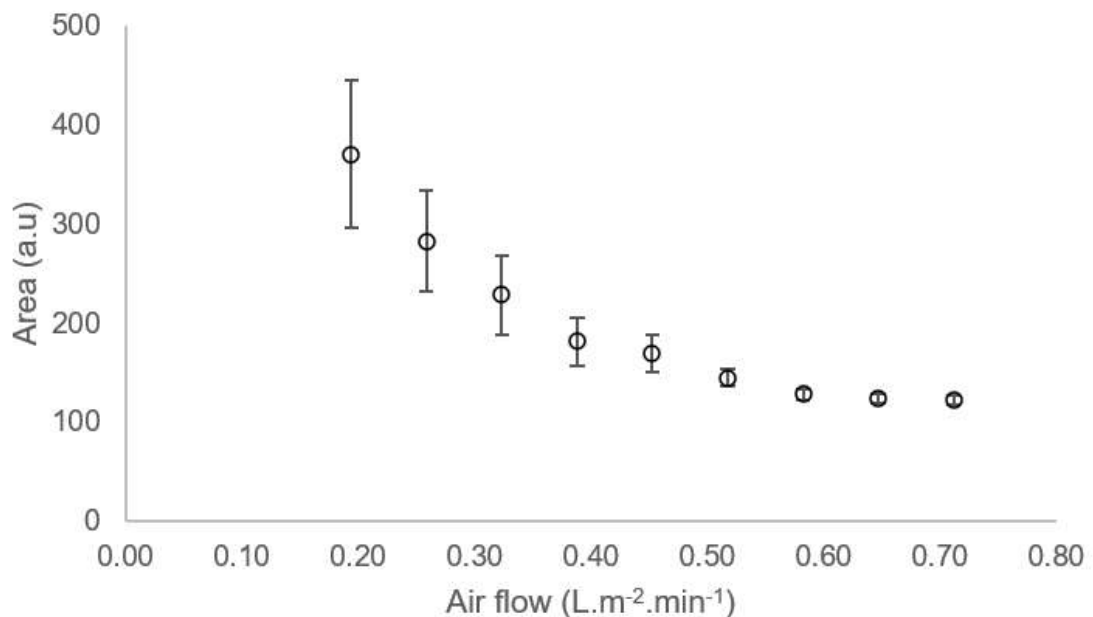


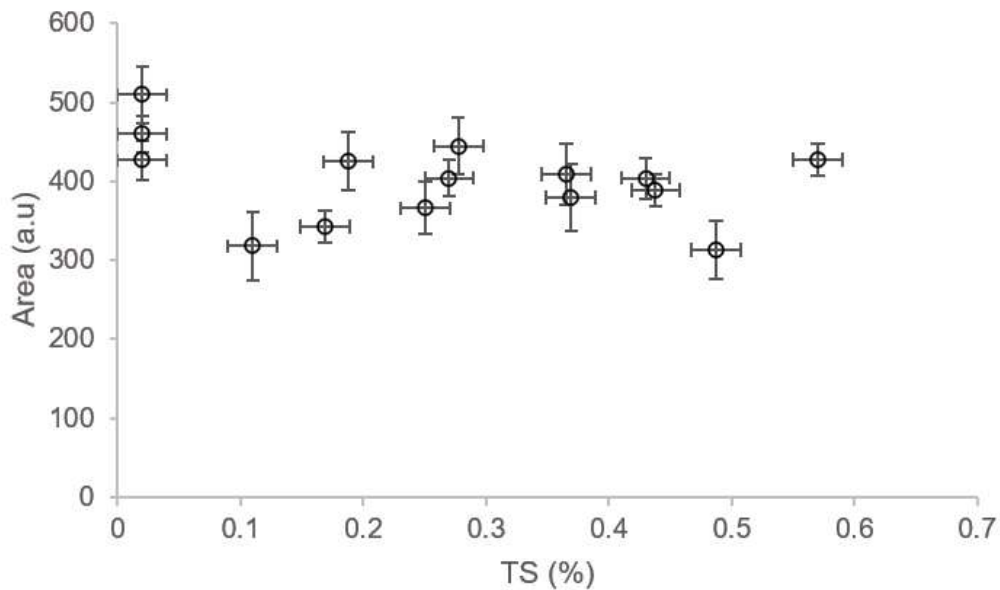
Figure 27 – Signal area in aerobic sludge with 0.3% of TS for different air flow



The tests made with sludge carry out in a much lower area value, since attenuation was greater, compared to the tests evaluated in water (Figure 26 and Figure 27). The results confirm previous tendency of attenuation by solids concentration. Despite the difference on attenuation with mixed water and sludge, it was not possible to correlate the TS of the anaerobic sludge with the signal area, with a flow rate of 0.58 L.m⁻².min⁻¹ (Figure 28). The explanation to that is that besides absorbing the ultrasonic waves, bubbles can also provoke scattering, which can increase or decrease the echo signal back to the transducer. In that sense, with the tested Arduino routine, it was not possible to establish a good correlation between TS and the signal attenuation

in a high flow rate of bubbles. However, Neves *et al.* (2021) found a good correlation with TS from sludge and attenuation with the presence of bubbles', but the flow rate and bubbles' size were not reported. It was probably a lower flow rate, thus the area calculation in such conditions may still be a simple and effective way to correlate attenuation and TS. Furthermore, even with a high flow rate, a more complex routine could probably be adapted to eliminate the bubbles' interference.

Figure 28 – Correlation between the area of the signal and the TS concentration at 22 °C and flow rate of $0.58 \text{ L.m}^{-2}.\text{min}^{-1}$



Several sensors already present the bubbles' compensation algorithm on their software, however, as shown in this chapter, it depends on the flow rate. Therefore, for air diffusion in the aeration tank of an activated sludge system, for instance, the flow rate can be easily controlled. However, in UASB reactors, the biogas production is variable and certainly with a much lower flow rate compared to aeration tanks.

6.4 Conclusion

The effect of bubbles on the sensor reading was confirmed on this test. Mainly three conclusions could be drawn from the results. First, that the accumulation of bubbles in the transducer can blind the sensor if there is no way for the bubbles to "escape". Second, that the attenuation is proportional to the air flow rate until a saturated point. And third, that the correlation of the signal attenuation and TS concentration was not possible with the tested Arduino routine in a high flow rate ($0.58 \text{ L.m}^{-2}.\text{min}^{-1}$). Moreover, tests with lower flow rate and different type of gases are recommended, so a more compatible comparison can be done with the biogas effect from UASB reactors.

7 SIGNAL ANALYSIS FOR DIFFERENT TYPE OF SOLIDS

7.1 Introduction

Solids particles present different characteristics. The main characteristic that it is known that can interfere in ultrasonic attenuation are the physical properties of the particles (e.g shape, density and size) (YOUSEFIAN *et al.*, 2018; BOUDA; LEBAILI; BENCHAAALA, 2002). The attenuation coefficient is well-known for different type of liquids and tissues, especially because of its application for medicine (CAROVAC; SMAJLOVIC; JUNUZOVIC, 2011; ALPEN, 1998). However, the effect of the physical properties of the particles on the ultrasonic signal also depends on the ultrasound frequency. For the frequency of 200 kHz, that is used for the US sensor, there is a lack of information about its effects on the signal attenuation due to the solids characteristic.

7.2 Methodology

7.2.1 Setup and materials

It was evaluated the behavior of the signal and the attenuation for anaerobic sludge, aerobic sludge, sludge ash and soil, all of them separately mixed with tap water. Anaerobic sludge was collected from the digestors of the STP of Leeuwarden. Anaerobic sludge grain size reported by NEVES (2020) was mostly below 0.3 mm. Sludge ash was obtained from SusPhos project (Figure 29) that was occurring inside the WAC in the city of Leeuwarden. Souza and Agostinho (2022) reported the ash composition that can be seen in Table 11. The soil was collected at the parking lot of Van Hall Larenstein university, in Leeuwarden (The netherlands) and sieved with an opening of 4.5 mm (Figure 30). A general characterization of the soil composition was considered for this analysis according to Römken and Oenema (2004) and can also be seen in Table 11. An open reactor made of glass and two mechanical stirrers were used to mix the materials with water at 100 rpm (Figure 31 and Figure 32). The US sensor was suspended inside the reactor by the transducer's transmission cable and a rope glued in the back of the reflection surface. A temperature sensor was installed inside the reactor. Temperature variate from 17 to 19 °C in all experiments.

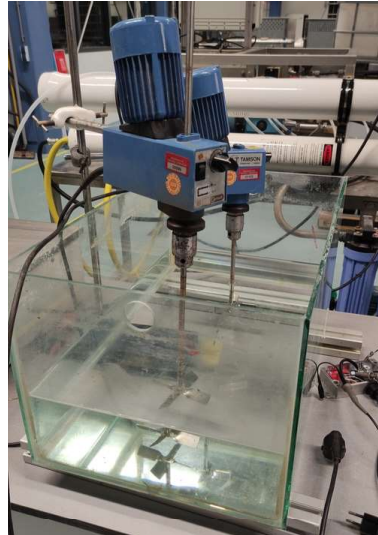
Table 11 – Substrates characteristics

Materials	VS/TS	Particle size	Mainly composition
Soil	0.21	<4.5 mm	Organic matter (20%), clay, Cd, Pb, Hg, As, Cu, Zn, Ni, Cr*
Sludge ash	0.00	<0.06 mm	Al ₂ O ₃ , Fe ₂ O ₃ , P ₂ O ₅ , SiO ₂ , SO ₃ (>90%)
Anaerobic sludge	0.71	<0.30 mm**	Organic matter (71%) and inorganic matter (29%) present in sludge ash

*RÖMKENS, 2004; ** NEVES, 2020;

The tests were performed in the water application center (WAC) in the city of Leeuwarden (The Netherlands).

Figure 29 – Sludge ash used for the tests**Figure 30 – Soil used in the tests**

Figure 31 – Setup - mechanic mixing**Figure 32 – US sensor inside the setup with water**

7.2.2 Correlation between attenuation and solids concentration

For better understanding the correlation between TS concentration and the signal attenuation three different substrates were tested: anaerobic sludge, sludge's ashes and soil. Anaerobic sludge contains a high value of organic matter, sludge's ashes is the same sludge without the organic fraction and soil was choose due to its different type of solid and greater amount of metals. After the substrates were added to the system, two samples were collected for the gravimetric test. The time was marked immediately after the substrate's addition. The first sample was collected at the minute 1, and the second at the minute 10, as a duplicate. At the minute 7 a sample of the signal was collected and saved for the MATLAB calculation of the maximum potential of the reflection peak. For that, it was considered an average between the maximum potential of 500 images generated from the oscilloscope.

Ideally the tests should cover the TS correspondence from a low concentration, when the signal amplitude is high, until it is completely attenuated (TS superior limit detection). However, that was performed only for soil (range concentration 0-0.2%). For the anaerobic sludge the signal increased after a certain TS concentration level, therefore, the signal was not completely

attenuated even for a sludge concentration higher than 1%. For the sludge's ashes the limit access to it carry out in a maximum range until 0.5% of TS for that substrate.

7.2.3 Signal behavior over time

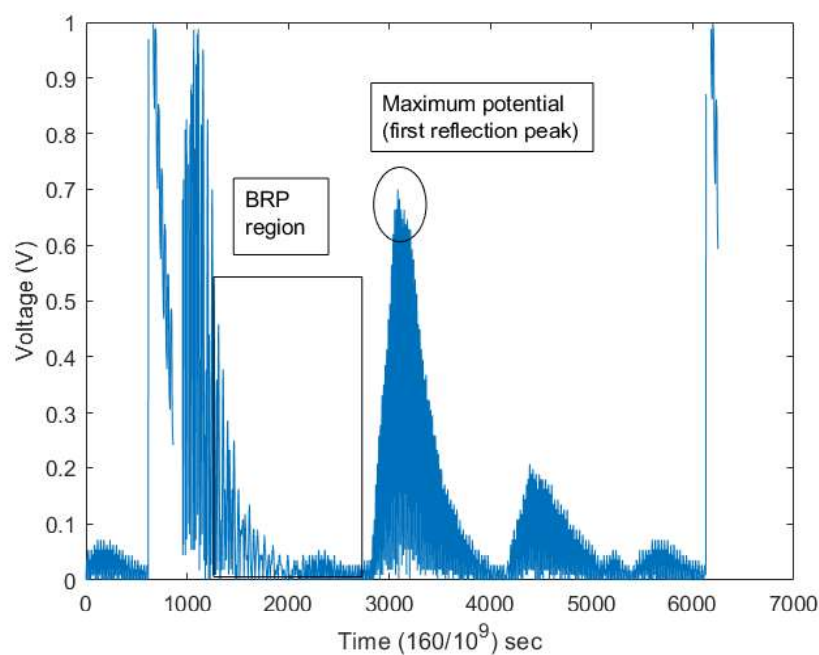
In order to see the behavior of the signal over time it were evaluated 5 different substrates: anaerobic sludge, aerobic sludge, sludge's ash, and soil, that were mixed with distilled water. An Arduino routine was used to calculate the area of the first reflection peak with a homemade routine. The software realterm stored 4 values in every second. The US sensor started to measure after the substrate was added to the system. The durability of the test were different from each other, depending on the velocity recover of the signal.

7.2.4 Aerobic sludge still and mixing comparative

In order to evaluate the signal from the carousel of the RWZI Grou, two liters of sample were collected from the carousel. The sludge was added to the same setup already described in this chapter in the Water Application Center. Distilled water was added to the system so the sensor could stay underwater. The fresh aerobic sludge collected was tested in four scenarios. First, with water, as a standard comparative. Second, with the sludge still. Third, with the sludge mixing for one hour. Four, with the sludge still after one hour of mixing (10 minutes later).

Two aspects were evaluated during these experiment, BRP (Before reflection peak) region peak sums, and the maximum potential correspondent to the first reflection peak.

Figure 33 – Signal module identification of BRP and maximum potential region



7.3 Results and discussion

7.3.1 Correlation between attenuation and TS concentration

The results obtained from three different type of solids (anaerobic sludge, sludge ash and soil) showed a different attenuation coefficient. Mixing water and soil (Figure 34) resulted in a high attenuation of the signal, since TS concentration below 0.2% showed almost complete attenuation. In contrast, sludge ash (Figure 35) and anaerobic sludge (Figure 36), showed a similar attenuation level for the same TS concentration range. It is relevant to notice that sludge ash has a much smaller particle size compared to anaerobic sludge. The differences and similarities from the attenuation can be confirmed by the angular coefficient of the linear regression from Maximum potential signal x TS of all substrates. While sludge ash and anaerobic sludge share similar composition, regarding inorganic components, the soil has a greater presence of metals. Therefore, solids presence that are not sludge in the reactors, for instance, sand (mainly at grit chambers and at the bottom of UASB reactors), plastic and hair, may greatly interfere in the signal, even with a small relative concentration. Nevertheless, the synergistic effect of the solids in full-scale have to be tested, with all variables simultaneously.

Figure 34 – Correlation between TS of soil and the signal potential of the US sensor

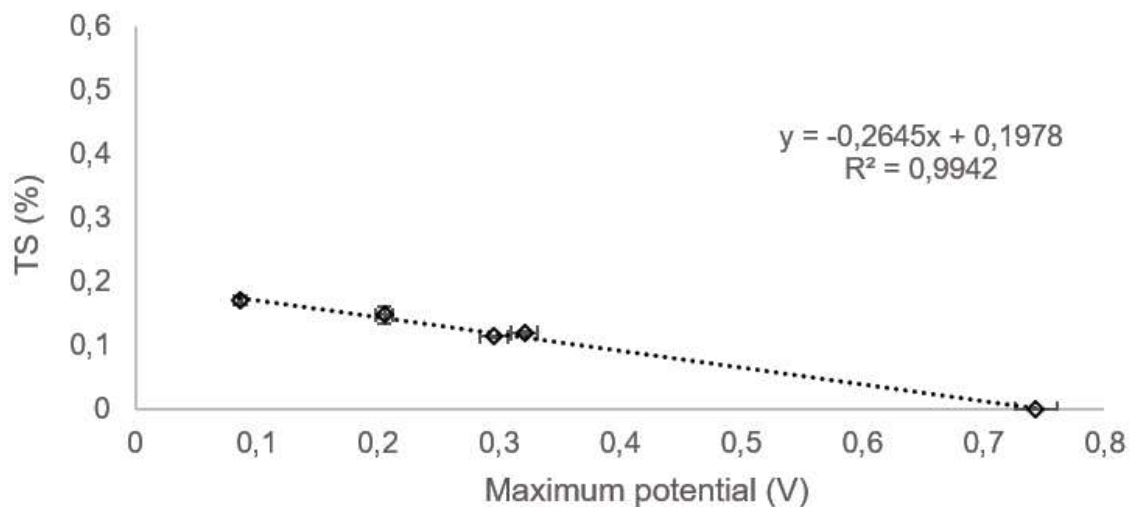


Figure 35 – Correlation between TS of sludge ash and the signal potential of the US sensor at a range below 0.5%

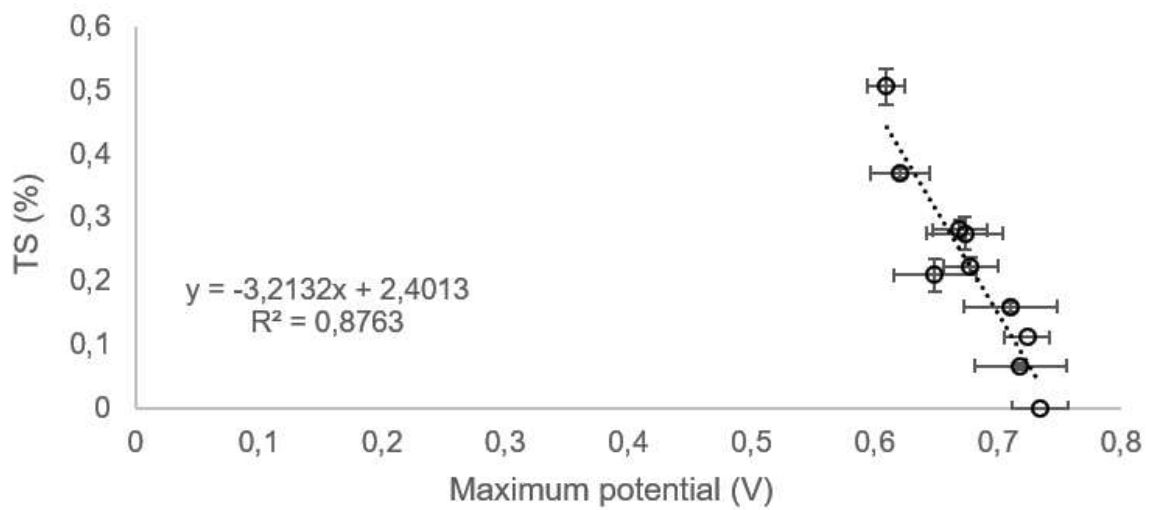
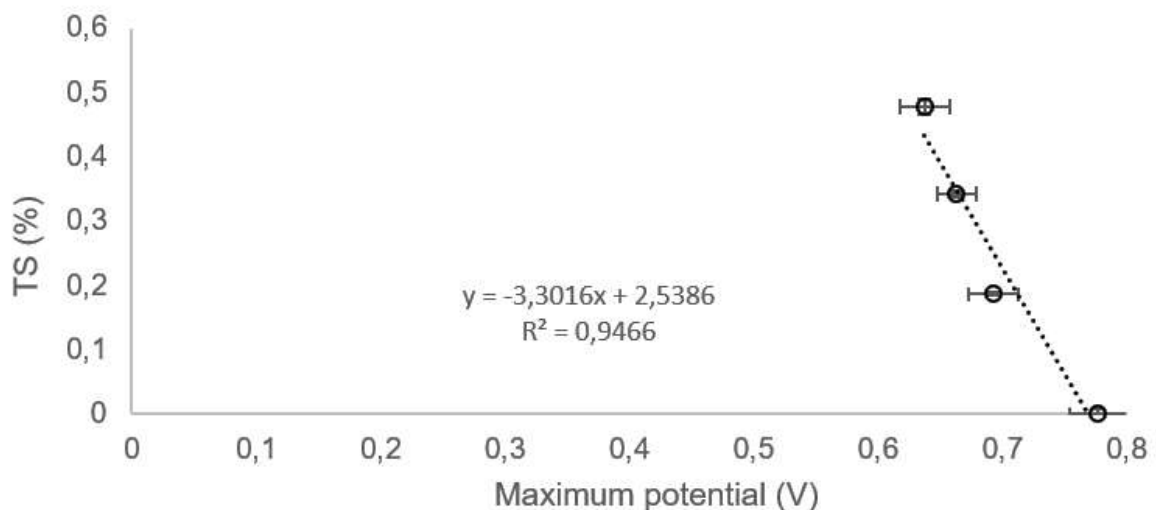
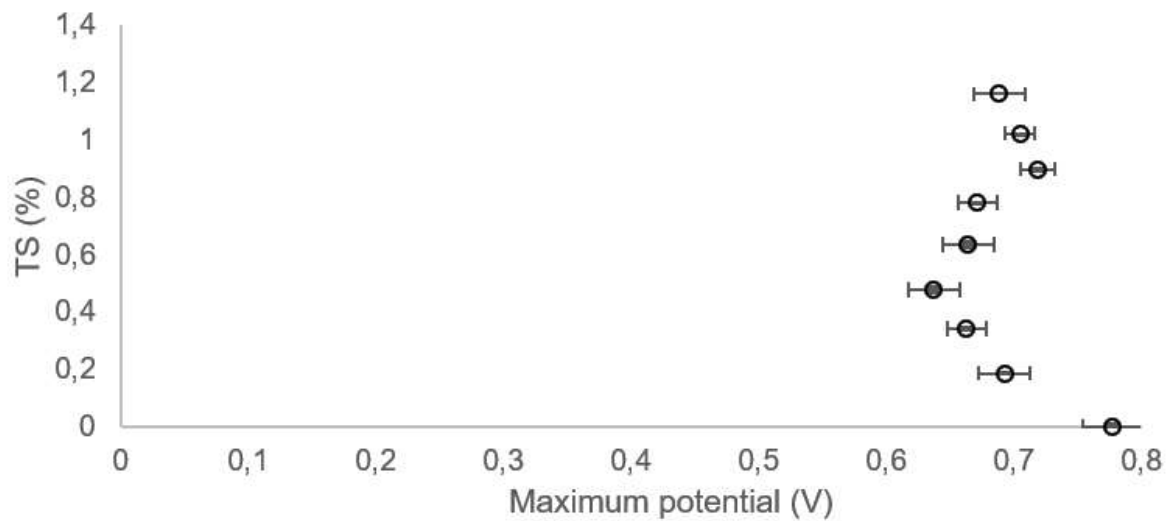


Figure 36 – Correlation between TS of anaerobic sludge and the signal potential of the US sensor at a range below 0.5%



During laboratory analysis, internal reflections provoked by the setup perhaps were crucial for incomprehensible results. For example, in Figure 37, anaerobic sludge start to increase the signal maximum potential after a TS concentration level of 0.5%, which is completely against attenuation theory predictions. Furthermore, real scale test have a much larger space for signal scattering and most of the structures are built with concrete which do not have good reflection properties. Therefore, it is expected better results on full-scale application.

Figure 37 – Correlation between TS of anaerobic sludge and the signal potential of the US sensor (until 1.16% TS)



7.3.2 Signal behavior over time

After the substrates were added to the system, in every case, a high attenuation level was detected at the begin of the measurements followed by a signal recovery. Probably the greater attenuation at the beginning is related to settleable solids that could not maintain suspended with the chosen mix rotation level. However, settling may explain only part of it, since, TS concentration was measured by the time attenuation was high and low, and presented similar concentrations. Air bubbles captured by the solids may be another factor that explains the decrease following by increasing of the signal, as they could be released after some time of mixing.

Greater attenuation can be seen in Figure 38 where it was possible to identify two different concentrations of soil. A higher concentration of soil and sludge ash showed greater attenuation and greater recovery time of the signal (Figure 38 and Figure 39). When suspended particles concentration is small, approximately $< 1\%$ v/v, the particles settle with negligible impact on each other (IWA, 2022). Hence, settling effect on soil and ash can be considered discrete sedimentation. Considering that, sedimentation for a TS concentration of 0.07% and 0.10% of soil should have the same velocity, thus the recovery signal should be similar and it is not what happened. Therefore, air bubbles captured by the solids may be another factor that explains the decrease following by increasing of the signal, as they could be released after some time of mixing. In that case, greater TS will carry out a larger presence of bubbles within the setup where the sensor is measuring

Considering the larger particles from the soil that contained heavy metals, it was expected a faster settling by the soil, thus a faster recovery of the signal area. However, sludge's ashes presented a much faster signal recovery. However, smaller sizes from the ashes (< 0.06 mm) could explain the signal longer recovery time when it is compared to soil (< 4.5 mm). Probably larger particles have a better capacity of trapping air, which can explain the signal longer recovery time by the soil.

Figure 38 – Signal area over time for soil compared to water

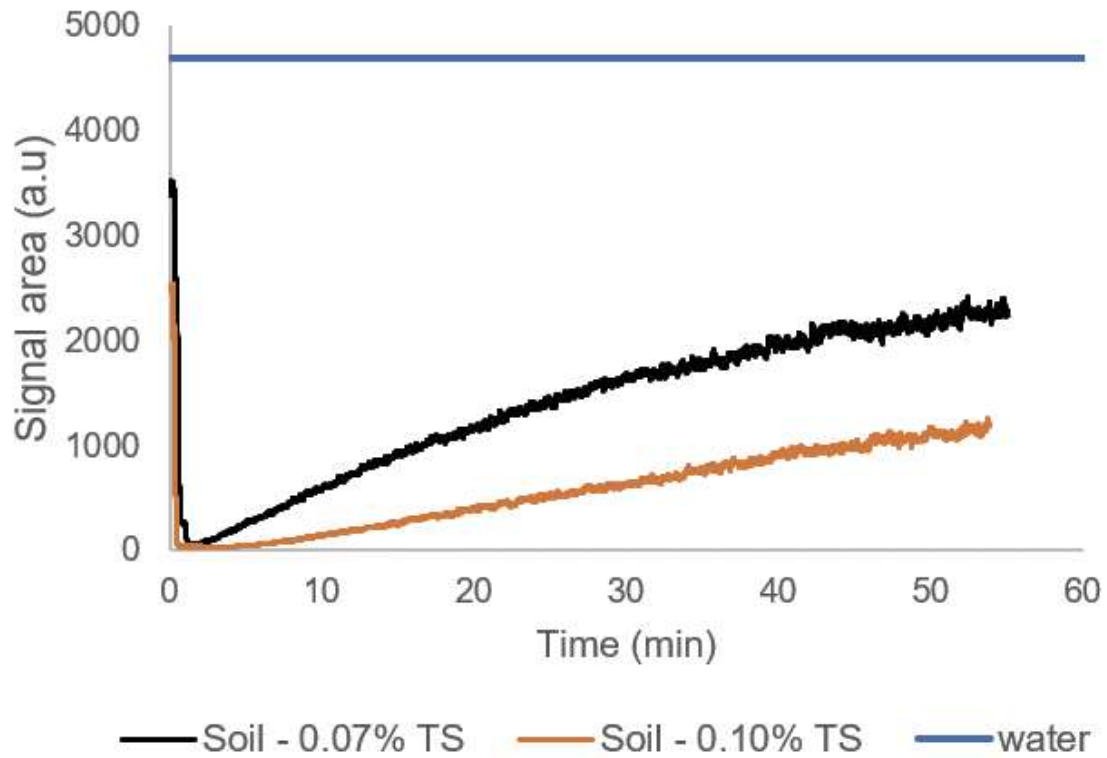
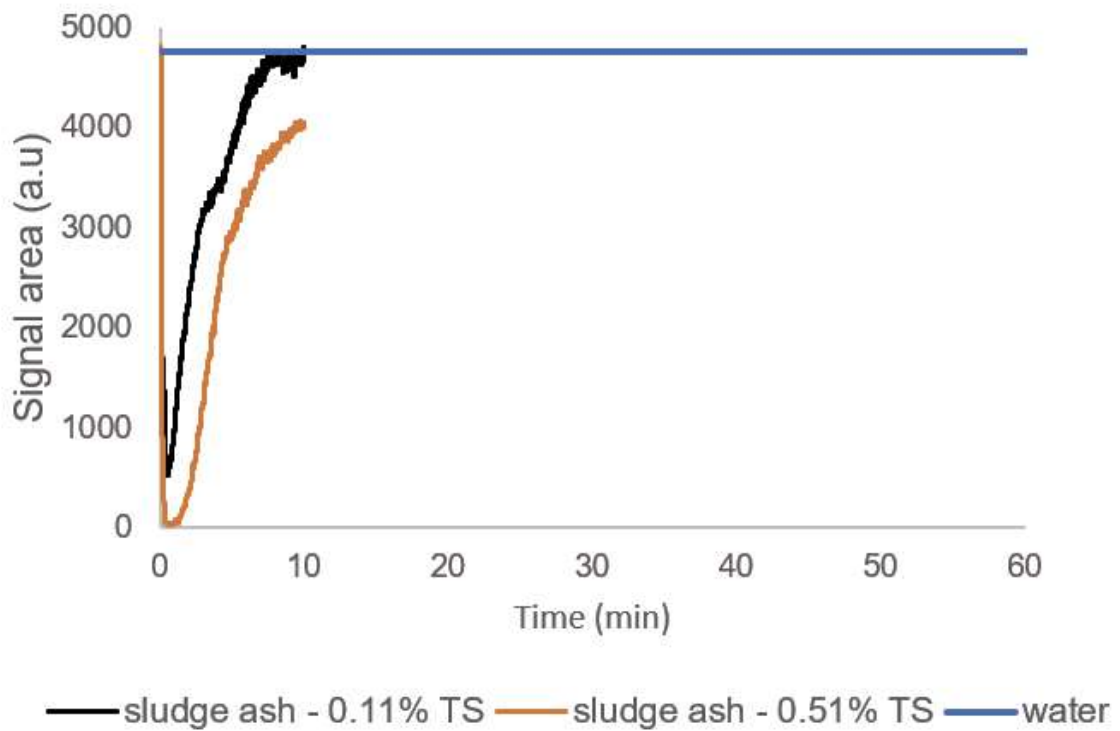


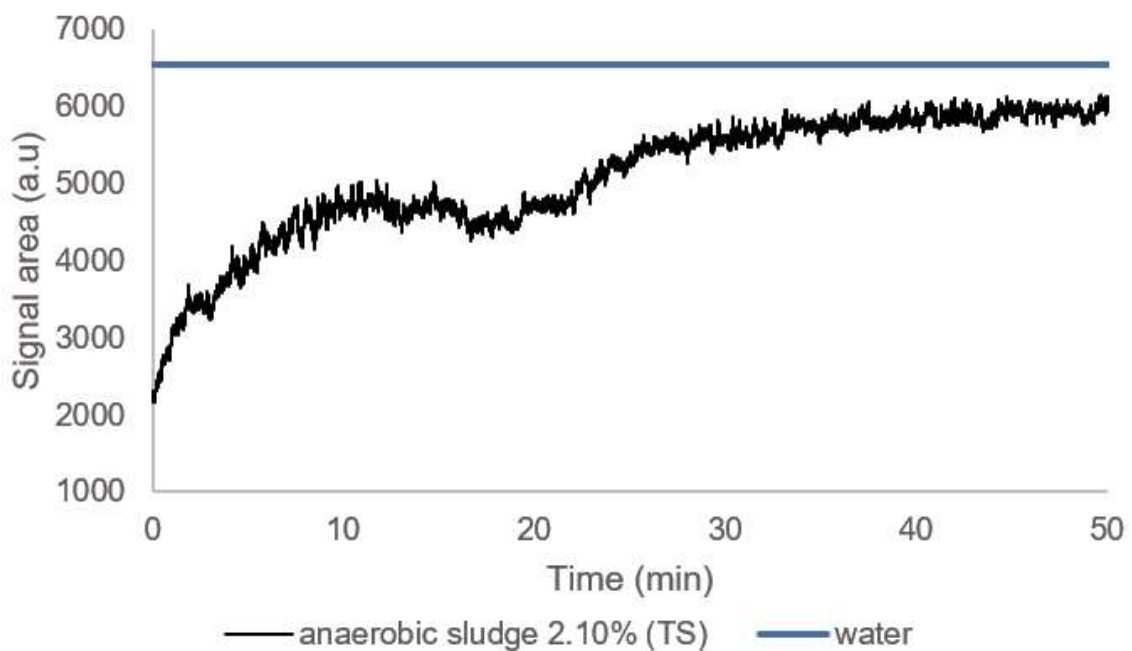
Figure 39 – Signal area over time for ash sludge compared to water



The result obtained from ash and anaerobic fresh sludge (Figure 39 and Figure 40)

indicate that, if the air theory is correct, then probably the sludge grain particles do not have effect on attenuation in the frequency of 200 kHz, as the signal after some time return to the same level as water. Considering that anaerobic sludge was fresh, it could not have air trapped in the particles. However, dissolved methane from anaerobic sludge could be released as mixing occurred. Nevertheless, a synergistic effect that occur in a full-scale STP with hair, plastic, sludge and chemical reactions (eg. Transformation of organic matter into water and CO₂ for aerobic treatment or transformation of organic matter into biogas and other subproducts in anaerobic treatment) may be sufficient to indicate, by ultrasonic attenuation, the TSS or TS concentration present in sewage.

Figure 40 – Signal area over time for anaerobic sludge compared to water



7.3.3 Aerobic sludge still and mixing comparative

In Table 12 it is notable that still sludge BRP region was greater than the mixing sludge. On the other hand, reflection peak maximum potential was greater than the sludge still. Greater values for the BRP region area while the sludge is still, could mean that sludge physical characteristic in this situation provide a greater reflection of the signal back to the transducer. At the same time, it reduces the signal amplitude (maximum potential), since most of the signal could not pass through the sludge present between the transducer and the reflection surface. Even when the sludge is mixed for a short time (10 seconds) and returns to the still status, physical properties probably do not return for the original configuration. That can be inferred by the similar results obtained for the sludge (1 hour mixing) and sludge mixed and still.

Table 12 – Signal analysis for the sludge still and mixing compared to water

Matrix	Maximum potential (V)	Maximum potential -Std	BRP potential	BRP- Std	ERT (160.10 ⁻⁹ sec)	ERT - Std
Aerobic sludge still	0.076	0.001	8.99	0.12	3167	38.40
Aerobic sludge (mixed and still)	0.440	0.001	3.54	0.29	3090	7.40
Aerobic sludge (1h mixing)	0.719	0.031	3.76	0.22	3100	0.39
Water	1.382	0.025	11.85	0.24	3078	0.35

ERT values also confirms that the presence of sludge in still state increases time necessary for the signal return from the reflection surface. Probably part of the signal is refracted in the sludge particles and part of it, due to diffraction, increase the distance traveled by the signal. It is notable that the ERT for water is lower compared to all the situations with sludge, which is expected since there is no obstacles in water for the signal. Furthermore, ERT standard deviation (ERT - Std) had a large variation comparing to mixing status. This is probably and indicative of settling, since at mixing status most of the solids were maintained suspended.

7.3.4 Conclusion

Different type of solids have different acoustic response from ultrasonic emitter. Attenuation from sludge ash and anaerobic sludge (for TS up to 0.5%) showed similar attenuation within the same TS concentration range, regarding a similar composition (slope coefficient -3.2132 and -3.3016, respectively). Probably volatile solids do not interfere in the signal as inorganic matter does, since the content of organic matter in sludge ash is almost null. Nevertheless, greater concentration of anaerobic sludge (TS of 2.1%) presented similar attenuation compared to water, which indicates that the setup could probably interfere in some in loco sludge characteristic. This behavior was confirmed by the anaerobic sludge analysis, which, with TS concentration above 0.5% started to decrease attenuation. Sludge still, and mixing differences, confirms that probably synergistic effect within a biologic reactor is essential to make the US sensor measurement viable. Moreover, for further tests the solids should be placed at same conditions, since sludge's ash and soil were dried and then mixed in water, and the sludge was mixed previously in the STP.

8 US SENSOR FULL-SCALE APPLICATIONS

This chapter will evaluate the US sensor application in 3 STPs in full-scale. It was firstly tested in Brazil, in a UASB reactor (STP Betim), with an older version of the US sensor, thus only with the oscilloscope data collection system, and the results were compared to the gravimetric test. Then the US sensor was improved in the Netherlands with an Arduino system, thus continuously data collection was possible. The US sensor was installed in a small STP in Grou (The Netherlands) and a medium STP in Leeuwarden (The Netherlands), both in a carousel unit of an activated sludge system. The applications in the Netherlands were compared with a commercial optic sensor and double-checked with the gravimetric test.

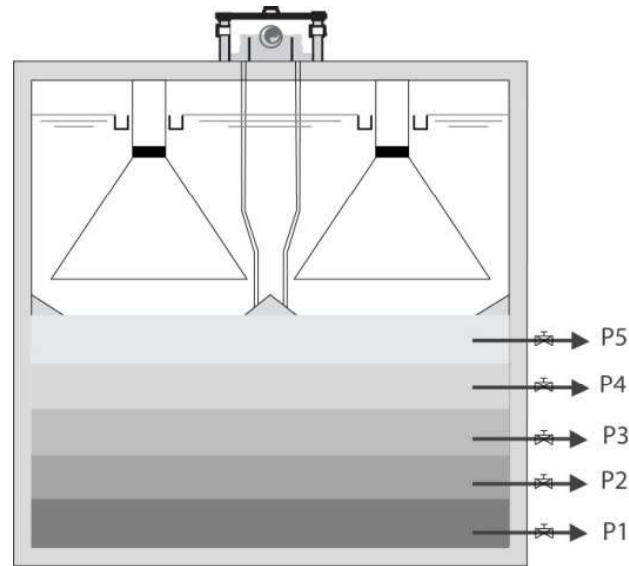
8.1 UASB reactors

8.1.1 Introduction

In Brazil, UASB reactors began to be deployed on full-scale in the 1980s, after a successful bench-scale test carried out in the city of Cali, in the 1970s (LETTINGA, 2014). Moreover, the experiences acquired and the evolution of research in the sector, have provided relevant contributions, which result into the resumption of confidence in this technology, mainly with the Basic Sanitation Research Program (PROSAB) carried out between 1997 and 2007 and later the contributions by the National Institute of Science and Technology in Sustainable Sewage Treatment Plants (INCT ETEs Sustentáveis), starting in 2017 (CHERNICHARO *et al.*, 2018).

The UASB reactors work through anaerobic digestion, which can be explained, in summary, by the conversion of organic matter by anaerobic microorganisms into methane, carbon dioxide, water, hydrogen sulfide, ammonia, and the addition to new bacterial cells. In matter of solids, UASB reactors don't present uniform solids concentration along the digestion compartment (Figure 41), therefore samples should be taken in different heights in order to determine the vertical solids profile of the reactor. Thus, at the upper layer of the sludge blanket, there is a lower concentration of solids compared to the bottom of the reactor, at the sludge bed (CHERNICHARO; BRESSANI-RIBEIRO; LOBATO, 2019; CHERNICHARO, 2016). Currently, Brazil has the largest park of UASB reactors in the world, 40% of the STP uses the technology in the South, Southeast and Midwest regions of Brazil (CHERNICHARO, *et al.*, 2018).

Figure 41 – Sludge sampling points along the digester compartment in UASB reactors



Chernicharo (2016)

Notably, many UASB reactors operate with a high concentration of solids due to the lack of systematic routines for sludge withdrawal. Hence, solids washout compromises not only the quality of the final effluent, which can harm the post-treatment steps, but also compromises the sludge retention and storage capacity inside the reactor (CHERNICHARO; BRESSANI-RIBEIRO; LOBATO, 2019). For this reason, it is essential that the sludge is discharged before the loss of solids to the settling compartment occurs (LOBATO *et al.*, 2018a). Furthermore, the washout of the lighter biomass can also be consequence of a high upflow velocity and decreased filtration capacity of the sludge bed, which can cause besides the loss of solids throw the effluent, an organic overload in post-treatment steps and inhibition of the methanogenic activity (LEITÃO *et al.*, 2006). The inhibition of methanogenic activity may reduce the biogas recovery potential, which can be used for energetic purpose. The reasons for the lack of routines or proper routines for the sludge withdrawal can be seen in Table 13 :

To prevent solids washout in UASB reactors, the sludge's mass in the reactor should be controlled and operate in a specific range. A minimum sludge's mass it is essential to maintain the microorganism activity on the reactor. The minimum sludge's mass (SM_{min}) can be determined dividing the removed organic load (ROL) and the specific methanogenic activity (SMA) as shows the equation 8.1 according to Lobato *et al.* (2018a).

$$SM_{min} = \frac{ROL (Kg.COD.d^{-1})}{SMA (Kg.COD_{CH_4}.Kg^{-1}.TVS^{-1}.d^{-1})} \quad (8.1)$$

SMA can be defined as the maximum capacity of methane production in a controlled lab environment. SMA represents the capacity of the sludge to produce methane from an organic substrate (CHERNICHARO, 2016).

Determine the maximum sludge's mass within the UASB reactor is essential to avoid the solids washout. For that, is necessary to trace the sludge profile and infer which is the maximum sludge's mass that carry out in the effluent deterioration (CHERNICHARO, 2016). Lobato *et*

Table 13 – Main factors that can affect the management of sludge from UASB reactors treating sewage

factors that can affect the operational routine of sludge management	Non-compliance source
Sludge sampling points, used to monitor the growth and concentration of the sludge along the height of the reactor digestion compartment, are insufficient and/or installed in the wrong position	Design and construction
Sludge withdrawal pipes in insufficient numbers or poorly distributed along the height of the digestion compartment	Design and construction
Manuals or operating guidelines for UASB reactors and dewatering systems that do not provide adequate detail on the procedures to be followed by the operators.	Design
Lack of systematic removal of excess sludge from UASB reactors and drying beds because of logistical and administrative problems (e.g. service contract for sludge transport incompatible with the required frequency, preventing sludge withdrawal from the reactor)	Operational management
Failures in the designs of drying beds or mechanized dewatering systems, with capacity below the need to process the sludge produced in the STP or incompatible with the characteristics of the sludge to be dewatered, as important factors were not considered, e.g. local specificities, climatic and operational conditions, such as the time scale of the operators, transport of sludge, availability of chemical products and spare parts, need for preventive maintenance, possibility of shutdowns because of corrective maintenance, and the like.	Design and operational management
Equipment of the mechanized dewatering system (e.g. sludge pumps, polymer doses, centrifuges, and the like) not in operation owing to difficulties with preventive and corrective maintenance.	Operational management

al. (2018b) recommends discharging the sludge on the top and bottom layers of the blanket, with at least 50% of the excess sludge mass from the upper piping (1.00 to 1.50 m above the bottom), which represents a more diluted sludge. A smaller portion should be discharged from the bottom (higher concentration of TS) in order to preserve the sludge bed and reduce the sludge withdrawal volume. However, the lack of sampling points or its inappropriate distribution along the digester compartment represent a barrier for this application. Because of these limitations Lobato *et al.* (2018) recommends to monitoring TS concentration at the highest point at the digestion compartment, just below the deflectors, at a maximum TS concentration of 0.5% (5000 mg.L⁻¹). Therefore, when TS concentration is above 0.5% in the upper part of the reactor, sludge withdrawal should be done to avoid the solids washout.

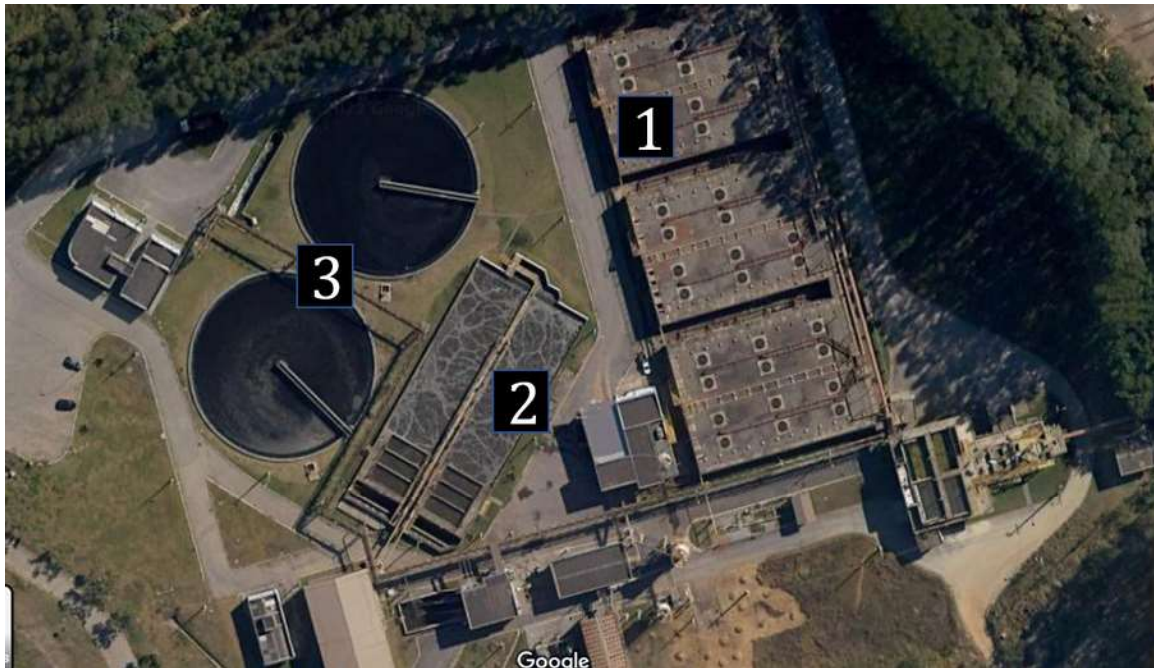
The withdrawal of sludge on the top layer and on the bottom has different implications. On the top of the sludge blanket, the solids are more diluted, therefore, it is necessary a greater sludge volume discharge, which demands a bigger and more expansive dewatering system. The sludge bed, located at the bottom of the reactor, is more concentrated and can retain several inert solids such as sand, depending on the quality of the preliminary treatment, that need to occasionally be removed from the reactor. Thus, the discharge of a more concentrated sludge can be an advantage because it removes several inert solids and also requires lower areas for the dewatering system. However, sludge bed has usually greater settleability quality, and the microorganisms' activity are usually higher and essential for sludge stabilization. Moreover, the denser sludge at the bottom of the reactor can function as a 'filter' that prevents inert solids to get into the reactor. Ozgun *et al.* (2019) reported that the sludge stabilization level in a UASB reactor with anaerobic membrane variate according to the height that the sludge is located through the blanket. While Mahmoud *et al.* (2004) reported the VS/TS relation through the sludge blanket was constant in a UASB reactor without post-treatment.

Furthermore, there are some recent auxiliary tools to the sludge management in a UASB reactor that can be used in different scenarios. The Integrated System of Sludge Management (SIG-Lodo) it's a software which can carry out different strategies for the sludge management, considering the interface between the production sludge unit (UASB reactor) and dewatering sludge process, therefore, being a helpful tool for the manager choose an effective sludge discharge plan (EMRICH *et al.*, 2021). For the proper function of SIG-Lodo tool, it is mandatory that data input is collected in a certain frequency and real time monitoring would be ideal for a better accuracy of the software.

8.1.2 Methodology

The test was evaluated on full-scale UASB reactor in ETE Betim Central (STP Betim), located in the city of Betim (Brazil). The sewage treatment plant is composed by anaerobic technology (UASB reactors) and an aerobic technology (conventional activated sludge system) (Figure 42). The average inflow rate during the analyzed period was 478 L.s⁻¹.

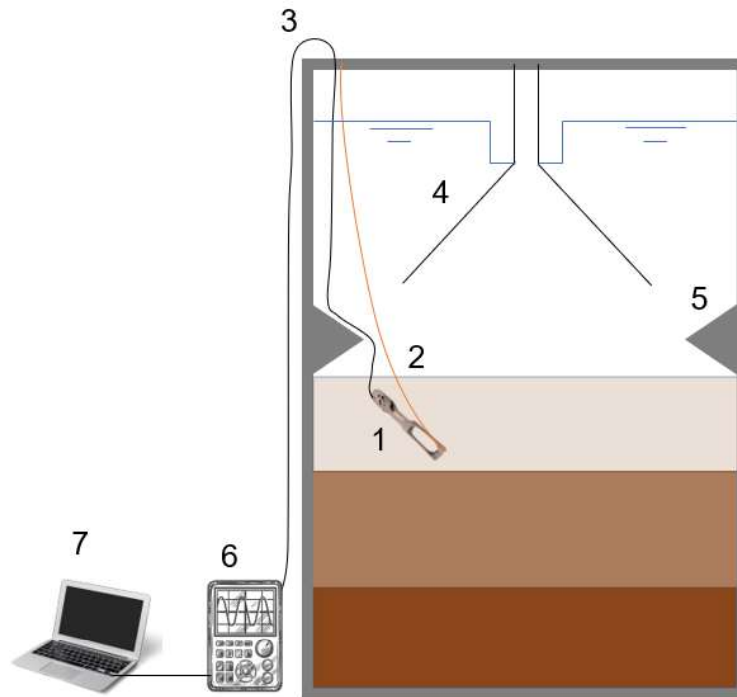
Figure 42 – ETE Betim Central (STP Betim) - 1: location of the ultrasonic sensor (UASB reactors), 2: aeration tank (activated sludge system), 3: Secondary sedimentation tanks



The instrumentation was the same as used by Neves *et al.* (2021), only an oscilloscope and a laptop were used for the data collection and gravimetric test for TS were realized at the correspondent height in which the sensor was installed. It is important to notice that this was the first test realized in this research, from 30 July until August 27 of 2021, therefore the new sensor with the Arduino was not available and some aspects that interfere in the signal were unknown by that time. The lack of time for this research was an impeditive for further tests with the upgraded sensor already with the Arduino for the real time data collection in UASB reactors.

There was mainly four differences from the tests evaluated by Neves *et al.* (2021). Firstly, the position of the sensor that was previously installed in the center of the UASB reactor close to the reactor's walls, just below the deflector. The change happened because the sanitation companies involved in the project advise it would be easier and safer to install the sensor there, since in the center it is located most of the biogas produced by the reactor. Secondly, the support of the sensor was previously a metal bar that kept the sensor still, this time it was used two flexible cables, thus the sensor have some movement due to the reactor's flow. The change occur also because of a demand of the companies. According to them, a rigid bar would not be viable to reach the desire height (just below the deflectors). The third difference, would be the support of the reflection surface. In both cases it was the same material, a PVC tube. What changed was the distance of the reflection surface from the transducer. Previously the distance was 45 cm, and for this test, the distance was 20 cm. The different values was an attempt to measure higher concentration of TS, since the limit detection of the sensor reported by Neves *et al.* (2021) was 1% of TS. The fourth difference is the system itself that the sensor was installed. While the sensor was installed previously in demo-scale UASB reactor, this time it was installed in a full-scale UASB reactor, that also receives excess sludge from the activated sludge system. A scheme of the evaluated test can be seen on Figure 43.

Figure 43 – UASB reactor Betim Central scheme - 1: Ultrasonic sensor position; 2: Support cable; 3: Transmission cable; 4: Gas-Liquid-Solid separator; 5: Deflector; 6: Oscilloscope and control box; 7: Laptop



During the sludge removal from the UASB reactor, it was compared the signal measurement at its beginning and after one hour in order to test the sensibility of the sensor for the removal of solids from the reactor.

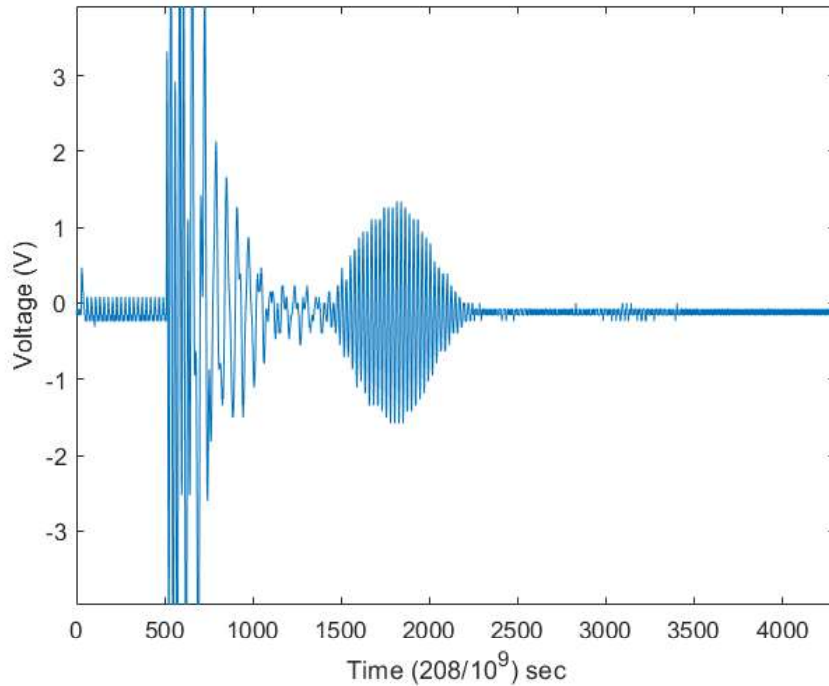
8.1.3 Results and discussion

The correlation between the attenuation of the signal and the TS gravimetric measurements did not present a good match on the few samples made during the period of one month. However, there are a large number of reasons that can explain it. Firstly, it was found that the reactor was operating with an overload of coarse solids in the upper part of the UASB reactor, which was reported by the operators from the plant after emptying the reactor. Secondly the recirculated sludge flow from the activated sludge system may exceed the UASB reactor capacity, which could cause a disorder on the stratification of the sludge blanket.

Furthermore, the sensor itself was moving freely inside the reactor and close to the reactor's structures. Such characteristic could influence the signal, for example, if the sensor was located in a dead zone of the reactor, which has a greater possibility of occurrence at the side part of the reactor comparing to its center. Moreover, the reflections from the reactor's structures could also cause some interference, as it occurred in laboratory scale. Nevertheless, there was no visual indicative of such reflections (Figure 44), although a low resolution signal was used during the UASB test and data collection was not continuously obtained. Therefore, as the sensor moves in the reactor, interference reflections could have occurred while the oscilloscope was not collecting the data. In that sense, a continuous data obtained from an Arduino would be a

valuable result for full-scale application in UASB reactors.

Figure 44 – 1 out of 500 images from the ultrasonic sensor for TS gravimetric measurement of 0.1% at the same height position of the sensor location inside the UASB reactor of ETE Betim Central obtained by an oscilloscope



During the sludge removal process of the reactor that last for 6 hours, it was measured the signal at its beginning and after one hour (Table 14). The greater difference between both situation may be explained because of adhered bubbles at the solids, that could be released after the sludge withdrawal begins. The sludge without the adhered bubbles, or at least with less adhered bubbles, could greatly increase the maximum potential mean, since bubbles greatly increase attenuation as seen in chapter 6. Moreover, the decrease of solids within the reactor probably also contributed to increase on the maximum potential mean. However, the gravimetric test were not possible to be performed during that time.

Table 14 – Signal amplitude before and during the sludge withdrawal in a UASB reactor

Status	Maximum potential mean (V)	Standard deviation
Before sludge withdrawal	0.25	0.05
One hour after the sludge withdrawal begin	1.61	0.08

After the period of two months, the sensor was removed from the reactor, with a great amount of solids adhered around its support. Different design and position of the sensor should be tested in order to evaluate the cleaning frequency. This result showed another challenge when testing in full-scale STPs compared to the demo-scale test reported by Neves *et al.* (2021). Cleaning routines of a sensor installed in a UASB reactor could be quite laboriously, since the reactor need to be closed to avoid air entrance. A cleaner design was developed already for further tests (Figure 9), however a better solution would be to use the US sensor in the settling compartment of the UASB reactor, that have a lower amount of solids. Self-cleaning sensors already exist in the market, nevertheless, manual cleaning is always necessary and recommended, besides the self-cleaning device.

Figure 45 – Solids accumulation on the US sensor after two months inside the UASB reactor from ETE Betim Central



8.1.4 Conclusion

A low-cost ultrasonic sensor was previously tested in a demo-scale with promising results regarding its correlation with gravimetric test, however, full-scale application showed to be quite challenging and this correlation was not possible to be observed. Further tests with the sensor with an Arduino control is recommended in order to generate a continuous data, therefore a more representative data. Moreover, the tests in full-scale carry out important lessons for further researches and tests. For example, the possible difference on the application of the US sensor in the lateral position of the UASB reactor and in the center. Two sensors in the same reactor (at the side and the central location within the reactor) could bring more consistent results and eliminate uncertainty regarding the possible interference on the sensor reading. The cleaning demand is also a relevant aspect to be evaluated, since a high cleaning frequency could simply replace the work regarding the gravimetric test.

8.2 Activated Sludge

8.2.1 Introduction

Conventional activated sludge treatment, unlike UASB reactors, occurs by the aerobic digestion of the organic matter. This technology was named in 1914, when Arden and Lockett published a paper that carried out that the production of an activated mass of aerobic microorganisms can increase the stabilization of organic matter in wastewater (ARDERN; LOCKETT, 1914). The effluent is usually aerated by diffusers or the system is mechanically aerated. This discovery was greatly impacted by Clark and Adams research, few years before, that found out that the injection of air could increase the purification of wastewater (CLARK; ADAMS, 1914 *apud* METCALF EDDY, 2003).

Activated sludge system contains mainly 3 components. The aeration tank, in which the microorganisms are kept suspended homogeneously receiving oxygen; liquid-solids separation (e.g clarifiers); and a recycle system for the returning of the solids removed from the sedimentation tank back to the aeration tank (METCALF EDDY, 2003). Usually conventional activated sludge systems are preceded by primary sedimentation tanks, that can remove most of the settleable solids. However, depending on the robustness of the preliminary treatment, some plants dispense the use of primary settlers.

Aeration can be provided by several forms and is always an energetic cost involved on it. The type of aeration will depend on the geometry, function to be performed and installation cost. The main types of aeration are: diffused-air systems, mechanical aeration and high purity oxygen systems (METCALF EDDY, 2003). Aeration has a secondary objective of mixing the sewage, thus the substrate-microorganism relation can be balanced over all the reactor (VON-SPERLING, 2016).

In order to increase the solids retention in the system, the sludge from the secondary sedimentation tank is returned to the aerated tank. For the proper operation of activated sludge system, it is essential that the return ratio keeps on a range between 0.7 and 1.2. The typical values of TSS in the aerated tanks are between 2000 mg.L⁻¹ and 4000 mg.L⁻¹, while the typical concentration on the return line is between 6000 mg.L⁻¹ and 12 000 mg.L⁻¹. In general, the more concentrated the sludge from the secondary sedimentation tank, the lower the return sludge flow need to be, which is an important control factor for the sludge age of the system (VON SPERLING, 2016).

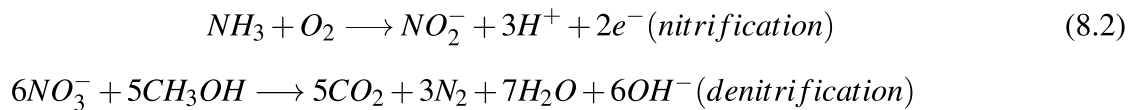
For the solid control in the activated sludge system, several methods can be applied. The Sludge Volume Index (SVI) indicates the settleability of the sludge, and is a usual parameter to indicate the presence of a bulking sludge. Thus, it is possible to increase or decrease the sludge return ratio in order to improve the settling in the secondary sedimentation tank. Furthermore, a principle of controlling the return sludge flow according to the sludge blanket in secondary sedimentation tanks is very effective against the loss of solids to the effluent. Whenever the sludge blanket reaches a specific height in the settler, a sensor can detect it and send a signal so that the sludge outlet valve in the sedimentation tanks opens more, increasing the sludge

flow. This procedure can be done manually, which is more common in Brazil (VON-SPERLING, 2016).

Furthermore, several parameters in matter of settling theory can be useful in an activated sludge system. For instance, when the applied flow in the settler is superior to the limit flow and the hydraulic application rate is superior to the sludge's sedimentation velocity, then the secondary sedimentation tank has an overload in the thickening and clarification issue (VON SPERLING, 2016). Therefore, the sedimentation velocity of the sludge is an important parameter to maintain an appropriate control of the system.

The excess sludge from conventional activated sludge, unlike UASB reactors, need to be stabilized and thickened before the dewatering process (LEITÃO *et al.*, 2006). If the activated sludge is a post-treatment of the UASB reactor, the aerobic excess sludge can be returned into the UASB, where it will be stabilized and thickened. However, the returning fraction concentration has to be compatible with the solid capacity of the UASB reactor (LOBATO *et al.*, 2018).

More recently, at the end of century XX, activated sludge systems were adapted to remove nutrients, mainly nitrogen and phosphorus (METCALF EDDY, 2003). For nitrogen removal, nitrification-denitrification process can occur with a component called selector, that can operate in anoxic or aerobic condition (VON-SPERLING, 2016). The ammonia content in sewage can be converted into nitrite and nitrate by aeration process (nitrification), then it can be converted into gas nitrogen in anoxic condition (denitrification) as shown in the equation 8.2 reported by EPA (2007):



The adherence of nitrogen bubbles at solids is considered a problem, for example, when they enter to the secondary sedimentation tank unit and fluctuate instead of settle, thus it is recommended to mix or aerate it before going to the settling units (VON-SPERLING, 2016).

Modelling of activated sludge processes has become a common part of the design and operation of STPs. Activated sludge models (ASM) started at the 80s, helped researches to achieve more efficient experimental designs and operators to better organize and understand information available at their plants. This occurred for several parameters, including nitrogen and phosphorus removal. TSS were introduced into the biokinetic models in order to compute their concentration via stoichiometry. Since phosphorus removal and precipitation introduce mineral fractions into the activated sludge, prediction of TSS is important (HENZE *et al.*, 2000). Modelling is a valuable tool to control automation in STP by feedforward systems. The feedforward control is an efficient strategy in activated sludge process because of the high hydraulic delays. Feedforward control advantage is to act on the process when the influent disturbances appear and before they cause major changes in the effluent. Feedforward control can also be combined with slow feedback control to compensate for model approximations. (VRECKO; HVALA; CARLSSON, 2003).

Abusam and Mydlarczyk (2018) reported that operational issues in activated sludge are rarely discussed in developing countries. However, they found out huge operational problems in a waste water treatment plant in Kuwait. The STP's was operating with overload of solids and the transfer of oxygen to the system was not enough. In Brazil, most of activated sludge system are located in big cities (ANA - AGÊNCIA NACIONAL DE ÁGUAS E SANEAMENTO BÁSICO, 2020), which means a great amount of sewage is treated by this technology, however most of them do not have an automation regarding solids control.

8.2.2 Methodology

A more detailed explanation about the instrumentation and data collection can be seen in chapter 3.

8.2.2.1 STPs overview

8.2.2.1.1 Overview of RWZI Grou (small STP)

The STP of the city of Grou (RWZI Grou) treat the sewage of an equivalent population of 17 000 people. An overview of the STP can be seen in Figure 46. The US sensor was installed in the end of the aeration step of the carousel, as shown in Figure 47, thus probably a region that may occur denitrification. The aeration begins at the mixers position, and the dissolved oxygen decreases as the mixed liquor gets away from the aeration mechanic machine (located in the selectors position). The US sensor was installed in the same height (50 cm from the surface) and close to the optic sensor for TSS that the STP already had (Figure 48). A wire of 5 meters length connected the US sensor to a control box, which was connected to a laptop that was responsible for collecting and storing the data with the software realterm. The laptop and the control box were inside a house, protected from rain and wind.

Figure 46 – RWZI Grou: 1 - Preliminary treatment; 2 - Carousel units; 3- Secondary sedimentation tanks; 4 - Sludge thickener; 5 - Sludge dewatering units



Google maps, modificado (2022)

Figure 47 – RWZI Grou carousel unit: 1 - Mixers; 2 - Position of the US sensor and optic sensor for TSS.



Google maps, modificado (2022)

Figure 48 – US sensor (on the left) and optic sensor (TSS) in the carousel

8.2.2.1.2 Overview of RWZI Leeuwarden (medium STP)

RWZI Leeuwarden is a medium STP located in the capital of Fryslân (The Netherlands). The plant was design to treat sewage of an equivalent population of 200 000 inhabitants (Figure 49). The US sensor was installed in a carousel unit with a 10 meters cable connected to a control box and a datalogger (EL-USB-4). The carousel unit works similarly to RWZI Grou. Control box and the datalogger were kept inside a safe house. US sensor was located around 68 meters from the already installed optic sensor (for TSS measurements) (Figure 47) and 40 cm below typical surface level (Figure 51). Samples for the gravimetric test (TSS) were collected at the same height where US sensor was located.

Figure 49 – RWZI Leeuwarden: 1 - Preliminary treatment; 2 - Carousel units; 3- Sludge thickening, dewatering, anaerobic digestors and biogas treatment; 4 - Secondary sedimentation tanks. The circled area correspond to the carousel unit where the sensors were installed.

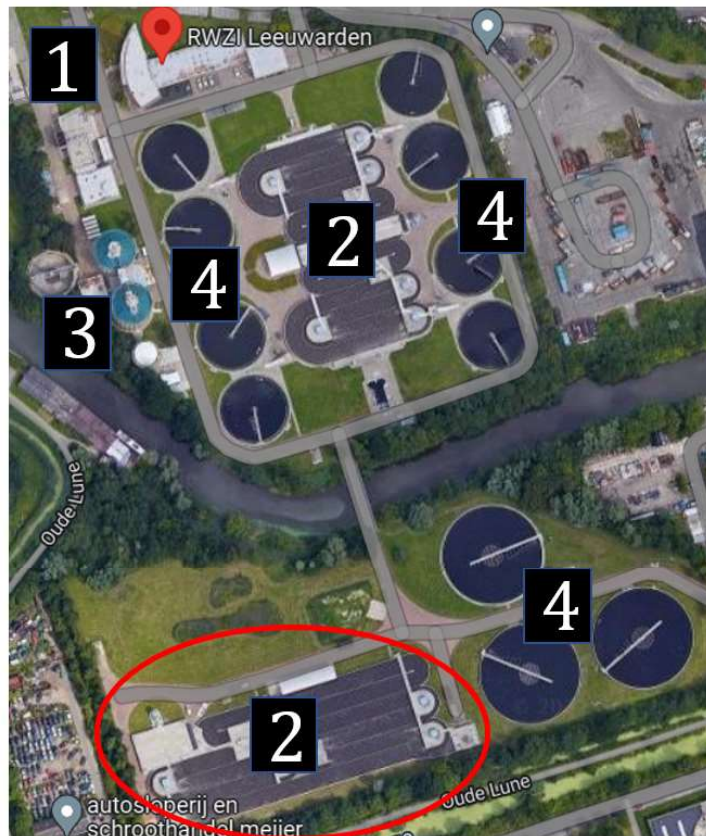


Figure 50 – RWZI Leeuwarden carousel unit: 1 - Optic sensor location; 2 - Ultrasonic sensor location

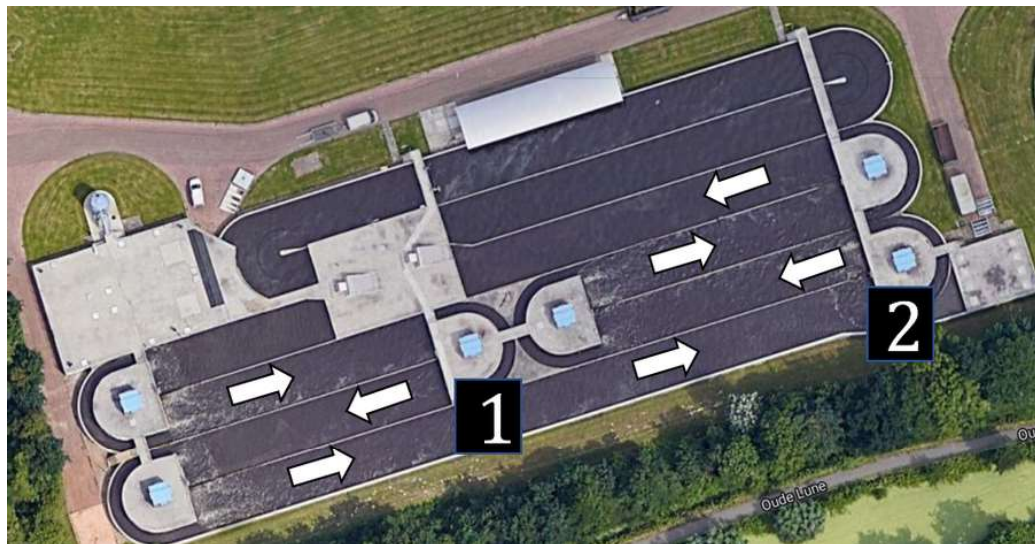
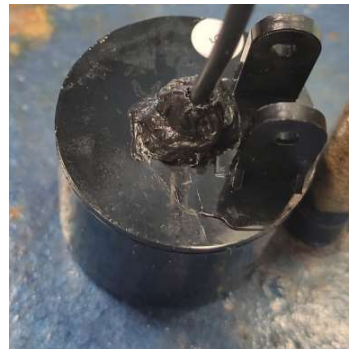


Figure 51 – US sensor in RWZI Leeuwarden, on the right

While in RWZI Grou instrumentation follow the scheme previously described with a laptop to record the data (Realterm software), the control box (with the arduino), and the US sensor (Figure 3), in RWZI Leeuwarden the configuration was different. Since the laptop stopped recording the data for unknown reasons, a datalogger EL-USB-4 was used instead. The new configuration is more similar to the US sensor real application, since no laptop is needed.

Since the transducer was damaged because the water entrance in RWZI Grou, a new transducer was used in RWZI Leeuwarden. It was added Beral uni-seal on it, in order to protect the new transducer interior from water (Figure 52)

Figure 52 – Beral uni-seal added to the transducer for water-tight protection

8.2.3 Calibration

The US sensor was calibrated with results obtained from TSS gravimetric test done according to APHA/AWWA/WEF (2017). In RWZI Grou MLSS kept in a short range level of 0.31% - 0.35%, thus calibration was performed with approximately the same level of solids concentration. TSS gravimetric test were compared with the arduino routine calculation for the peak area measured by the US sensor. For RWZI Leeuwarden calibration could be done with more points, since it was tested for a longer time and the variation of solids in the mixed liquor was greater during that period (0.28%-0.41%) according to the gravimetric tests performed. TSS gravimetric test was compared with the current measured by the US sensor and stored by a data

logger. In both situations tap water was used as reference for 0% of TSS. Calibration curve in Grou and Leeuwarden can be seen in Figure 53 and Figure 54.

Figure 53 – US sensor calibration in RWZI Grou

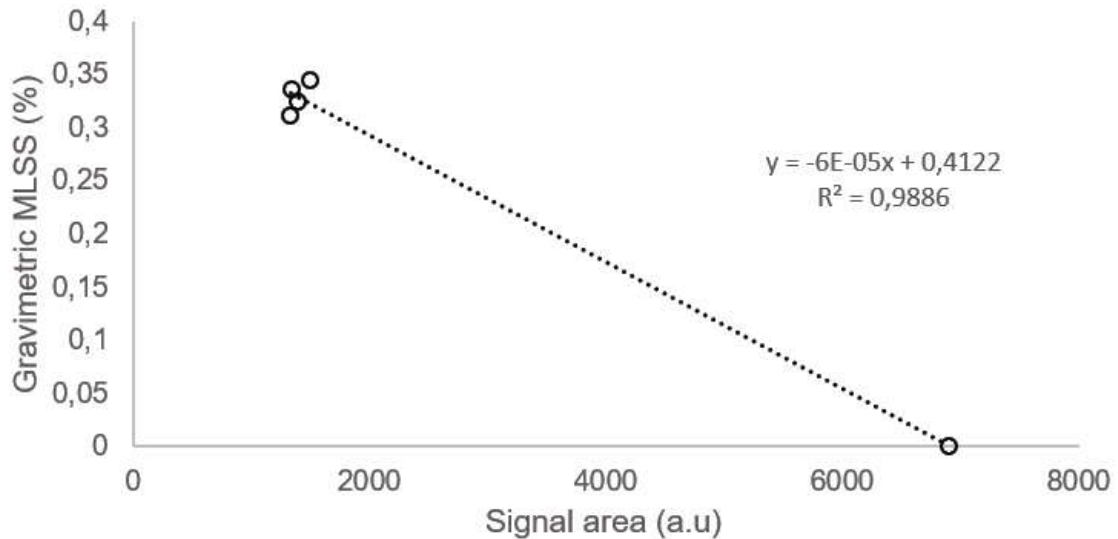
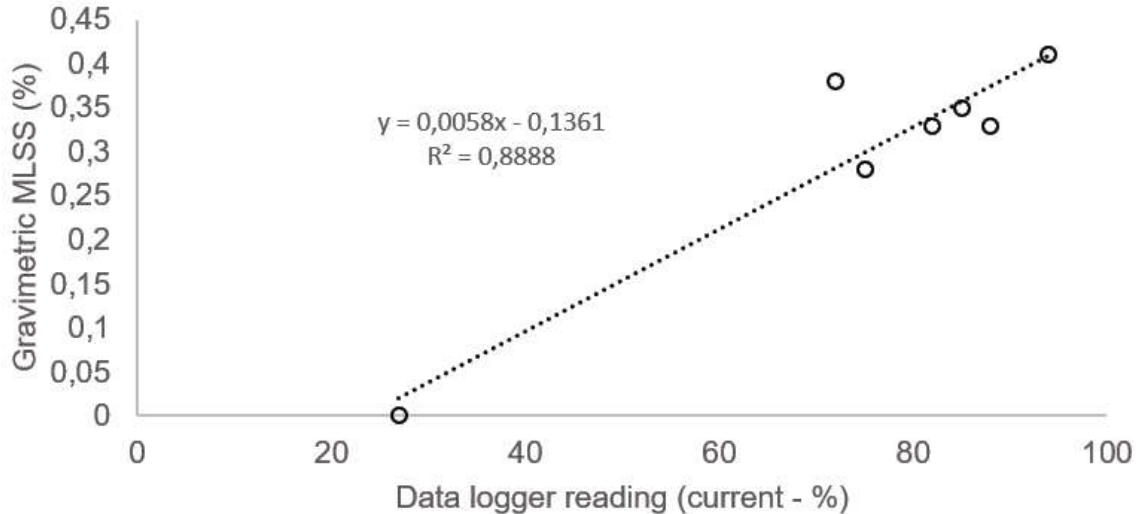


Figure 54 – US sensor calibration in RWZI Leeuwarden



- **Hypothesis statistical tests - Correlation of parameters**

For both STP descriptive statistic was evaluated for the measurements of US sensor, optic sensor, inflow rate and gravimetric test (MLSS). Shapiro Wilk test on MATLAB was used to determine the normality of each data (BENSAÏDA, 2009). In order to evaluate the correlation between the parameters, spearman coefficient and pearson coefficient were calculated, regarding the data normality. Spearman coefficient is used for non-parametric data, while pearson for parametric data (VON-SPERLING; VERBYLA; OLIVEIRA, 2020).

The hypothesis created for the statistical analysis were, (for TSS parameters x TSS parameters) :

H_0 : correlation between both analyzed parameters is ≤ 0 for a confidence level of 99%.

H_A : correlation between both analyzed parameters is > 0 for a confidence level of 99%.

The hypothesis created for the statistical analysis were, (for inflow x TSS parameters):

H_0 : correlation between both analyzed parameters is 0 for a confidence level of 99%. H_A : correlation between both analyzed parameters is different from 0 for a confidence level of 99%.

H_0 is the null hypothesis, and H_A is the alternative hypothesis.

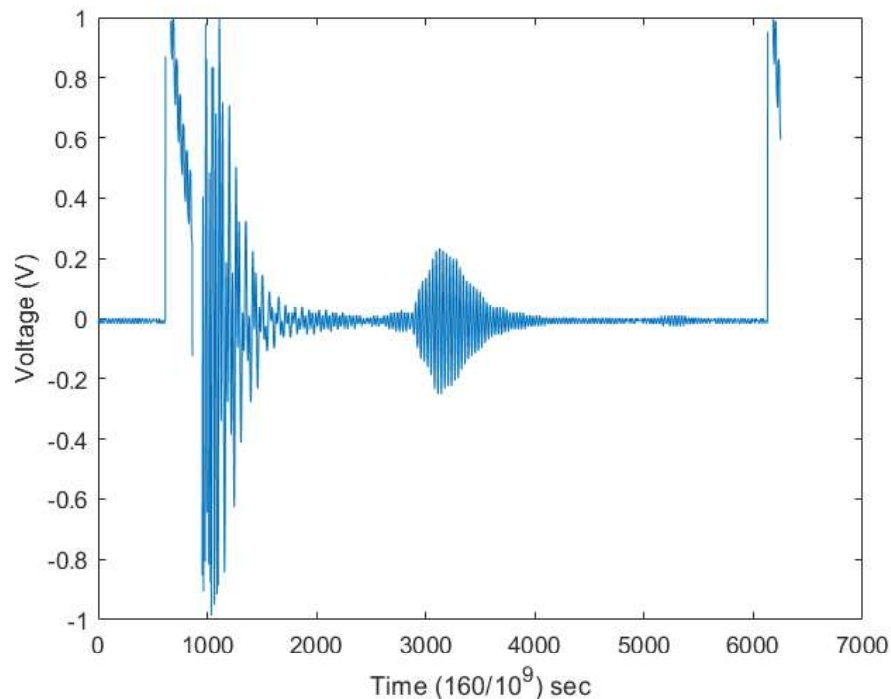
For all statistic analysis, measurements from US sensor and optic sensor were considered below 0.46% of TSS. High TSS estimation values are most probably because of solids accumulation in both sensors.

8.2.4 Results and discussion

8.2.4.1 RWZI Grou

In the oscilloscope view of the signal (Figure 55) it is noticeable that after the reflection peak, no other peak appeared. In lab scale, after the reflection peak, others peaks appeared because of the setup reflection.

Figure 55 – Signal visualization from the oscilloscope in Grou - 17-03-2022



Distribution of the data was evaluated within a period between March 24 and April 1 of 2022. Figure 56 indicates a normal distribution by the ultrasonic measurement during the period of one week in RWZI Grou. MLSS estimated concentration around 0.34% were more frequent. It is a different tendency when compared to the application of the US sensor in still water (Figure

57). Hence, as the variation of the US sensor measurement occur in a smaller scale with still water, the variability of the MLSS estimated by the US sensor in the plant is probably because of real variations on the MLSS concentration.

Figure 56 – Frequency distribution of US sensor MLSS estimation from 24/03/2022 to 01/04/2022 - RWZI Grou

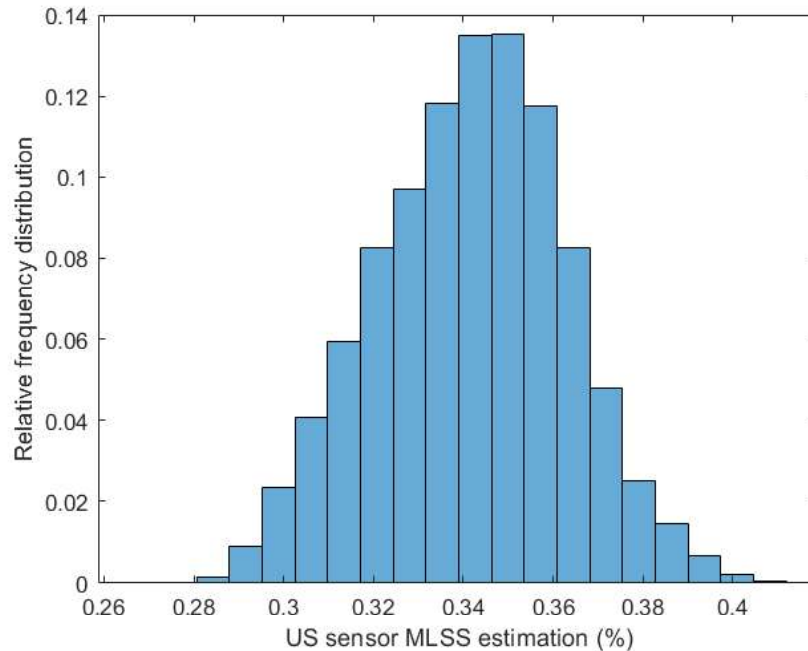
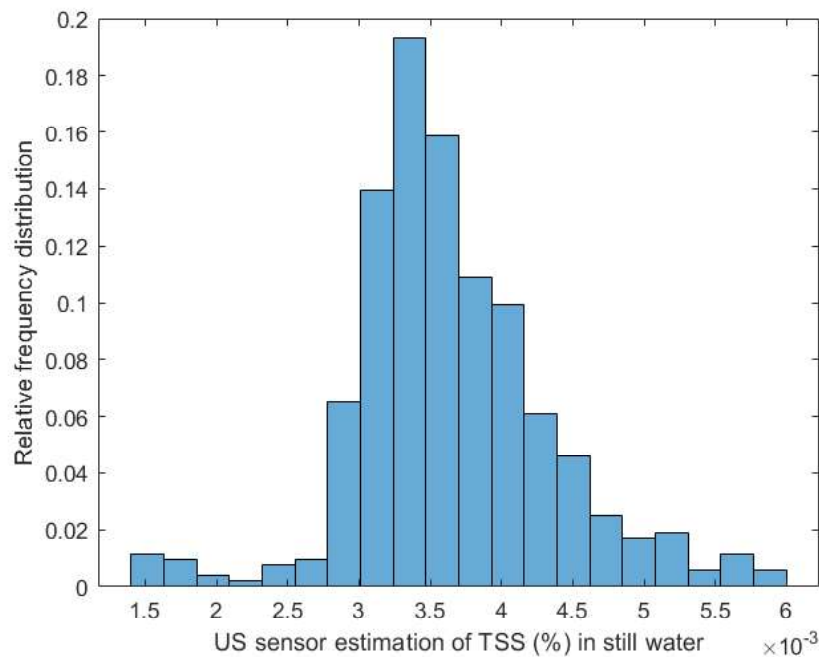


Figure 57 – Frequency distribution for the US sensor estimation of TSS in still water



The US sensor and the optic sensor presented similar performances during the testing period. However, the ultrasonic sensor presented bigger data variance, even though the standard

deviation is still very low (Table 15). The descriptive statistic of the measurements indicate a similar range between the MLSS average and the gravimetric tests, the optic and ultrasonic sensors, all of them with a low standard deviation. The variation of the TSS estimation by both sensors in a time series can be seen in Figure 58. Although there were only a few gravimetric analyses done in the period, they match well with the values estimation by both sensors. It is expected that the variation of the TSS values observed in the ultrasonic sensor data probably reflects real variations of the solids concentration in the mixed liquor, even though more solids analysis would be necessary to prove this hypothesis.

Table 15 – Descriptive statistics of the optic sensor, ultrasonic sensor and the inflow rate

Parameter(s)	Mean	Standard deviation	Maximum	Minimum	n
Optic sensor (MLSS %)	0.32	0.01	0.34	0.31	178
US sensor (MLSS %)	0.34	0.02	0.40	0.28	178
Gravimetric test (MLSS %)	0.34	0.01	0.35	0.33	4
Inflow rate (m ³ .h ⁻¹)	124.00	112.08	755.70	0.70	178

Figure 58 – Time series of the MLSS measurement for the ultrasonic sensor, optic sensor and gravimetric test - RWZI Grou

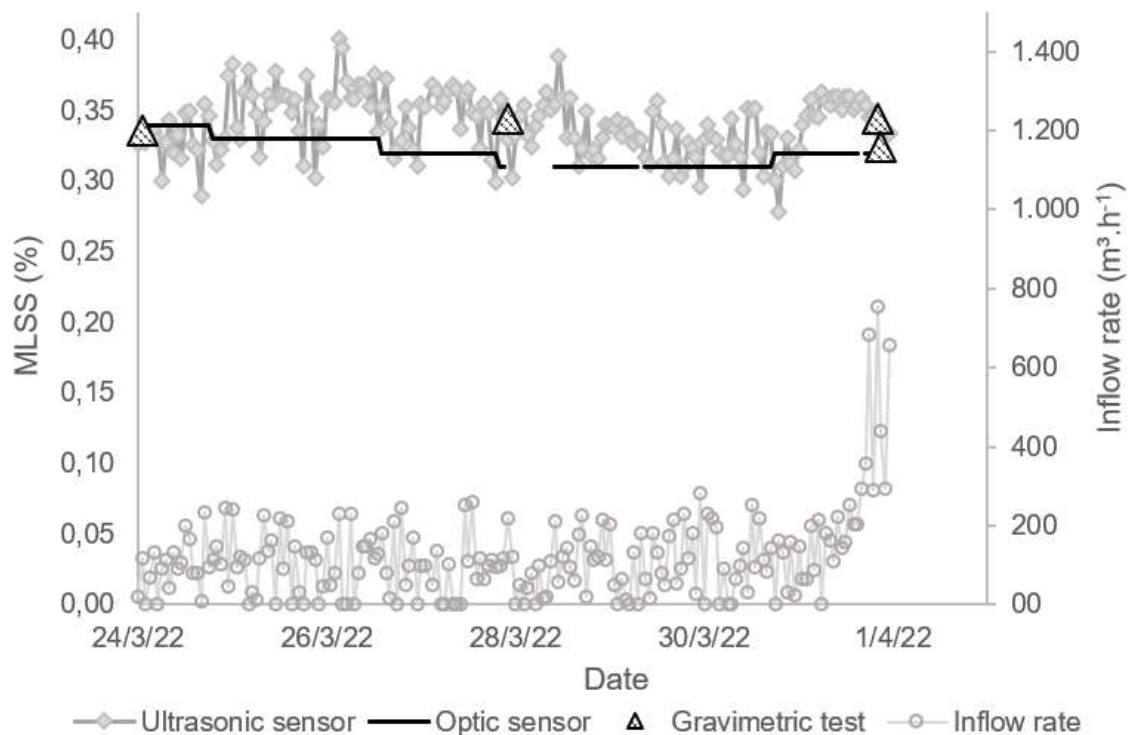


Figure 58 shows that TSS range in the effluent stayed within expected values of 0.20-0.40 % (METCALF EDDY, 2003) during the tested period. von-Sperling (2016) reported that MLSS should maintain in a range below 0.45-0.50 % as bigger values may cause overload of the secondary sedimentation tanks.

Most of the data obtained by the ultrasonic sensor in a UASB reactor kept in the range of 0.1-0.2 % of TS (NEVES *et al.*, 2021). The application in the carousel had an average TS concentration of 0.5 %. Such results reinforce previous prediction in which the sensor could be used within a range of 0.1-0.5 % of TS. For activated sludge, however, TSS is a more typical parameter to monitoring solids. The already commercial optic sensor was already calibrated to give the measurements in terms of TSS, therefore, the same was done for the US sensor.

- **Statistical hypothesis tests - Correlation of parameters**

The low spearman and pearson coefficient and the low covariance (cov) indicates that the correlation between the US sensor and optic sensor is low, although the correlation is greater than 0 for a confidence level of 99 % (Table 16). However, since MLSS was kept in a similar range level during the analyzed period, the variations were too small for a more complete evaluation. Inflow rate was also an important information in order to confirm, whether the sensor is affected by it or not. From march 24, until march 31, the inflow rate variate in the range of $0.7 \text{ m}^3 \cdot \text{h}^{-1}$ - $300 \text{ m}^3 \cdot \text{h}^{-1}$. On April 1, the inflow rate raised to values around $600 \text{ m}^3 \cdot \text{h}^{-1}$. Nevertheless, the shift in the inflow rate did not correlate to either US sensor measurements or optic sensor. Low covariance and the non rejection of H_0 even with a high number of samples (n), explain this conclusion. Furthermore, the correlation with both sensors with the gravimetric measurements had a high p-value, thus, H_0 could not be rejected. This result can be explained because of the low number of samples collected for the gravimetric test during the analyzed period. Moreover, although gravimetric test is more trustable than both sensors, error on collecting a representative sample could generate a non representative result.

Table 16 – Correlation parameters in RWZI Grou for a period of one week.

Parameter(s)	Spearman coef.	p-value	Pearson coef.	p-value	Cov.	Conclusion
US sensor x Optic sensor	0.25	<0.01	0.20	<0.01	<0.01 and >0	Reject H_0 (p-value<0.01). Correlation is significantly greater than 0 for a confidence level of 99%, however, with a low correlation coefficient.
US sensor x Inflow rate	0.01	0.86	0.01	0.86	<0.01 and >0	H_0 can not be rejected (p-value>0.01), therefore, correlation is not significantly different from zero at a confidence level of 99%
Optic sensor x Inflow rate	-0.04	0.60	-0.05	0.48	<0.01 and >-0.01	H_0 can not be rejected (p-value>0.01), therefore, correlation is not significantly different from zero at a confidence level of 99%
Gravimetric test x US sensor	0.00	0.67	0.34	0.33	0.18	H_0 can not be rejected (p-value>0.01), therefore, correlation is not significantly different from zero at a confidence level of 99%
Gravimetric test x Optic sensor	-0.63	0.91	-0.28	0.64	-0.03	H_0 can not be rejected (p-value>0.01), therefore, correlation is not significantly different from zero at a confidence level of 99%
Gravimetric test x Inflow rate	-0.80	0.33	-0.78	0.22	<0.01 and >0	H_0 can not be rejected (p-value>0.01), therefore, correlation is not significantly different from zero at a confidence level of 99%

- ***Mechanical and electronic problems with the US sensor***

In the analyzed period both sensors were not cleaned. Solids accumulation on the optic sensor can be seen in Figure 59, while solids accumulation from the US sensor after one week can be seen in Figure 60. Most of the solids adhered to the sensors was hair. However, even that no cleaning was conducted during the tests, no significant change was perceived in the measurements. MLSS kept in the same range for both sensors, which was confirmed by the gravimetric test. Probably, solids adhered on the sensor, kept floating on the flow direction,

which may have avoided the deposit of these solids in the region between the transducer and the reflection surface. However, if the amount of solids is too heavy, probably the mixed liquor flow will not be enough to avoid those deposit, which can occur after a longer period of time or a greater presence of hairs in the mixed liquor.

Figure 59 – Solids accumulation on the optic sensor (RWZI Grou)



Figure 60 – Solids accumulation on the ultrasonic sensor after one week (RWZI Grou)



8.2.4.2 RWZI Leeuwarden

For a better visualization of the data during the analyzed period it was plotted a time series of the US sensor, optic sensor and gravimetric measurements (Figure 61). The plot indicates a good match between the gravimetric, optic and ultrasonic sensor until 08 of June. After that time, US sensor estimation for MLSS reached a minimum value of 0.08% (Table 17), which is below typical values in activated sludge system. However, optic sensor measurements continuous on the range of 0.3%, and the same occurred for the gravimetric test. The amount of nitrogen bubbles adhered to the solids could be an aspect that may explain this difference, depending on the denitrification efficiency, since the sensor is located in an anoxic zone. However, more information is needed to confirm this hypothesis, such as dissolved oxygen, nitrate and the removal of TKN (Total Kjeldahl Nitrogen) in the unit.

Moreover, optic sensor by June 12, suffer a great increment on MLSS estimation measurement (up to 1.1%). The responsible for cleaning the sensor was on vacation by that time, hence, the optic sensor was not cleaned, as it usually is twice a week. Compared to Grou, inflow rate did not show a good correlation with MLSS concentration as well. Table 17 complement the tendency of a better match by the optic sensor with gravimetric test pointed on Figure 61, considering only the measurements when both sensors were cleaned.

Figure 61 – Time series - Ultrasonic sensor, optic sensor, gravimetric test for MLSS measurement in RWZI Leeuwarden

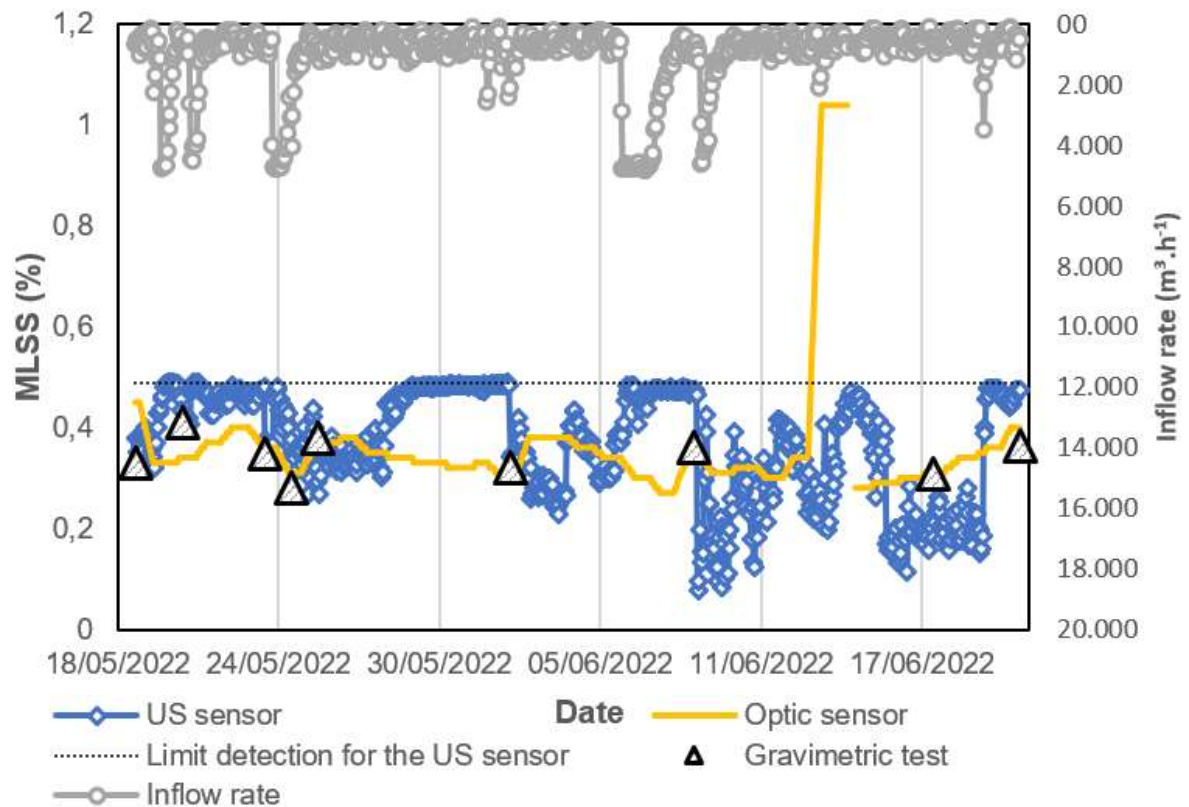
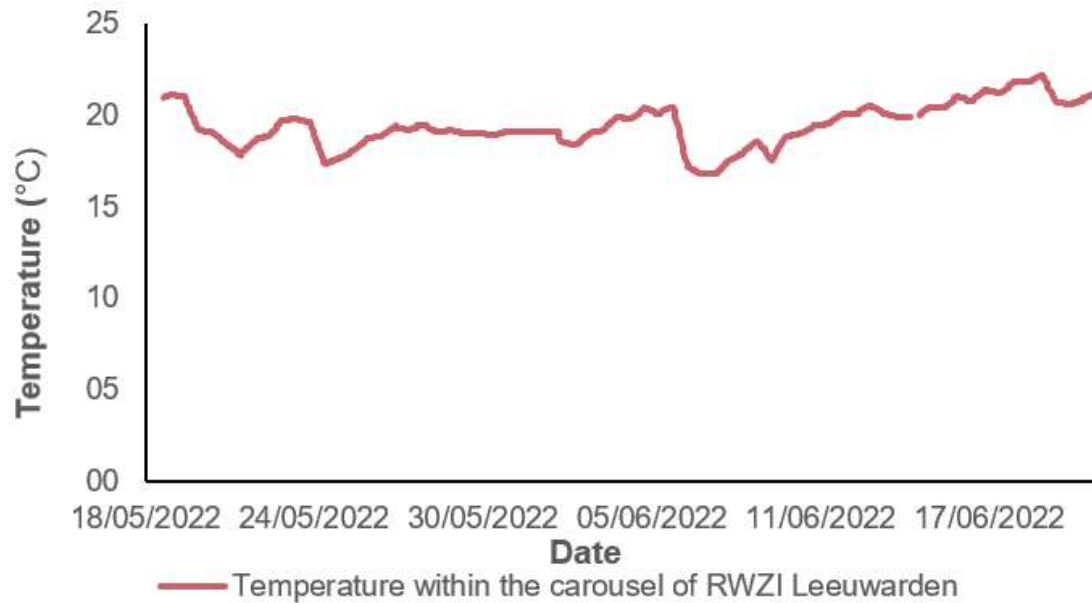


Table 17 – Descriptive statistics of the data collected in RWZI Leeuwarden during the period of 18/05/2022 to 20/06/2022

Parameters	Median	Mean	Standard deviation	Maximum	Minimum	n
US sensor (MLSS %)	0.33	0.31	0.09	0.45*	0.08	512
Optic sensor (MLSS %)	0.34	0.34	0.03	0.45*	0.27	751
Gravimetric test (MLSS %)	0.35	0.34	0.04	0.41	0.28	9
Temperature (°C)	19.20	19.42	1.18	22.20	16.80	785
Inflow rate (m ³ .h ⁻¹)	706.20	1079.90	1147.40	4824.70	109.80	785

*Measurements for US sensor and optic sensor were adjusted (below 0.46), so the solids accumulation do not interfere on the statistic analysis

The test in RWZI Leeuwarden seems to repeat a unknown behavior that occurred on the WAC laboratory . From December of 2021 to January of 2022, the sensor was kept inside water in the WAC of Van Hall Lareinstein University. Surprisingly, signal amplification increased by that time without any mechanical or electrical adjustment. The same behavior seem to occur in RWZI Leeuwarden. Strangely, this behavior did not correspond to Neves *et al.* (2021) results that kept the same sensor inside a UASB reactor for 25 weeks without new calibrations. Underestimated MLSS by the US sensor seems to be occurred after one month within the carousel. Hence, calibration should probably be evaluated at least once a month. Moreover, for further tests, temperature should be corrected from the US sensor measurement since it can affect the signal as seen in chapter 5. During one month, however, temperature range kept in the same range (Figure 62).

Figure 62 – Time series of the mixed liquor temperature in RWZI Leeuwarden

Considering gravimetric measurements as reference, even though it may not be representative, it was calculated the relative error comparing optic and ultrasonic sensor measurements (Table 18). However, the comparison was made only for the period until June 8, since after that US sensor seems to require a new calibration as it presented an error greater than 5%. The results confirm the similar accuracy presented by both optic and US sensor compared to the gravimetric measurement, with an average relative error (Avge) of around 1% in both cases. Nevertheless, a high error observed on optic sensor (4.36%), it was probably because the optic sensor was not cleaned, and solids accumulation masked the result.

Table 18 – Relative error comparative from US sensor and optic sensor in RWZI Leeuwarden

Gravimetric (MLSS -%)	US sensor (MLSS - %)	Relative Error (%)	Optic sensor (MLSS - %)	Relative Error (%)
0.33	0.38	0.76	0.45	4.36
0.41	0.40	0.02	0.34	1.20
0.35	0.38	0.26	0.36	0.03
0.28	0.38	3.57	0.31	0.32
0.38	0.29	2.13	0.36	0.11
0.32	0.34	0.13	0.30	0.13
		Avge = 1.14		Avge = 1.02

- **Statistical hypothesis tests - Correlation of parameters**

Statistical hypothesis test were evaluated in which concern the correlation between the parameters on Table 19. The normality of the data was evaluated with Shapiro-Wilk test on

MATLAB (BENSAÏDA, 2009). Data used for the correlation with gravimetric test (Gravimetric test x US sensor, Gravimetric test x Optic sensor, Gravimetric test x Inflow rate) carry out on a normal distribution with a confidence level of 95%, therefore, Pearson coefficient was considered for those parameters. However, the rest of correlations (US sensor x Optic sensor, US sensor x inflow rate, Optic sensor x inflow rate) pointed a non-normal distribution, therefore, spearman coefficient was considered for these parameters. The coefficients considered for the conclusions about the correlation were underlined on Table 19. The difference on the results could be explained by the numbers of samples (n) for each group of correlation. All correlation with gravimetric test had only a number of sample equal to 6, while the correlations that presented a non-normal distribution had an n equal to 489.

Table 19 – Correlation between parameters in RWZI Leeuwarden for a period of one month

Parameters	Spearman coef.	p-value	Pearson coef.	p-value	Cov.	Conclusion
US sensor x Optic sensor	<u>0.26</u>	<u><0.01</u>	0.29	<0.01	<0.01 and >0	Reject H ₀ (p-value<0.01). Correlation is significantly greater than 0 for a confidence level of 99%, however, with a low correlation coefficient.
US sensor x Inflow rate	<u>0.07</u>	<u>0.11</u>	0.16	<0.01	<0.01 and >0	H ₀ can not be rejected (p-value>0.01), therefore, correlation is not significantly different from zero at a confidence level of 99%.
Optic sensor x Inflow rate	<u>-0.13</u>	<u><0.01</u>	-0.15	<0.01	>0.01 and <0	H ₀ rejected (p-value<0.01), therefore, correlation is significantly different from zero at a confidence level of 99%.
Gravimetric test x US sensor	0.23	0.33	<u>0.24</u>	<u>0.32</u>	<0.01 and > 0	H ₀ can not be rejected (p-value>0.01), therefore, correlation is not significantly different from zero at a confidence level of 99%.
Gravimetric test x Optic sensor	0.41	0.22	<u>0.17</u>	<u>0.37</u>	<0.01 and >0	H ₀ can not be rejected (p-value>0.01), therefore, correlation is not significantly different from zero at a confidence level of 99%.
Gravimetric test x Inflow rate	-0.22	0.58	<u>-0.63</u>	<u>0.07</u>	>-0.01 and < 0	H ₀ can not be rejected (p-value>0.01), therefore, correlation is not significantly different from zero at a confidence level of 99%.

In summary all the results presented on Table 19 pointed a low or non correlation between all evaluated parameters. In spite of a positive correlation between Gravimetric test x US sensor, Gravimetric test x Optic sensor, US sensor x Optic sensor was significant for a confidence level of 99%, Spearman and Pearson coefficient were low for all of them. Low correlation can be explained by the distance between US sensor and Optic sensor (68 m) and mixing conditions. Moreover, although gravimetric test is more accurate than sensors, manual sampling could be a reason of a non representative result. Solids accumulation at the sensors could also have a partial interference on the results, even after eliminating those measurements above 0.46% of TSS by

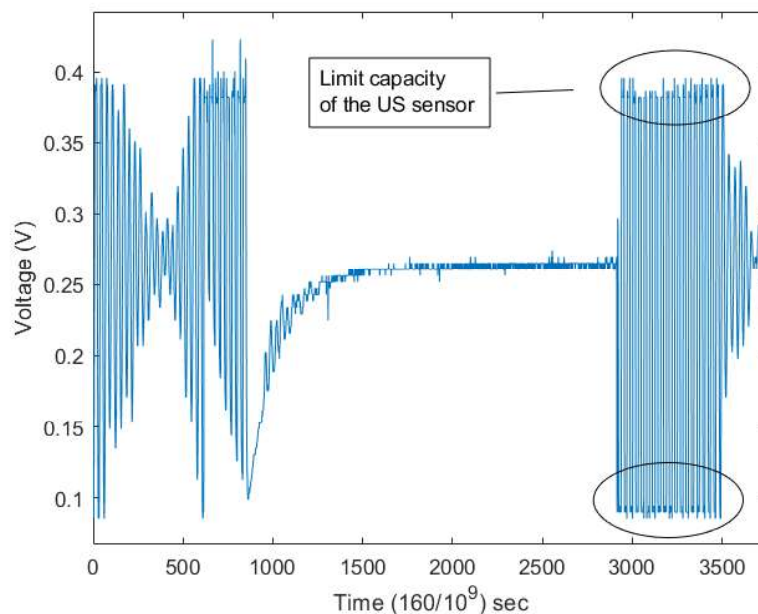
the sensors.

Inflow rate correlation with the sensors and gravimetric test presented a curious result. While the correlation with US sensor and gravimetric measurements was not significantly different from zero, the correlation with the optic sensor test were. Even more, presented a negative correlation with the inflow rate. Greater inflow rates are associated with rain, since the sewage system is unitary in the Netherlands. One possible explanation for the negative correlation is that rain (greater inflow rate) could dilute solids concentration of the mixed liquor. Gravimetric test x Inflow rate presented a relatively high negative correlation (Pearson coefficient), which corroborates with this hypothesis, even though low number of samples were not enough to reject H_0 .

- ***Mechanic and electronic considerations***

Limit detection from the US sensor during full-scale test was 0.49% of TSS. In order to increase this limit, calibration could be realized only with sludge measurements, not water. Calibration with water demands a limit amplification of the signal, otherwise the sensor reading will not correspond with actual scenario. Figure 63 is an example where signal was over ranged, hence the correspondence voltage is lower than it should be. A scenario only with water represent the best scenario for higher values of the signal, since there is almost no obstacle to attenuate it. Therefore, calibration only with sludge allows greater signal amplification without any over range.

Figure 63 – Example of signal overrate (DC)



Comparing the solids accumulation from Grou and Leeuwarden on the sensor, it is clear that plant size and characteristic can greatly influence on the amount of solids adhered to the sensor. Hence, cleaning routine should be adjusted for each specific STP. Solids accumulation in Leeuwarden can be seen in Figure 64.

Figure 64 – Solids accumulation on the US sensor after two days - RWZI Leeuwarden

Depending on the position of the solids accumulated at the sensor, it is possible to detect and alert operators to clean it. For that, the region before the first reflection peak should be analyzed and incorporated to the Arduino code. If this region has a high correspondent area value, it probably means that there is something blocking the signal.

Furthermore, the seal used to protect the transducer seem to work, at least for a period of two months (sensor was installed in RWZI Leeuwarden one month before data collection). No damage was observed during that period, while in RWZI Grou, after two weeks water entered the transducer and damage it.

8.2.5 Conclusion

The US sensor was compared to an optic commercial sensor in a small and medium full-scale activated sludge system, and showed similar measurements of MLSS double-checked with the gravimetric test. The relative error from US sensor and the optic sensor compared to the gravimetric test were 1.14% and 1.02% respectively, during a period of 5 weeks in the STP of Leeuwarden (medium scale). A cleaning routine of the sensors must be implemented in both cases and should be adjusted depending on the STP characteristics. Furthermore, at the medium STP, the US sensor had its signal increased after the third week without any electrical or mechanical adjustment, resulting on the underestimation of the MLSS (minimum 0.08% of TSS). Gravimetric test and optic sensor had their measurements around 0.3% of TSS at the same time. This probably indicate that a new calibration was necessary to maintain the sensor functional.

9 COST ANALYSIS (US SENSOR X GRAVIMETRIC TEST)

9.1 Introduction

Besides the initial cost for a real time monitoring sensor (Table 2), operational cost involving monitoring of solids is relevant to be evaluated not only considering the application for sanitation companies, but also for the research that is done in the universities. This chapter will evaluate energy consumption between the gravimetric test and the US sensor and the analysis cost for the gravimetric test.

9.2 Methodology

- **Energy costs**

In order to evaluate the operational cost of the US sensor for solids monitoring it was compared the energy cost between US sensor, a drying oven (DO) and water bath (WB) used in the Federal University of Minas Gerais (UFMG) at the chemical physicist laboratory for the gravimetric analysis.

To evaluate the energy consumption for the gravimetric test for TS it was considered a weekly frequency during a period of one year with two different scenarios. First scenario considering 24 hours of drying oven use (the worst scenario - WS), which is a common practice in a research laboratory and secondly considering 3 hours of warm bath plus 1 hour of drying oven (the best scenario - BS), which is the faster way to conclude the TS analysis. For the comparative of the TSS test, it was considered a daily monitoring, which correspond to the monitoring program for the MLSS reported by von-Sperling (2016). The power from the drying oven in the university is 1000 W, while the power from the warm bath is 1840 W.

For the US sensor, power was calculated considering the voltage of 12 V and a current of 0.2 A, that was measured with a multimeter. It was considered that the sensor will be functioning continuously.

The cost considered two tax values, “green flag” which means energy costs do not have additional taxes and “red flag”, which considered additional taxes for energy payment. The taxes values were obtained from the Energy Company of Minas Gerais in the year of 2021 (CEMIG, 2021).

- **Analysis costs**

Analysis costs were evaluated by TS and TSS quotation for each sample by a certified company in Brazil during the year of 2022. For TSS quotation, it was considered a daily monitoring, which is typical for activated sludge systems. For TS quotation it was considered a weekly monitoring, with one sampling point and three sampling point (sludge profile). Sampling costs were not considered on this analysis, since it will depend on the distance between the laboratory company and the STP.

9.3 Results and discussion

- **Energy costs**

Considering the moment of scarcity of financial resources and with an increasing energy demand, a comparison was made between the US sensor and the equipment used for the gravimetric test. Thus, it was evaluated the energy expenditure and its financial cost. The results can be seen in Table 20. Even gravimetric test for TSS that had the lower energy demand of the gravimetric tests, showed a much greater energy consumption compared to the US sensor, that had a very small energy consumption. The US sensor had an energy cost 59 times lower than the prediction to the gravimetric test, considering the worst case scenario (WS). Greater energy consumption had an important environment impact, but it depends on the source of the energy. In Brazil, for example, most of the energetic matrix is hydroelectric, a renewable energy. However, the dependency of such matrix is a problem in Brazil, since the country is experiencing water crisis in several places (GRANZIERA; REI, 2015). Moreover, even renewable energy can cause environmental impacts. Hydroelectric plant demands the construction of dams and causes the flooding of immense areas, forcing in many cases the local population exodus, which can cause complex damages to cultural and social values. In addition, irreparable damage to local fauna and flora, with possible loss of biodiversity and alteration of the navigability of rivers may also occur. The flood of great areas generates the decomposition of existing vegetation, compromising local biodiversity and inducing the release of methane gas, responsible for the greenhouse effect and decrease on ozone layer (INATOMI; UDAETA, 2005).

Table 20 – Comparison of energetic cost for TS and TSS monitoring by US sensor and the gravimetric test

Parameter(s)	US sensor	Gravimetric test for TS (WS)	Gravimetric test for TS (BS)	Gravimetric test (TSS)
Power (W)	1.04	1000 (DO)	1840 (BW) & 1000 (DO)	1000
Annual consumption (kWh)	9.15	1248	339	365
Weekly up time (h)	168	24	4	7
Annual cost (R\$)	13.00 - 13.81	771.41 - 819.57	245.73 - 256.80	241.07-256.12

- **Analysis costs**

Analysis costs involving the gravimetric test by a certified laboratory in Brazil (Table 21) showed that for one year of TSS analysis the same value was observed for an already commercial low-cost optic sensor (Table 2). TS single sample point compared to energy cost had similar values. Nevertheless, TS monitoring for the sludge profile carry out in a much higher cost considering laboratory analysis. The estimated costs considered typical monitoring frequency for each parameter (TS and TSS) regarding the application in activated sludge system (mixed liquor) and UASB reactors. However, in Brazil most of the STPs do not have a proper routine for monitoring control, hence, effluent quality is compromised.

Table 21 – Laboratory cost for TS and TSS analysis

Parameter	TSS	TS (single sample point)	TS (sludge profile)
Period (days)	365	365	365
Analysis frequency	daily	weekly	weekly
*Analysis cost (unit) - R\$	15	15	15
Annual cost - R\$.year ⁻¹	5,475.00	780.00	2,340.00

Quotation from 2022, in Belo Horizonte.

9.4 Conclusion

Lower energy demand is always a positive aspect when sustainability is an objective to be achieved. Besides lower environmental impact due to energy demand, real time monitoring also showed to be much cheaper option for the TS and TSS monitoring, regarding operational costs. That was even more evident when comparing laboratory analysis costs for TS and TSS. Annual cost for TSS monitoring in an activated sludge system, that usually requires a daily monitoring was R\$ 5,475.00, which is similar to an already commercial optic sensor (\$ 950.00) However, the acceptance and confidence on the technology by the operators and researchers is an essential requirement in order to change paradigm for either researching (by using more data from sensors, which can save a lot of time for the researcher evaluate more important aspects of their researches) and operating (Cleaning routines for the sensor is better than collecting and processing samples?).

10 FINAL CONSIDERATIONS

10.1 *Signal interference*

The research determined how several factors can interfere in the ultrasonic signal. Temperature can be predicted by the ultrasonic sensor, by calculating the ERT, thus, it can be applied in regions with a large amplitude of temperature. However, a more consolidated model to predict temperature interference on attenuation should be realized together with other variables such as solids concentration and bubbles flow rate. ERT can be used to predict distances from the transducer and the reflection surface. Moreover, depending on the distances, maximum potential response from the sensor varies proportionally in a range within 20 cm, which can be predicted as well. The minimum safe distance to optimize the potential signal from the transducer was found out to be 23 cm.

Attenuation of the signal can vary according to the air flow rate. Low flow rate is recommended for the frequency of 200 kHz, and the sensor's position should be horizontal to avoid the accumulation of bubbles in the transducer surface. However, with the current data treatment routine, correlation between solids concentration and the presence of bubbles were not observed, in a flow rate of $0.58 \text{ L}\cdot\text{m}^{-2}\cdot\text{min}^{-1}$. Furthermore, a model capable of compensate bubbles effect should be developed for a wider application of the US sensor. Depending on the type of solids, ultrasonic signal showed different attenuation levels. Therefore, a large variation on the sludge composition can greatly interfere on the measurements. For instance, a punctual high concentrated industrial discharge and/or the presence of sand in the mixed liquor, specially for technologies that do not precede primary sedimentation tanks.

10.2 *Sludge blanket level*

Sludge blanket level determination in real time is an effective way of controlling the sludge from clarifiers of primary and secondary sedimentation tanks. However, the US sensor did not show a positive correlation with the manual test, although it was only tested for the range between 0.05 and 0.10 m. The results are still inconclusive, probably the sensor will need a frequency above 200 kHz for better results which will carry out in a high-cost for a technology that should be low-cost. In that case, testing the US sensor with a wider range and expecting a lower accuracy may be a better option for further tests.

10.3 *Full-scale application*

The ultrasonic sensor was compared to an optic commercial sensor in a small (STP Grou) and medium (STP Leeuwarden) full-scale activated sludge system in the Netherlands, and showed similar measurements of MLSS double-checked with the gravimetric test. The relative error from US sensor and the optic sensor compared to the gravimetric test were 1.14% and 1.02% respectively, during a period of 5 weeks in the STP of Leeuwarden (medium scale).

A cleaning routine of the sensors must be implemented in both cases and should be adjusted depending on the STP characteristic. Furthermore, at the medium STP, the US sensor had its signal increased after the third week without any electrical or mechanical adjustment, resulting on the underestimation of the MLSS (minimum 0.08% of TSS). Gravimetric tests and optic sensor had their measurements around 0.3% of TSS at the same time. This probably indicate that new calibration was necessary to maintain the sensor functional.

Application of the US sensor in a full-scale UASB reactor showed several perspectives regarding the sensor position within the reactor, despite no correlation between TS and attenuation were observed. Solids accumulation on the sensor in UASB reactors will be probably more challenging compared to activated sludge system, since anaerobic reactor are closed and more difficult to access. However, the application of the US sensor with an Arduino system, and the continuous data generated, could provide important information regarding its use in UASB reactors. A comparative between the application in the center and lateral part of the reactor, above and below the deflectors are recommended.

It is expected in future application of the US sensor that a new design for the reflection surface will be used. A cleaner design with less surface to prevent sensor fouling in between the reflection surface and the transducer is recommended. Moreover, the low-cost attraction of the US sensor and the national domain of the technology can make it dissemination easier, since maintenance and communication with the producers would be favored. The few alternatives currently offered on the market for low-cost sensor opens the possibility of the improvement and conclusion of the US sensor. Such possibility can make the US sensor an important tool for real time monitoring of solids in developing countries, especially Brazil, which contain the know-how of such technology.

11 RECOMMENDATIONS

- Full-scale application in UASB reactors with an Arduino control and a data logger in two different position simultaneously (central position and lateral position above the deflectors).
- Temperature correction in full-scale application
- Full-scale application for sludge thickening units and sludge digestors.
- Correlation between biogas production and attenuation from an ultrasonic sensor with a frequency below 200 kHz in different regions within the reactor.
- Sludge blanket level determination by an ultrasonic sensor with a greater range of the blanket height (0.3 m - 0.6 m)
- Bubbles effect on attenuation with different type of gases and with a flow rate compatible to UASB reactors

REFERENCES

- ABDA, F.; AZBAID, A.; ENSMINGER, D.; FISCHER, S.; FRANÇOIS, P.; SCHMITT, P.; PALLARÈS, A. Ultrasonic device for real-time sewage velocity and suspended particles concentration measurements. *Water Science & Technology*, IWA Publishing, v. 60, n. 1, p. 117 – 125, July 2009.
- ABUSAM, A.; MYDLARCZYK, A. Assessment of the operational performances of two activated sludge systems in Kuwait. *Environ Monit Assess*, v. 190, n. 514, 2018. Available at: <https://doi.org/10.1007/s10661-018-6879-9>.
- ALPEN, E. L. *Radiation Biophysics*. 2. ed. [S.l.]: Elsevier Inc. All, 1998. ISBN 978-0-12-053085-4.
- ANA - AGÊNCIA NACIONAL DE ÁGUAS E SANEAMENTO BÁSICO. *Atualização da base de dados de estações de tratamento de esgotos no Brasil*. Brasília: Atlas esgotos, 2020.
- ANDREOLI, C. V.; VON-SPERLING, M.; FERNADES, F. *Lodo de esgotos: tratamento e disposição final*. 2. ed. Belo Horizonte: Editora UFMG, 2014. v. 6. 444 p. (Princípio do tratamento biológico de águas residuárias, v. 6). ISBN 978-85-423-0085-71.
- APHA/AWWA/WEF. *Standard Methods for the Examination of Water and Wastewater*. 23. ed. Washington DC: American Public Health Association, 2017. ISSN 55-1979. Available at: www.standardmethods.org.
- ARDERN, E.; LOCKETT, W. T. Experiments on the oxidation of sewage without the aid of filters. *Journal of the Society of Chemical Industry*, v. 33, n. 10, p. 523 – 539, May 1914. Available at: <https://doi.org/10.1002/jctb.5000331005>.
- BAMBERGER, J. A.; GREENWOOD, M. S. Using ultrasonic attenuation to monitor slurry mixing in real time. *Ultrasonics*, v. 42, p. 145 – 148, abril 2004. Available at: <https://doi.org/10.1016/j.ultras.2004.02.016>.
- BENSAÏDA, A. *Shapiro-Wilk and Shapiro-Francia normality tests*. 2009. MATLAB Central file exchange. Available at: <https://www.mathworks.com/matlabcentral/fileexchange/13964-shapiro-wilk-and-shapiro-francia-normality-tests>. Accessed on: 16 de março de 2022.
- BHASKARAN, P. K. Role of Gas Bubbles in the Attenuation of Acoustic Waves at the Air-Sea Interface. *Current science*, v. 107, n. 6, p. 983 – 993, September 2014.
- BOLLER, C.; CHANG, F.; FUJINO, Y. *Encyclopedia of Structural Health Monitoring*. [S.l.]: wiley, 2009. v. 1.
- BORGES, A. N.; RODRIGUES, C. G. *Introdução à Física Acústica*. 1. ed. São Paulo: Editora Livraria da Física, 2017. ISBN 978-85-7861-484-3.
- BOUDA, A. B.; LEBAILI, S.; BENCHAAALA, A. Grain size influence on ultrasonic velocities and attenuation. *NDT&E International*, Elsevier Science Ltd, v. 36, n. 1-5, Julho 2002.
- BOURGEOIS, W.; BURGESS, J. E.; STUETZ, R. M. On-line monitoring of wastewater quality: a review. *Chemical Technology and Biotechnology*, v. 76, n. 4, p. 337 – 348, Março 2001. Available at: <https://doi.org/10.1002/jctb.393>.
- BRASIL. Conselho Nacional do Meio Ambiente. *Resolução CONAMA 357*, Diário Oficial da União, Brasília, Março 2005.

- BRASIL. Conselho Nacional do Meio Ambiente. *Resolução CONAMA 430*, Diário Oficial da União, Maio 2011.
- BRASIL. DIÁRIO OFICIAL DA UNIÃO. *Resolução CONAMA nº 498*, n. 161, p. 265 –, Agosto 2020. ISSN 1677-7042.
- CAROVAC, A.; SMAJLOVIC, F.; JUNUZOVIC, D. Application of Ultrasound in Medicine. *Journal of Academy of Medical Sciences of B&H*, v. 19, n. 3, p. 168 – 171, Setembro 2011.
- CEMIG. *Valores de tarifas e serviços*. 2021. Available at: <https://www.cemig.com.br/atendimento/valores-de-tarifas-e-servicos/>. Accessed on: June, 07, 2021.
- CHEEKE, J. D. N. *Fundamentals and Application of Ultrasonic Waves*. [S.l.]: CRC press LLC, 2002. ISBN 0-8493-0130-0.
- CHEN, H.; NI, Y. Data Acquisition, Transmission and Management. In: CHEN, H.; NI, Y. (Ed.). *Structural Health Monitoring of Large Civil Engineering Structures*. John Wiley & Sons Ltd., 2018. chap. 3, p. 51 – 67. Available at: <https://doi.org/10.1002/9781119166641.ch3>.
- CHERNICHARO, C. A. L. *Reatores Anaeróbios*. 2. ed. Belo Horizonte: Editora UFMG, 2016. v. 5. 379 p. (Princípio do tratamento biológico de águas residuárias, v. 5). ISBN 9788542301724.
- CHERNICHARO, C. A. L.; BRESSANI-RIBEIRO, T.; LOBATO, L. C. Chapter 6: Operation of UASB Reactors for Sewage Treatment. In: PUBLISHING, I. (Ed.). *Anaerobic Reactors for Sewage Treatment: Design, construction and operation*. [S.l.]: IWA Publishing, 2019. chap. 6. ISBN 9781780409238.
- CHERNICHARO, C. A. L.; BRESSANI-RIBEIRO, T.; PEGORINI, E. S.; POSETTI, G. C.; MIKI, M. M.; SOUZA, S. N. Contribuição para o aprimoramento de projeto, construção e operação de reatores UASB aplicados ao tratamento de esgoto sanitário- Parte 1: Tópicos de Interesse. *Revista DAE*, v. 66, n. 214, p. 5 – 16, 2018.
- CLARK, H. W.; ADAMS, G. Sewage treatment by aeration and contact in tanks containing layers of slate. *Record*, v. 69, p. 158 – 159, 1914.
- COLLIVIGNARELLI, M. C.; ABBÀ, A.; FRATTAROLA, A.; MIINO, M. C.; PADOVANI, S.; KATSOYIANNIS, I.; TORRETTA, V. Legislation for the Reuse of Biosolids on Agricultural Land in Europe: Overview. *Sustainability*, v. 11, n. 21, October 2019. Available at: <https://www.mdpi.com/2071-1050/11/21/6015>.
- COLLIVIGNARELLI, M. C.; BERTANZA, G.; ABBÀ, A.; DAMIANI, S. Process auditing and performance improvement in a mixed wastewater-aqueous waste treatment plant. *Water Science & Technology*, v. 77, n. 4, p. 891 – 898, 2018.
- CUCCARO, R.; MAGNETTO, C.; ALBO, P. G.; TROIA, A.; LAGO, S. Temperature increase dependence on ultrasound attenuation coefficient in innovative tissue-mimicking materials. *Physics Procedia*, p. 187 – 190, 2015.
- DAKERS, J. L. Automation and Monitoring of Small Sewage Treatment Works. In: DRAKE, R. (Ed.). *Instrumentation and Control of Water and Wastewater Treatment and Transport Systems*. Pergamon, 1985. p. 413 – 417. ISBN 978-0-08-032591-0. Available at: <https://www.sciencedirect.com/science/article/pii/B9780080325910500592>.

EMRICH, A. L.; LOBATO, L. C. S.; ALMEIDA, P. G. S.; PORTO, M. F.; ALVES, L. V. R.; CHERNICHARO, C. A. L. Ferramenta computacional para gerenciamento de lodo e melhoria de desempenho de reatores UASB tratando esgoto doméstico. In: *Congresso Nacional de Saneamento, Associação Nacional de Serviços Municipais de Saneamento. Gramado (RS)*. [S.l.: s.n.], 2021.

EPA. *Wastewater Management Fact Sheet - Denitrifying Filters*. 2007. Available at: https://www.epa.gov/sites/default/files/2019-08/documents/denitrifying_filters_fact_sheet_p100il79.pdf. Accessed on: 12/06/2022.

GAO, X.; ALVO, M.; CHEN, J.; LI, G. Non parametric multiple comparison procedures for unbalanced one-way factorial designs. *Journal of Statistical Planning and Inference*, Elsevier Science Ltd, v. 138, n. 8, p. 2574 – 2591, August 2008.

GRANZIERA, M. L. M.; REI, F. *Energia e Meio Ambiente: Contribuições para o necessário diálogo*. Santos- SP: Editora universitaria Leopoldianum, 2015. 240 p. ISBN 978-85-60360-57-4.

GRIDLING, G.; WEISS, B. *Introduction To Microcontrollers*. [S.l.]: Vienna University of Technology, 2006.

GÜVEN, Y.; COŞGUN, E.; KOCAOĞLU, S.; GEZICI, H.; YILMAZLAR, E. Understanding the concept of microcontroller based systems to choose the best hardware for applications. *International Journal of Engineering and Science*, v. 7, n. 9, p. 38 – 44, 2017.

HAN, J.; LV, S.; WU, Z.; ZHANG, M.; BAI, J. Study on measurement of sound attenuation coefficient in bubble wake by pool. In: *2020 2nd International Conference on Geoscience and Environmental Chemistry*. EDP Sciences, 2020. v. 206. Available at: <https://doi.org/10.1051/e3sconf/202020603013>.

HENZE, M.; GUJER, W.; MINO, T.; LOOSDRECHT, M. van. *Activated Sludge Models ASM1, ASM2, ASM2d and ASM3*. [S.l.]: IWA Publishing, 2000. ISSN 1025-0913. ISBN 1 900222 24 8.

HIRAO, M.; OGI, H. *EMATs for Science and Industry: Noncontacting Ultrasonic Measurements*. [S.l.: s.n.], 2003. ISBN 978-1-4419-5366-7.

INATOMI, T. A. H.; UDAETA, M. E. M. *Análise dos Impactos Ambientais na Produção de Energia Dentro do Planejamento Integrado de Recursos*. 2005. Available at: https://scholar.google.com.br/citations?view_op=view_citation&hl=pt-BR&user=xyGjcrQAAAAJ&citation_for_view=xyGjcrQAAAAJ:9yKSN-GCB0IC. Accessed on: 10/06/2022.

ITIS FOUNDATION. *Speed of Sound*. 2021. Available at: <https://itis.swiss/virtual-population/tissue-properties/database/acoustic-properties/speed-of-sound/>. Accessed on: 07 de maio de 2021.

IWA. *Sedimentation Processes*. 2022. Available at: <https://www.iwapublishing.com/news/sedimentation-processes>. Accessed on: June, 07, 2022.

JONATHAN, J. K.; XU, W.; CHIABRERA, A. E.; SIFFERT, R. S. Diffraction Effects in Insertion Mode Estimation of Ultrasonic Group Velocity. *Institute of Electrical and Electronics Engineers*, v. 42, n. 2, p. 232 – 242, Março 1995.

KANDEMIR, M. H.; BEELEN, M.; WAGTERVELD, R.; YNTEMA, D. R.; KEESMAN, K. Dynamic acoustic fields for size selective particle separation on centimeter scale. *Journal of Sound and Vibration*, 2020. ISSN 0022-460X.

KONDAVEETI, H. K.; KUMARAVELU, N. K.; VANAMBATHINA, S. D.; MATHE, S. E.; VAPPANGI, S. A systematic literature review on prototyping with Arduino: Applications, challenges, advantages, and limitations. *Computer science review*, Elsevier Science Ltd, v. 40, May 2021. ISSN 1574-0137.

LEE, J.; SU, Y.; SHEN, C. A Comparative Study of Wireless Protocols: Bluetooth, UWB, ZigBee, and Wi-Fi. In: *The 33rd Annual Conference of the IEEE Industrial Electronics Society (IECON)*. Taipei: [s.n.], 2007. p. 46 – 51.

LEITÃO, R. C.; HAANDEL, A. C.; ZEEMAN, G.; LETTINGA, G. The effects of operational and environmental variations on anaerobic wastewater treatment systems: A review. *Elsevier*, v. 97, n. 9, p. 1105 – 1118, June 2006. Available at: <https://doi.org/10.1016/j.biortech.2004.12.007>.

LEONEL, L. F. *Desempenho de estações de tratamento de esgoto – uma análise de sistemas de lagoas de estabilização de pequeno e médio porte integrada à avaliação da qualidade dos corpos hídricos na UGRHI 12 – Baixo Pardo/Grande*. 2016. 206 p. Dissertation (Departamento de Hidráulica e Saneamento – SHS) — Universidade de São Paulo.

LETTINGA, G. *My Anaerobic Sustainability Story*. [S.l.]: LeAF, 2014. 200 p.

LOBATO, L. C. da S.; BRESSANI-RIBEIRO, T.; SILVA, B. S. da; FLÓREZ, C. A. D.; NEVES, P. N. P.; CHERNICHARO, C. A. de L. Contribuição para o aprimoramento de projeto, construção e operação de reatores UASB aplicados ao tratamento de esgoto sanitário – Parte 3: Gerenciamento de lodo e escum. *DAE*, v. 66, n. 214, p. 30 – 55, novembro 2018.

LOBATO, L. C. S.; BRESSANI-RIBEIRO, T.; SILVA, B. S. D.; FLÓREZ, C. A. D.; NEVES, P. N. P.; CHERNICHARO, C. A. L. Contribuição para o aprimoramento de projeto, construção e operação de reatores UASB aplicados ao tratamento de esgoto sanitário. Parte 3: Gerenciamento de lodo e espuma. *Revista DAE*, v. 66, n. 214, p. 30 – 55, 2018.

LOCATELLI, F.; FRANÇOIS, P.; LAURENT, J.; LAWNICZAK, F.; DUFRESN, M.; VASQUEZ, J.; BEKKOUR, K. Detailed Velocity and Concentration Profiles Measurement During Activated Sludge Batch Settling Using an Ultrasonic Transducer. *Journal Separation Science and Technology*, v. 50, 2015. Available at: DOI:10.1080/01496395.2014.980002.

LUBBERS, J.; GRAAF, R. A simple and accurate formula for the sound velocity in water. *Ultrasound in Medicine & Biology*, Elsevier Science Ltd, v. 24, n. 7, p. 1065 – 1068, Setembro 1998.

MARÇAL, D. A.; SILVA, C. E. Avaliação do impacto do efluente da estação de tratamento de esgoto ETE-Pirajá sobre o Rio Parnaíba, Teresina (PI). *Eng. Sanit. Ambiental*, v. 22, n. 4, p. 761 – 772, jul/ago 2017.

MARTIN, C. C. *Ultrassom*. São Paulo: ABENDI, 2012. 342 p. ISBN 978-85-99153-06-2.

MCCLEMENTS, D.; FAIRLEY, P. Ultrasonic pulse echo reflectometer. *Ultrasonics*, Butterworth-Heinemann Ltd, v. 29, p. 58 – 62, Janeiro 1991.

METCALF EDDY. *Wastewater Engineering: Treatment and Reuse*. 4. ed. [S.l.]: McGraw-Hill Companies, Inc., 2003. 1819 p. ISBN 0071122508.

MORAIS, D.; RODRIGUES, D. L.; POSSANI, D.; CORREIA, F. C. Ondas Ultrassônicas: Teoria e aplicações industriais em ensaios não-destrutivos. *Revista Brasileira de Física Tecnológica Aplicada*, Ponta Grossa, v. 4, n. 1, p. 16 – 33, Maio/Jun 2017. ISSN 2358-0089.

- MURUGAN, K. H. S.; SUMATHI, M. Wireless data acquisition system for underwater environment. In: *2017 Second International Conference on Electrical, Computer and Communication Technologies (ICECCT)*. Coimbatore: [s.n.], 2017. p. 1 – 6.
- NEVES, P. *Contribuição para o aprimoramento de reator UASB aplicado ao tratamento de esgoto sanitário: Inoculação e controle da manta de lodo*. 2020. Dissertation (Programa de Pós Graduação em Saneamento, Meio Ambiente e Recursos Hídrico) — Universidade Federal de Minas Gerais.
- NEVES, P. N. P.; AZEVEDO, L. S.; HOEP, M.; BRESSANI-RIBEIRO, T.; WIERSMA, M.; FERREIRA, R. N.; WAGTERVELD, R. M.; YNTEMA, D.; CHERNICHARO, C. A. L.; AGOSTINHO, L. L. F. Real-Time Determination of Total Solids in UASB Reactors Using a Single Emitter Ultrasonic Sensor. *Water*, v. 13, n. 11, Maio 2021. Available at: <https://doi.org/10.3390/w13111437>.
- OLIVEIRA, S. M. A. C.; VON-SPERLING, M. Evaluation of 166 treatment plants operating in Brazil, comprising several technologies. Part 1: performance analysis. *Engenharia Sanitaria e Ambiental*, v. 10, n. 4, p. 358 – 368, Dezembro 2005. ISSN 1809-4457.
- OLYMPUS. *Introduction to Phased Array Ultrasonic Technology Application*. 2007. Available at: www.olympus.com.br.
- PANDIN, T. Application of Oscilloscope Technology in the Early 21st Century: A Systematic Literature Review. 2021. Available at: <https://www.preprints.org/manuscript/202106.0090/v1>. Accessed on: 21/06/2022.
- PARRA, L.; ROCHER, J.; ESCRIVÁ, J.; LLORET, J. Design and development of low cost smart turbidity sensor for water quality monitoring in fish farms. *Aquacultural Engineering*, Elsevier Science Ltd, v. 81, p. 10 – 18, Maio 2018.
- PAULA, A. C. *Avaliação Integrada do Desempenho de Reatores Anaeróbios do Tipo UASB Tratando Esgoto Doméstico em Escala Real*. 2019. 210 p. Dissertation (Pós-Graduação em Engenharia de Recursos Hídricos e Ambiental) — Universidade Federal do Paraná.
- PÉTRIER, C. The use of power ultrasound for water treatment. In: PÉTRIER, C. (Ed.). *Power ultrasonics*. Woodhead Publishing, 2015. chap. 31, p. 939 – 972. Available at: <https://www.sciencedirect.com/science/article/pii/B9781782420286000314>.
- POWLES, A. E. J.; MARTIN, D. J.; WELLS, I. T.; GOODWIN, C. R. Physics of ultrasound. *Elsevier*, v. 19, n. 4, p. 202 – 205, 2018. Available at: <https://doi.org/10.1016/j.mpaic.2018.01.005>.
- RAFIQUZZAMAN, M. *Microcontroller Theory and Applications with the PIC18F*. 1. ed. [S.l.]: Wiley Publishing, 2011.
- RAVEAU, M. P. A review of theoretical models for attenuation of sound by bubble clouds. In: *22rd International Congress on Acoustics*. Buenos Aires: [s.n.], 2016.
- ROCHER, J.; SENDRA, S.; PARRA, L.; SHU, L. Low Cost Sensor to Measure Solid Concentrations in Wastewater. *IECON 2018 - 44th Annual Conference of the IEEE Industrial Electronics Society*, p. 5234 – 5239, Outubro 2018.
- RÖMKENS, P.; OENEMA, O. *Quick Scan Soils in The Netherlands: - Overview of the soil status with reference to the forthcoming EU Soil Strategy*. Wageningen, 2004.

SANCHEZ, A.; CASTRO, A. de; ELVIRA, S.; GLEZ-DE-RIVERA, G.; GARRIDO, J. Autonomous indoor ultrasonic positioning system based on a low-cost conditioning circuit. *Measurement*, Elsevier Science Ltd, v. 45, n. 3, p. 276 – 283, April 2012.

SCHEWERDA, J.; FÖRSTER, G.; HEINRICHMEIER, J. Novel method for sludge blanket measurements. *Water Science & Technology*, IWA Publishing, v. 64, n. 4, p. 775 – 782, 2014. Available at: <https://doi.org/10.2166/wst.2013.775>.

SHUNG, K.; ZIPPURO, M. Ultrasonic transducers and array. *Institute of Electrical and Electronics Engineers*, v. 15, n. 6, p. 20 – 30, 1996.

SOUZA, B. F. de; AGOSTINHO, L. L. F. Sewage Sludge Ash Characterization for P Recovery. 2022.

STAKUTIS, V. J.; MORSE, R. W.; DILL, M.; BEYER, R. T. Attenuation of Ultrasound in Aqueous Suspensions. *The Journal of the Acoustical Society of America*, Elsevier Science Ltd, v. 27, n. 3, Maio 1955.

TECHAVIPOO, U.; VARGHESE, T.; STILES, T. A.; CHEN, Q.; ZAGZEBSKI, J. A.; FRANK, G. R. Temperature dependence of ultrasonic propagation speed and attenuation in excised canine liver tissue measured using transmitted and reflected pulses. *The Journal of the Acoustical Society of America*, v. 115, n. 6, June 2004.

TREEBY, B. E.; COX, B. T.; ZHANG, E. Z.; PATCH, S. K.; BEARD, P. C. Measurement of Broadband Temperature Dependent Ultrasonic Attenuation and Dispersion Using Photoacoustics. v. 56, n. 5, p. 1666 – 1676, Agosto 2009.

VON-SPERLING, M. *Lodos ativados*. 4. ed. Belo Horizonte: Editora UFMG, 2016. v. 4. 461 p. (Princípio do tratamento biológico de águas residuárias, v. 4). ISBN 978-85-423-0173-1.

VON-SPERLING, M. *Princípios básicos do tratamento de esgotos*. 2. ed. Belo Horizonte: Editora UFMG, 2016. v. 2. ISBN 9788542301748.

VON-SPERLING, M.; VERBYLA, M. E.; OLIVEIRA, S. M. *Assessment of Treatment Plant Performance and Water Quality Data: A guide for students, researches and practitioners*. 1. ed. [S.l.]: IWA Publishing, 2020. 668 p.

VRECKO, D.; HVALA, N.; CARLSSON, B. Feedforward-feedback control of an activated sludge process: A simulation study. *Water Science & Technology*, IWA Publishing, v. 47, n. 12, p. 19 – 26, February 2003.

WADE, G. Human uses of ultrasound: ancient and modern. *Ultrasonics*, Elsevier Science Ltd, v. 38, n. 1-6, p. 1 – 5, Março 2000. Available at: [https://doi.org/10.1016/S0041-624X\(99\)00063-3](https://doi.org/10.1016/S0041-624X(99)00063-3).

WEF. *Clarifier Design*: Water Environment Federation Manual of Practice No. FD-8. 2. 2. ed. Virginia: McGraw-Hill, 2005. 746 p.

WEF - WATER ENVIRONMENT FEDERATION. *Automation for Optimization of Thickening and Dewatering*. 2019. Available at: <https://www.wef.org/globalassets/assets-wef/3---resources/topics/a-n/biosolids/technical-resources/002-automation-for-optimization-of-thickening-and-dewatering-final.pdf>. Accessed on: 10/06/2022.

WINATA, H. N.; NOGUCHI, R.; AHAMED, T.; NASUTION, M. A. Prediction of Microalgae Total Solid Concentration by Using Image Pattern Technique. *Journal of the Japan Institute of Energy*, v. 98, n. 5, p. 73 – 84, May 2019. Available at: DOI:10.3775/jie.98.73.

YOUSEFIAN, O.; WHITE, R. D.; KARBALAEISADEGH, Y.; BANKS, H. T.; MULLER, M. The effect of pore size and density on ultrasonic attenuation in porous structures with mono-disperse random pore distribution: A two-dimensional in-silico study. *The Journal of the Acoustical Society of America*, v. 144, n. 2, August 2018. Available at: <https://asa.scitation.org/doi/10.1121/1.5049782>.

ZHANG, G.; LI, X.; ZHANG, S.; KUNDU, T. Investigation of frequency-dependent attenuation coefficients for multiple solids using a reliable pulse-echo ultrasonic measurement technique. *Measurement*, Elsevier Science Ltd, v. 177, n. 109270, Junho 2021. ISSN 0263-2241. Available at: <https://doi.org/10.1016/j.measurement.2021.109270>. Accessed on: 06 de maio de 2021.